Investigation into Transient Stability of a Nuclear Power Plant using DIgSILENT

Prepared by:

Paul Emmanuel

EMMPAU001

Department of Electrical Engineering
University of Cape Town

Prepared for:

Komla Folly

Department of Electrical Engineering
University of Cape Town

October 2015

Submitted to the Department of Electrical Engineering at the University of Cape Town in partial fulfilment of the academic requirements for a Master of Science degree in Electrical Engineering.

Declaration

I declare that this dissertation is my own, unaided work. It is being submitted for the degree of Master of Science in Electrical Engineering in the University of Cape Town. It has not been submitted before for any degree or examination in any other university.

Name: **Paul Emmanuel**

Signature: Signed **Date:** 21 April 2016

Acknowledgements

I would like to thank the following people for assisting and supporting me through my thesis project and undergraduate degree:

- my wife Megan, and son Joel, for allowing me the time to complete my study's;
- Professor Komla Folly, for his guidance and assistance throughout my thesis, and his encouraging words allowing me to complete these study's;
- Mr. David Oyedokun, for his patience, guidance and help throughout my thesis;
- Mr Gregory Karsten, for his continuous support;
- Mr Mike Hadingham, for his expert advice and contribution;
- Mr Willem Stemmet, who encouraged me to complete this study; and
- Eskom for their sponsorship throughout this study.

Abstract

The current electricity crisis, coupled with the lack of generation, has led to a major focus on continuity of supply. The Western Cape has been severely affected, as it only has a limited number of generation sources, namely Koeberg Nuclear Power Station (base supply) along with other power stations used for peak load running such as Ankerlig, Palmiet, etc. Koeberg Nuclear Power Station is located at the end of a long transmission line with no other base-load generation for 1500km, between the power station and the mass pool of coal-fired generation in Mpumalanga.

Koeberg Nuclear Power Station (herein referred to as “Koeberg”) plays a significant role in ensuring the stability of the Western Cape’s electricity network. Without this power stattion, the network power flow is greatly affected, and is placed under severe strain. Koeberg is the determining factor when the system-operators control the Western Cape network. The network is modelled having one of Koeberg’s unit offline, using contingency analysis N-1. The one Koeberg unit being the N-1 contingency factored into the transmission network. The network should be able to withstand a disturbance with one Koeberg unit out of service and maintain stability after the disturbance. With the Eskom's decision to increase Koeberg power plant’s electrical output power, it became apparent that the impact of this upgrade needed to be assessed. In the past, various hand calculations and assumptions were made before implementation of these types of changes could occur. With the advent of technology, modern computer-based software simulation tools have reduced the time to analyse such changes and aid engineers to quickly assess the impact it would have on various components.

A load flow and short circuit studies of the Koeberg internal networks were performed and verified against plant data. The original data was compared to simulated data using a computer-based simulation package. The simulation software package used to validate the results is the DIgSILENT software package. This is one of the standard software packages used by Eskom to validate models on the network. Load flow studies for Koeberg have been completed in the past, but many changes have since been made to the plant. There was thus a requirement to re-calculate the original load flow studies and ensure that all plant and protection settings are within an acceptable criterion. This new study found that there were minor errors in the on-site documentation and that the software is compatible with the plant data.

The South African electricity network is made up of many components. To gain understanding, and to reduce computation time, a reduced network was built into DIgSILENT to assess the impact the increase in the output generation has on the nuclear plant’s ability to remain stable during grid disturbances. Two classical mathematical assessments were made, namely, the equal area criterion and the modified Euler method, to validate the simulated results for the critical clearing times associated with the nuclear power plant. In all the simulated results, a decrease in critical clearing times was noted when the output of the generator was increased. A further reduction in critical clearing time is achieved when both generators are

coupled to the common coupling in the High Voltage (HV) yard. DIgSILENT has the ability to build models of Automatic Voltage Regulators (AVR), Power Systems Stabilisers (PSS) and Turbine control systems. However, only a transient stability assessment of the AVR was completed, as the PSS and the turbine control models have not been validated yet. It is shown that the AVR has very little impact on the critical clearing time of the nuclear power station during transmission-grid faults, as the response of the excitation system of the plant is a rotating-type exciter, which responds slowly to faults. The simulation validated this and allows system engineers to motivate for a replacement of excitation system when the need arises.

The nuclear power station has five back-up emergency diesel generators used to bring the plant power down safely if all off-site supply is lost, and it is no longer able to supply itself. DIgSILENT was used to perform a critical clearing time assessment for faults at the HV busbar close to the nuclear power station. This critical clearing time only comes into play when the emergency diesel generator is coupled to the network during routine testing to prove the diesel generator's output capability. A critical clearing time has now been established for the emergency diesel generators following the thermal power upgrade, and, although no pole slip protection is available, the information is valuable for the thermal power upgrade project.

The effect of increased generation on critical clearing times was determined. The Western Cape transmission system was simulated taking into account all the generation sources in the province. Three-phase faults were placed both at HV busbar close to the power station and far away (i.e., 800 km) following the new electrical generation parameters. The nuclear power plant would be stable for both close and far away faults; however, cascading pole slipping occurs in all the generators in the province when the generators at the nuclear plant pole slip.

Protection systems ensure stability of supply by only isolating the defective component/equipment and ensuring continuity of supply. Although the protection scheme at Koeberg has been in operation for quite some years, a verification of settings needs to be completed from time to time. The settings have been based on network and plant parameters. These parameters will change when the thermal power upgrade settings are applied to generator and the protection scheme needs to be adapted accordingly. The protection setting of interest for this study was the pole slip protection. However, validation of protection models is outside the scope of this work.

Based on all the simulations conducted, it was concluded that Koeberg Nuclear Power Station would be transiently stable following a network disturbance even after the increase in the electrical output power.

Table of Contents

List of Figures

List of Tables

1. Introduction

1.1 Introduction

South Africa's electricity supply has been dominated by the Electricity Supply Commission (ESCom), which was established in 1923 [1]. The name was changed to Eskom in 1986. Eskom generates approximately 95% of the electricity used in South Africa and approximately 45% of the electricity used in Africa [1]. The Eskom network is part of the Southern African Power Pool (SAPP), which connects Eskom to the networks of other utilities in neighbouring countries. Eskom generates, transmits and distributes electricity to industrial, mining, commercial, agricultural and residential customers together with redistributors [1]. The power-generation pool comprises of the following sources, namely, coal, nuclear, hydro with pump storage, gas, wind and solar. Eskom's total generating capacity is 45656MW as of June of 2015. Eskom's generation can be broken up into the different technologies associated with the South African national electrical grid, which is illustrated in Figure 1.1 below.

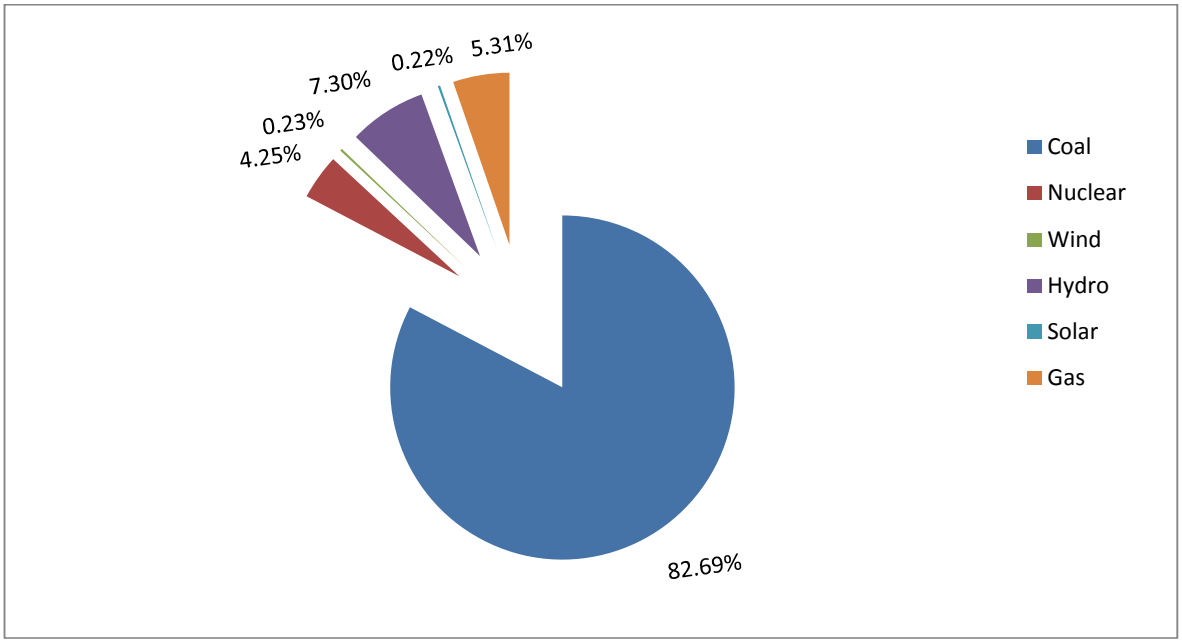

Figure 1.1 Electricity technology distribution

Eskom's generating capacity is as follows, namely, coal 82,7%, nuclear 4,25%, wind 0,23%, hydro 7,3%, gas 5,3% and solar 0,22% [2]. The power stations can be further divided into base-load power generations and peaking power generations. Base-load power stations are characterised by power stations that run continuously; and examples are Kendal, Koeberg, Matla and Majuba, to name a few. While peak power stations refer to generation stations that are used only during high consumption periods, examples are Ankerlig, Gourikwa, and Palmiet [2]. The base-load stations contributed up to 90% of the generation source, compared to peaking stations that make up 10% of the generation sources [2]. In South Africa, coal and

nuclear dominates the base-load supply power stations, whereas wind and hydro (renewable energy), gas and solar constitutes the peaking contingent of the generation sources.

This study focuses on the Western Cape network; therefore the development of the Western Cape network is briefly discussed below.

The first Eskom power station erected in Cape Town was the Salt River 1 power station in 1928 [3]. It was the first coal-fired power station that was operated by the utility. As the load demand in the Western Cape province increased, Eskom and the Western Cape Provincial Council decided to increase the generating capacity in the Western Cape by building the Athlone power station in 1962 and the Salt River 2 power station in 1967 [3]. The province was eventually linked to the national grid in 1969, which reduced the generating requirement for power stations in the province [3].

As the load in South Africa increased and the Western Cape was no longer an islanded network, Eskom decided to build a nuclear power station, and the first unit at Koeberg Nuclear Power Station was commissioned in 1984 [2]. This increased the generating capacity in the Cape Province by 1800MW, which, at the time, was sufficient to supply the Western Cape and even to export power northwards on the transmission lines connecting the Cape and Orange Free State to the Highveld region of South Africa [4].

From the 1980s through to the early 2000s, the growth in demand for electricity followed a trend averaging between 2% and 3% per annum [5]. However, over the past few years, the annual growth in peak demand for electricity has been higher than an average of 4% per annum. The Government's accelerated and shared growth initiative for South Africa (ASGISA) projected growth of the economy by approximately 6% per annum into the future [5]. This 6% projection implies a 4% increase in the demand for electricity. Eskom's future planning, with reference to the demand for electricity capacity, is therefore based on an average annual growth rate of 4% [5]. Figure 1.2 illustrates the growth in load demand taken in 2006 and projects that the future electricity reserve margin will be reduced dramatically. In 2015, this reserve margin is being stretched on a daily basis and load shedding is a daily possibility as the load demands encroach on the reserve margin.

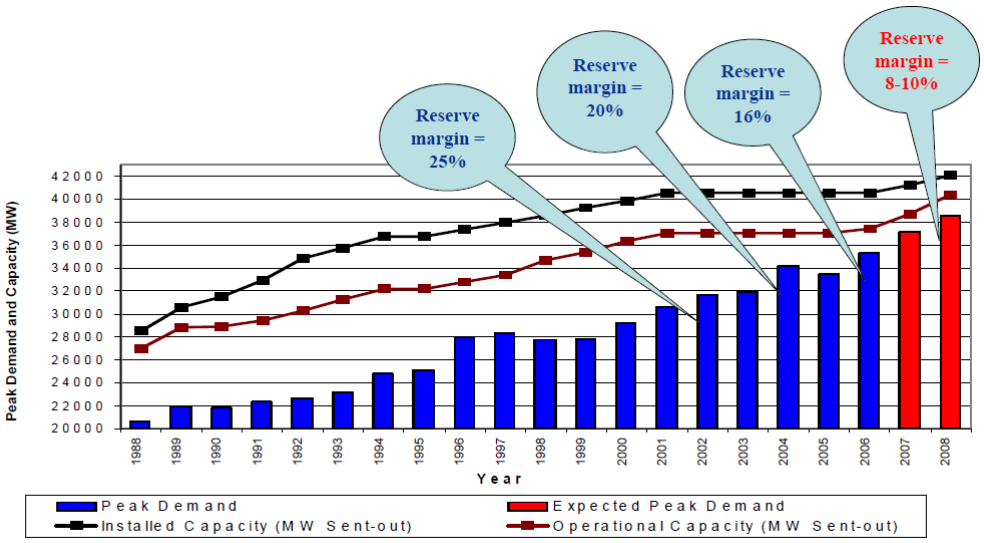

Figure 1.2 Electricity load demand increase [6]

Assuming the Western Cape's energy growth trend follows the country's growth trend, then the nuclear power plant would have been unable to supply the Western Cape grid on its own many years ago. For illustrative purposes, a snap shot of the Western Cape winter load profile in 2009 is shown in Figure 1.3. From this figure it can be seen that Koeberg Nuclear Power Station would be unable to supply the Western Cape load already since before 2009. Koeberg is only capable of sending out 1840MW (both units in operation), and the minimum load in the Western Cape was 2200MW in 2009 and the maximum load was 4100MW [4]. It should be noted that the Western Cape gets most of its electricity supply from the large generation source comprising of coal-fired power stations in the province of Mpumalanga [4]. This confirms the assumption that the Western Cape growth rate was at least as high as that of the country over the past ten years.

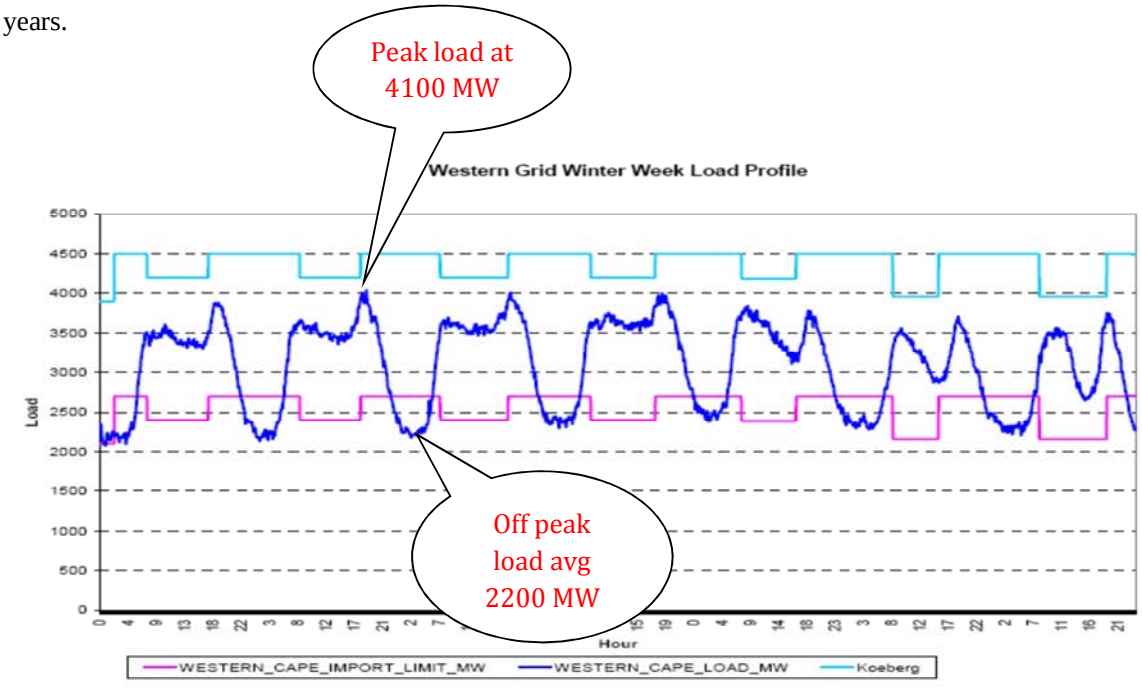

Figure 1.3 Western Cape winter load profile 2009 [4]

The government of South Africa is planning to increase the national nuclear generation from the current 4.4% to 9.5% in the next few years [7]. Although this is still in the planning phase, the project has been approved by Government, which affirmed its position regarding the use of nuclear technology to generate electricity. This will assist with the ever-increasing loading on the network and the lack of generation, especially the base-load which is much needed to ensure availability of supply [2]. Any increase in base-load generation could assist or help the power system, which is ailing owing to the lack of generation.

With the Koeberg Nuclear Power Station preparing to increase its generating capacity by a 130MW (per generating unit) in the Western Cape, a detailed analysis of the effect of this plant on the transient stability of the system is required. Transient stability studies are particularly important as they can indicate whether the generation in the Western Cape can stay in synchronism with rest of the Eskom generation and, hence, ensure that the all-important Koeberg auxiliaries can receive power from the transmission network [8]. Recently, the resurgence in studies completed for new technology included completing transient stability studies [8], [9], [10]. Here, High Voltage-Direct Current (HVDC) has received a lot of attention in many studies completed by many authors [11], [12], [13]. With the diversification of electrical technologies, wind generation studies have also been completed and transient stability studies have also been included in these studies [9], [14]. However, during the literature review, it was found that not much external research related to transient stability studies of nuclear power plants has been published.

This dissertation will therefore aim to address stability issues within the nuclear power plant, and allow for network engineers to adapt and protect the plant against network disturbances or faults. It also allows engineers to evaluate plant changes and give better insight into the behaviour of the nuclear power plant.

1.2 Background to the study

The South African electricity utility is under immense pressure to ensure continuity of supply. The South African power grid, especially in the Western Cape, is susceptible to instability owing to the long transmission lines that connect the Western Cape to coal-based power plants and the lack of adequate base-load power generation in the Western Cape [4].

It should also be noted that South Africa's only nuclear power station, namely Koeberg, has plans in place to increase its thermal power output by replacing the steam generators [15]. In the last 10 years, Koeberg Nuclear Power Station has performed various modifications to improve efficiency and electrical output. Modifications like the turbine blade modification allowed the electrical output power to be increased from 920MW to 970MW per generator unit. The steam generator replacement will allow an increase in electrical output power from 970MW electrical (MWe) to 1100MWe per generator unit, which is a 13.4% increase in generation capacity. The increase in electrical power output however requires analysis of the generator protection scheme and the stability of the generator following the thermal power upgrade. This has provided

an opportunity for developing a plant model to be used for the analysis of plant upgrades as well as fault simulations.

Nuclear power stations rely on internally generated power to supply their safety-related equipment [16]. As such, the output of the generator feeds the main power supply bus system of the station via a step-down transformer [16]. Serious faults can however occur more frequently as plants become older, and harsh weather conditions can further compound the ailing health of these plants. It is therefore imperative to perform transient stability analysis for ageing nuclear power stations to ensure minimal disruption to the continuity of supply during the said transient conditions [16].

On a global level, there have however been nuclear incidents in the past. The nuclear incident at the Fukushima nuclear power plant, in Japan, has demonstrated that a more rigorous approach to nuclear power plant operation is required [17]. Nuclear power plants are however designed and maintained to operate at maximum capacity at all times, and protection systems ensure stability of supply by only isolating the defective component/equipment and ensuring continuity of supply.

Although the protection scheme at the Koeberg nuclear power plant has been in place for some years, a verification of the settings needs to be completed from time to time [18]. The settings were based on network and plant parameters; when these parameters change, the protection scheme needs to be adapted accordingly. Similarly, the internal nuclear plant network, as well as the affected generation network, should be analysed to ensure that most power plants can withstand grid disturbances.

Transient stability studies are concerned with the ability of the power system to withstand large faults or disturbances. If the system can return to its original operating state or a new state once the disturbance is removed, the system is said to be stable [19] .The types of disturbances range from transmission-line loss owing to lightning strikes and broken conductors, loss of generation, increase in load demand, and a decrease in generating capability [19]. The nuclear power plant in this study, like many others, has been subjected to all of these types of disturbances at some point in its operational life. Some have been significant and others have gone unnoticed without any major incident or impact.

Usually numerous simulations are conducted to verify plant parameters and responses for different scenarios to give insight into the behaviour of the network under different conditions. The simulation results allow the system operator to adapt the network to pre-empt failure. Even a well-designed and normally operated system may face the threat of transient instability [19]. Computer-based stability analysis is therefore an important component of power systems' operations and planning. As a result, it is crucial that the models and parameters of the generators and associated excitation systems are accurately assessed to ensure that the results are representative of the real power system [4], [13].

The simulation software package used to validate the results in this dissertation is the DIgSILENT software package. DIgSILENT is a computer-based software package, providing power system modelling, analysis and simulation [20]. This software package is widely used by system operators to model the power system to quantify risk and uncertainty in simulation models. These studies are considered during the planning and design stages of a new power station, as well as when evaluating changes to an existing system during the operational phase [4].

1.3 Objectives of this study

The main objective of the thesis is to look at issues which ensure the safe operation of the Koeberg nuclear plant during grid disturbances by:

- validating the built DIgSILENT model against known parameters;
- analysing the plant response with or without the Automatic Voltage Regulator(AVR), with the main focus being the future plan to increase the generating output of the plant and the effect on the plant under various plant configurations;
- investigating the network response to transients emanating from switchyard faults close and far away from the nuclear plant, and the reaction of the Western Cape grid during these disturbances post thermal power upgrade; and
- examining the transient behaviour of the on-site emergency generators during faults on the 400kV transmission network with an increase in generation at the nuclear power plant.

1.4 Thesis development plan

A literature review was completed to provide insight into the topic. Once the literature review was completed, a decision was made to perform a transient analysis of a nuclear power plant. A development plan was put together and can be seen in Figure 1.4.

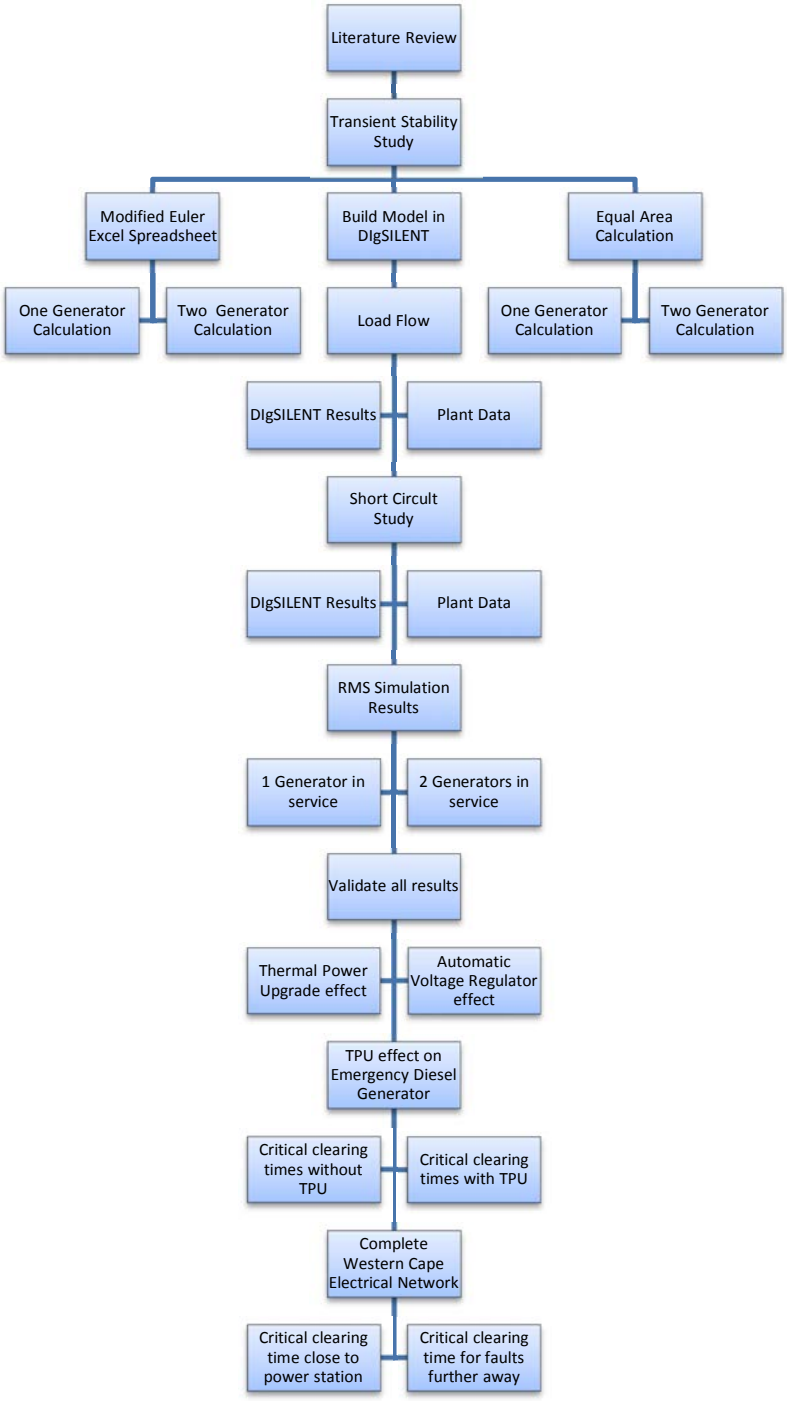

Figure 1.4. Development plan of the Dissertation

In order to conduct this study, it was decided to build a reduced network with an infinite bus representing the grid and the nuclear plant's generators and internal 6,6kV network. The complete Eskom reticulation was built in DIgSILENT by Eskom system operators, but limited to the transmission network and does not include generation plant parameters. Therefore, to fully understand the fundamentals of the study, a reduced network was built. It allows plant engineers to verify internal plant parameters and assess relevant data pertaining to modifications. It will allow the plant engineers to verify fault reports and put measures in place

to prevent inadvertent tripping of the nuclear power plant. Network system operators perform daily simulations relating to changes seen on the national electricity grid in order to validate data. The network is dynamic and changes all the time, and these system operators, based on their knowledge and training, adapt the network accordingly to prevent major loss of electrical power. Hence, this knowledge and training is not readily available and takes years to develop.

DIgSILENT was used to build the network. However, it was necessary to verify the reduced network to ensure that the model was valid, and thus two other methods were used to validate the models. The first approach was to perform the equal-area-criterion calculation for the nuclear plant connected to an infinite bus. The same parameters used in the previous two methods were used to perform the modified Euler method to compare the networks and to ensure model validity.

The load flow studies were completed using the DIgSILENT software. Load flow studies will determine the bus voltage magnitude, bus voltage angle, current, active power and reactive power. In addition to the load flow studies performed in DIgSILENT, a short-circuit analysis was completed and fault currents were compared to the original handover information supplied at commissioning. On completion of the short-circuit study, a transient stability analysis was completed using DIgSILENT to confirm various scenarios against which critical clearing times were assessed.

1.5 Scope and limitations

Limitations are based on the fact that a reduced network model was used in the analysis in Chapters 4 and 5. This includes the hand calculations completed for the equal area criterion; the modified Euler Excel spreadsheet analysis and the reduced network built in the DIgSILENT software. The South African reticulation network used in Chapter 6 neglected Static VAr compensators and capacitor banks. The study was also limited to the HV switchyard closest to the nuclear power plant, as well as another generating source 800km away, to gauge the effect of generation faults further away from the plant. The Power System Stabiliser (PSS) and turbine control model was not included in the scope of this work. The PSS installed on the plant is still being optimised and parameters have not been finalised yet. The turbine control has been modified and, owing to a lack of data, has not been included in the simulation.

1.6 Contribution of this thesis

The contributions of this thesis include:

- The development of a simplified network of the plant that could be used for future upgrades and plant/network fault interactions studies.
- The finding that the nuclear power plant would be transiently stable following a grid disturbances near and further away (800km) from the power plant following the thermal power upgrade.

- The discovery that the excitation system of the Koeberg nuclear power plant is slow in responding to the disturbances during the simulation.
- The clarification of the critical clearing times associated to the emergency diesel generator which was not known before.

1.7 Structure of thesis

This study is divided into seven chapters which are organised in the following manner:

Chapter 1 describes the background, scope and limitations of the dissertation. It also defines the reason for completing the study.

Chapter 2 presents the literature review by examining the background history related to power system stability. It also includes basic nuclear power fundamentals and initiates the discussion regarding the behaviour of synchronous machines under various conditions. This chapter is concluded by examining the effect that the excitation system has on transient stability.

Chapter 3 is an introduction to mathematical modelling and theory related to performing transient stability studies. It then delves into the fundamentals which form the basis of analysis of rotor angle stability. It also introduces the DIgSILENT software and its modelling capabilities.

Chapter 4 focuses on the simplified network and compares different methods to determine critical clearing times. A load flow and short-circuit studies were completed, analysed and compared with plant data to verify simulation accuracy.

Chapter 5 examines the critical clearing time of the emergency diesel generator when a network disturbance occurs and the diesel generator is connected to the network.

Chapter 6 takes into consideration all the generation sources in the Western Cape and assesses the critical clearing time for faults which occur nearby and faults some 800km away from the nuclear plant based on the thermal power upgrade generation capability.

Chapter 7 discusses the study's conclusions and recommendations based on the simulation results addressed in Chapters 4, 5 and 6.

2. Literature Review

Transient stability studies have been applied for many years to determine generator stability during major grid disturbances [11]. Grid disturbances, which can be categorised as the tripping of one or more power system components of the grid, have resulted in many nuclear power stations being disconnected from the grid and operated in islanding mode. However, many reports suggest that network disturbances can operate both network and generator protective devices which eventually could trip the nuclear power station [16], [21]. The ability of a nuclear power station to withstand a grid disturbance is vital, as the preferred mode of operation would be to supply its own auxiliaries and to ensure nuclear safety by supplying all the vital equipment [21].

Transient stability events are a reality and the severity of these events has major outcomes, depending on how well the network is controlled. Therefore, much emphasis has been placed on studying the network to prevent such an occurrence and various methods are used to determine transient stability, namely, Artificial Intelligence, Time-Domain and Numerical Integration methods [11], [12], [14]. These methods are further discussed at a later stage in this chapter and are confined to time domain and numerical integration methods. Transient stability however forms part of a much larger facet called power system stability.

2.1 Power system stability

Power system stability is defined as maintaining the stability of synchronous machines under different scenarios, and it can be categorised into three main types, namely rotor angle stability, voltage stability and frequency stability [11], [14], [19]. Each of these topics is of equal importance and are all based on the notion that the network will be stable if the network is able to withstand a disturbance without major power disruption.

Understanding the differences between the three types of stability, namely rotor angle, frequency and voltage, is critical in identifying possible shortfalls in the networks [11]. These types of stabilities are defined as follows:

- *"Rotor angle stability refers to the ability of synchronous machines of an interconnected power system to remain in synchronism after being subjected to a disturbance. It depends on the ability to maintain/restore equilibrium between electromagnetic torque and mechanical torque of each synchronous machine in the system. Instability that may result occurs in the form of increasing angular swings of some generators leading to their loss of synchronism with other generators*" [22].

- *"Voltage stability refers to the ability of a power system to maintain steady voltages at all buses in the system after being subjected to a disturbance from a given initial operating condition. It depends*

on the ability to maintain/restore equilibrium between load demand and load supply from the power system. Instability that may result occurs in the form of a progressive fall or rise of voltages of some buses. A possible outcome of voltage instability is loss of load in an area, or tripping of transmission lines and other elements by their protective systems leading to cascading outages. Loss of synchronism of some generators may result from these outages or from operating conditions that violate field current limit" [22].

- *"Frequency stability refers to the ability of a power system to maintain steady frequency following a severe system upset resulting in a significant imbalance between generation and load. It depends on the ability to maintain/restore equilibrium between system generation and load, with minimum unintentional loss of load. Instability that may result occurs in the form of sustained frequency swings leading to tripping of generating units and/or loads*" [22].

Figure 2.1 shows the various layers in which power system stability is analysed in a simplified way. It also indicates the various sub-sections which will be discussed further [12].

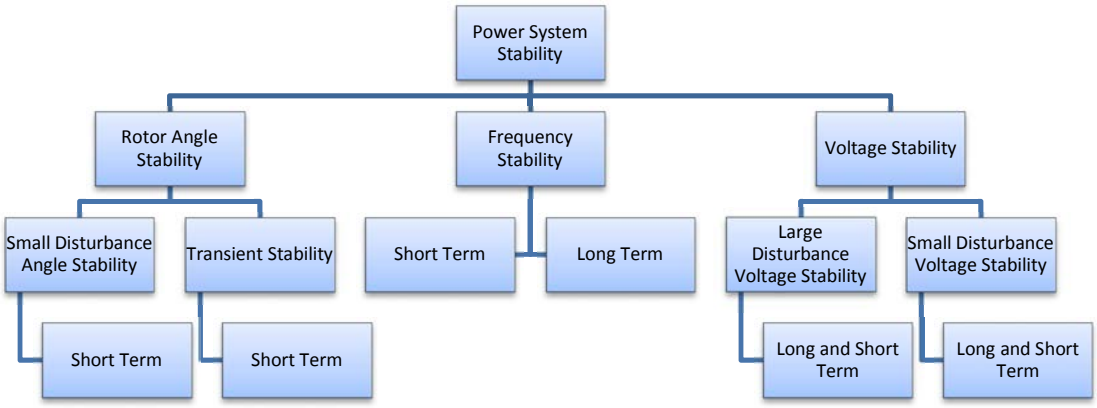

Figure 2.1 Classification of Power System Stability [11], [12]

As illustrated in Figure 2.1 above, the types of stability are further broken down into sub-sections. Here, the various types of stabilities together with their sub-sections are discussed below.

Small-disturbance rotor angle stability problems may be either local or global in nature. Local problems involve a small part of the power system, and are usually associated with rotor angle oscillations of a single power plant against the rest of the power system and are called *local plant mode oscillations* [22]. Stability (damping) of these oscillations depends on the strength of the transmission system as seen by the power

plant, generator excitation control systems and plant output [11]. Global problems are caused by interactions among large groups of generators and have widespread effects. They involve oscillations of a group of generators in one area swinging against a group of generators in another area and are called *inter- area mode oscillations* [22]. Their characteristics are very complex and differ significantly from those of local plant mode oscillations. Load characteristics, in particular, have a major effect on the stability of inter-area modes [22]. The time frame of interest in small-disturbance stability studies is in the order of a few seconds following a disturbance.

Large-disturbance rotor angle stability or *transient stability*, as it is commonly referred to, is concerned with the ability of the power system to maintain synchronism when subjected to a severe disturbance, such as a short-circuit on a transmission line [11]. The resulting system response involves large excursions of generator rotor angles and is influenced by the nonlinear power-angle relationship. Transient stability depends on both the initial operating state of the system and the severity of the disturbance. Instability is usually in the form of a periodic angular separation owing to insufficient synchronising torque, manifesting as *first swing instability* [11]. "*However, in large power systems, transient instability may not always occur as first swing instability associated with a single mode; it could be as a result of superposition of a slow inter-area swing mode and a local-plant swing mode causing a large excursion of rotor angle beyond the first swing* [11]. *It could also be a result of nonlinear effects affecting a single mode causing instability beyond the first swing. The timeframe of interest in transient stability studies is usually three to five seconds following the disturbance and it may extend to 10–20 seconds for very large systems with dominant inter-area swings*" [11], [23].

As identified in Figure 2.1, small-disturbance rotor angle stability, as well as transient stability, is categorised as *short-term* phenomena. "*The term 'dynamic stability' also appears in literature as a class of rotor angle stability. However, it has been used to denote different phenomena by different authors. In North American literature, it has been used mostly to denote small-disturbance stability in the presence of automatic controls (particularly, the generation excitation controls) as distinct from the classical 'steady-state stability' with no generator controls* [11] , [24] , [25]. *In European literature, it has been used to denote transient stability* [11], [24], [25]. *Since much confusion has resulted from the use of the term 'dynamic stability', we recommend against its usage, as did the previous IEEE and CIGRE Task Forces*" [11], [26], [27].

The voltage stability sub-category, "large-disturbance voltage stability", refers to the system's ability to maintain steady voltages following large disturbances such as system faults, loss of generation or circuit contingencies [11] , [28]. The sub-category "small-disturbance voltage stability" refers to the system's ability to maintain steady voltages when subjected to small perturbations such as incremental changes in system load [11], [28]. Voltage stability of the study period of interest may extend from a few seconds to tens of minutes. Therefore, voltage stability may be either a short-term or a long-term phenomenon.

2.2 Global examples of power system instability

The 1965 blackout in North East America and Canada caused widespread supply loss and could be perceived as the catalyst for focused stability studies in North America. This led to more focused studies which predominately were based on transient (angle) stability, but post incident concluded that a more in-depth analysis is required for small changes in the frequency (small signal stability) and voltage collapse occurrences [23].

Recent major events, as listed below, have shown that well-established networks can become unstable causing major power loss. The following are a few examples [23, 11]:

1. July 2, 1996 disturbance of WSCC (Western North American Interconnected) System;
2. August 10, 1996 disturbance of WSCC system;
3. 1998 power failure of Auckland business districts, New Zealand;
4. March 11, 1999 Brazil blackout;
5. July 29, 1999 Taiwan disturbance;
6. August 14, 2003 blackout of Northeast U.S. and Ontario;
7. Europe 2006; and
8. India blackout June-July 2012.

The aforementioned are all unrelated events, yet occurred under similar circumstances. This could imply that one cannot predict what will happen in the power system, but one is able to make a more informed decision based on contingency studies' simulations. One common theme throughout these events was that, at some point, the network was heavily loaded. However, another issue to examine is that inadequate protection settings caused cascading tripping due to protection relay mal-operation which caused widespread power loss. Insights given into the events depict a global issue that is not related to a specific network. What is not clear in all these events is the age of the protection equipment and whether the technology used had an impact on the operation of the protective devices. These factors could greatly affect the power system's reliability and security, which brings back the age old question of old vs. new technology [21].

Classical methods of performing power flow contingency analysis and transient stability requires an N-1 criterion, which means it always uses a single fault condition and does not investigate multiple outage scenarios [23]. This could be one of the reasons why such aforementioned incidents have re-occurred. These events have left millions of customers without supply of electricity for hours and negatively impacted the economy. Multi-contingency studies (i.e., N-2) of modern power systems are becoming more important, where two standing faults are considered.

2.3 South African examples of grid disturbances

Although the South African electricity grid has not suffered from severe grid instability, the possibility of an occurrence of grid instability is always there. As an example, in 2005-2006 the Western Cape grid suffered

load shedding due to a lack of generation and protective devices mal-operating for faults [29]. Such unforeseen incidents have sparked questions about diversifying supply and ensuring that the generating capability of the Western Cape grid is strengthened. The events also highlight the importance of the nuclear power station of the South Africa national grid and the role it plays in stabilising the Western Cape's electricity supply. As discussed earlier, nuclear power plants have stringent operating criteria and the system operators are constantly adapting the network to ensure that parameters such as voltage and frequency parameters are not violated.

The geographical layout of the Eastern and Western Cape transmission network at the time the incidents occurred in 2005-2006 can be seen in Figure 2.2. The incidents include:

- Switching occurring in the 400kV transmission yard that caused several transmission lines and the Koeberg generator 2 to trip. This event resulted in load shedding of 1326MW in the Western Cape [29].
- The Beta–Hydra line (referred as the Cape Corridor) incident which, together with its associated 765/400kV transformer, which tripped owing to a wire short on the tower, was caused by a bird building a nest. This resulted in a voltage dip that caused the auxiliary power at Koeberg to trip and to delay the start-up of the tripped Koeberg Unit 2 [29].
- The Droerivier-Muldersvlei 2; the tripping of 400kV transmission line in the Western Cape, which was caused by a fire under the line, and which resulted in a major voltage network dip. The voltage dip caused Koeberg Unit 2 to trip with the loss of 1230MW load [29].
- The Kendal Power Station Unit 6 based in Witbank, Mpumalanga tripped causing a major frequency dip and a subsequent under-frequency incident that caused Koeberg Unit 2 to trip. The following day, multiple flashovers occurred on the following sub-stations located in Muldersvlei, Acacia, Aurora, Droerivier and Bacchus, and the interconnecting transmission lines all tripped. This resulted in load shedding of about 1079MW [29].
- The Bacchus-Droerivier 400kV line trip, resulting in the islanding of the Western Cape. Once Koeberg Unit 2 islanded successfully, an attempt was made to re-synchronise to the network. The unit was unable to synchronise to the network, precipitating a Koeberg Unit 2 trip, which resulted in a major loss of load. In all cases, the network affected Koeberg plant and, consequently, the Eastern and Western Cape was adversely affected [29].

In all the aforementioned events, the Western Cape was adversely affected, which reiterates the point that the Western Cape grid is more susceptible to disturbances and has special requirements, in order to maintain the supply within the province. The Western and Eastern Cape grid is depicted in Figure 2.2 that follows:

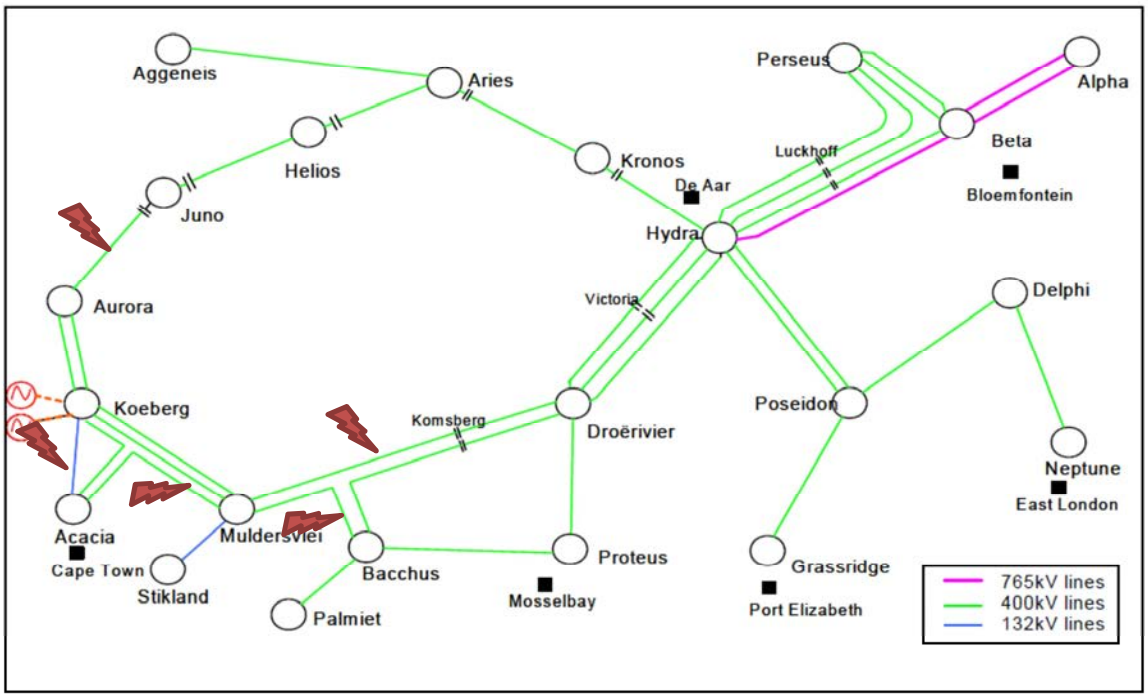

Figure 2.2 Transmission network for the Eastern and Western Cape [29]

The Western Cape grid is made of substations namely Koeberg, Juno, Kronos, Bacchus, Droerivier and ends at Hydra. The Eastern Cape grid includes substations called Poseidon, Delphi, Grassridge and Neptune. Figure 2.2 illustrates where the faults occurred, and, in most cases, the Koeberg nuclear power plant was affected. The incidents indicated above, highlighted the need to improve generating capacity on the Western Cape network. This was achieved by adding a 9 x 150 MW Open Cycle Gas Turbine (OCGTs) in Atlantis called Ankerlig and 5 x 150 MW OCGTs at Mossel Bay called Gourikwa [30]. This increase in generation and network improvements can be seen in Figure 2.3. The increase in generation was originally planned to be used during peak time; however, the network is nearing its maximum operation and these peaking stations are now required to operate more frequently [30]. This confirms that any increase in the networks spinning power aids the network power flows.

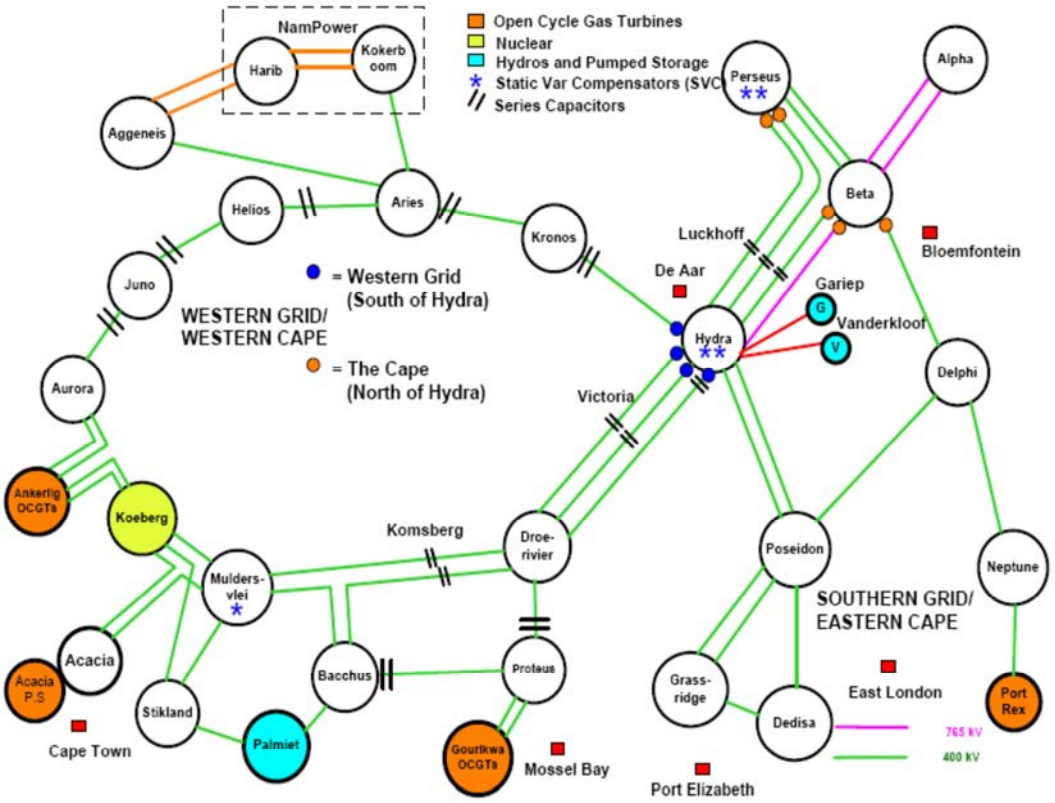

Figure 2.3 Transmission network improvements

2.4 Effect of grid disturbances on nuclear power generation

If the generator of a nuclear plant is subjected to transients and disconnects from the transmission system, the reactor control drop mechanism will insert control rods into the reactor. By inserting the rods, the rate of nuclear fission is reduced [16]. Steam flow needs to be reduced rapidly to prevent turbine over-speeding. Usually the generator disconnects from the network owing to the plant's protection system initiating. Excess steam flow is diverted to the condenser and residual heat is dissipated to the atmosphere, as the turbine no longer accepts steam as the main steam valves are closed [16]. Reactor core cooling is vital during this period and plant safety functions are critical in maintaining reactor core safety. Protection systems can operate for faults within the power station and operate for grid disturbances outside the nuclear power plant, to prevent damage. If a disturbance occurs outside the nuclear power plant and the grid protection system operate but the internal plant protection has not operated and the generator circuit breaker has not tripped, the power plant is said to have been "islanded" by reaching stability after the disconnection of the transmission system [16], [21]. That is, the nuclear power plant supplies only its own power from the generator output and the grid is disconnected.

By inserting the control rods into the reactor, by-products are created within the reactor, with important negative consequences; this process is called "reactor poisoning" [16]. One of the many and most important by-products of inserting the control rods is Xenon 135. Xenon 135 is a product of Uranium fission and has a

large neutron capture cross section. Its large cross-sectional area absorbs neutrons which reduces the reactor power. Eventually, reactor poisoning will lead to an extended shutdown period, possibly days [16]. For this reason, house loading or islanding is preferred for nuclear power plants when taking into account the time it takes to re-start the plant post trip. Here, the duration depends solely on the type of trip, when compared to fossil fuel plants that can start up almost immediately once the fault has been isolated and cleared.

Nuclear power plants (NPPs) rely on electrical power for operation of safety related pumps and valves, but without auxiliary supply the plant is unable to generate, as the auxiliary power feeds all the safety equipment used to produce safe nuclear power [21]. Without this auxiliary power, the nuclear reactor has no means of cooling the reactor, and it is unable to operate the control systems used to maintain acceptable reactor control.

An example of the above described phenomenon took place at the Forsmark Unit 1 Nuclear Power Plant, situated in Forsmark, Sweden, on 25 July 2006, that raised a number of issues related to the robustness of the electric power systems [21]. A grid disturbance (i.e., short-circuit) in the off-site switch yard, in combination with independent faults, resulted in a momentary over-voltage surge of ~120% on the on-site power supply systems, which resulted in failures of two of four redundant Uninterruptable Power Supply (UPS) units. Power was lost to all the safety components powered by these UPS units [20]. Although this incident is unrelated to transient stability, it can however give insight into grid disturbances that could cause failure in components within a Nuclear Power Generating context. Another contributory fact to the incident was that this system had been recently upgraded to a new system with new technology. This leads to the point of plant modifications for life extension with new technology, which could respond differently during grid disturbances.

Most nuclear power plants are nearing their end-of-life and require modifications to extend the life of the plant. Therefore, the technology chosen should be robust, tried and tested, ensuring that all scenarios are simulated to ensure that all electrical systems can withstand the changes, and that the modification does not have an adverse effect on the power grid [21].

In many countries the grid code rules requests that nuclear power plants should have the capability to switch over to house load operation (islanding) [21]. This will ensure continuity of supply to the auxiliary power for safety needs when a grid disturbance occurs, but it could also create on-site system problems, like voltage and frequency instabilities associated with such disturbances [21]. Hence, both aspects should be considered in the design of electrical systems. The Incident Reporting System (IRS) contains a number of events that are directly related to the disturbances in the plant's electrical systems. The IRS is operated jointly with the Organisational for Economic Co-Operation and Development (OECD)/Nuclear Energy Agency (NEA) to exchange information on unusual events at NPPs and to increase awareness of actual and potential safety

problems [21]. In 2006, a web-based IRS was created to allow quick reporting which subsequently increased the amount of reports of incidents [21].

In addition to the IRS, the World Association of Nuclear Operators (WANO) has established and operates a similar database of events that occurred at nuclear power plants operated within the WANO club, of which Koeberg Nuclear Power Station is an affiliated member [21]. In addition, WANO regularly publishes Significant Operating Experience Feedback Reports (SOER) in order to share valuable learning gained from the operating experience of colleagues in WANO [21]

When screening the IRS database, it was found that there were 88 grid disturbance events in 14 years [21]. It therefore appears that the disturbances in plant electrical systems are quite common events. The Licensee Event Reports (LERs) issued by NPPs in the USA are complementary to the IRS data base, and served as another important source of information about events that involved disturbance in the plant electrical systems [21]. Approximately 19 relevant reports that the plants reported to the United States Nuclear Regulatory Committee were also included to better illustrate the variety of events involved in grid or plant electrical system disturbances. The NPP's electrical grid connections allow various functions, namely, for the operation of the nuclear power station to export power and import power, and it also provides a source of electrical power to the power station auxiliaries to allow safe shutdown and post-trip cooling of the nuclear reactor [21].

Despite the fact that NPPs have on-site EDG's, the reliability and stability of the connected grid system has a significant effect on the reliability of post-trip cooling of the reactor core. [21]. Grid disturbances can result in a reactor trip with a subsequent loss of electrical supply to provide auxiliary power for essential safety system functioning. Hence, it is imperative that the design of nuclear power plants take these events into consideration, with the plant able to remain at power safely level for the complete range of grid related events and disturbances. A second requirement for the design is the safe shut down of the nuclear reactor when this occurs.

A modern aspect of power system stability is large signal disturbances which could result in loss of synchronism of any number of generators connected to the grid. Many studies have shown that automatic voltage regulation systems integral to large power plants are becoming increasingly important in solving the problem of stability. The performance and effectiveness of these systems to maintain terminal voltage within an acceptable range during disturbances and transients is critical to ensure overall stability of the network.

2.5 Generator's excitation systems

The basic function of an excitation system is to supply the direct current to the generator field winding, and it has added benefits as it performs a protective and controlling functions essential to maintain the performance of the power system by controlling the field voltage, which in turn controls the field current [11]. The

excitation system forms a major part of the energy production process. Primary energy in the form of coal, gas, water, wind, sun and nuclear (Uranium) is used to produce electricity. This form of energy is converted from mechanical energy to electrical energy, where the mechanical energy in the form of turbines drives the generator to produce electrical energy [31]. Synchronous machines are usually the preferred means of electrical conversion, which output voltage is maintained by an excitation system [31]. The complete process can be seen in Figure 2.4.

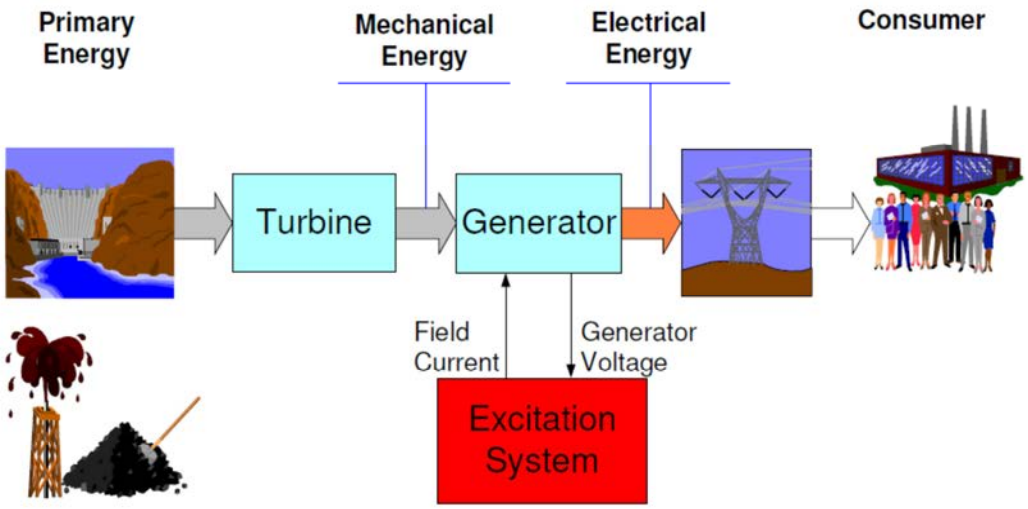

Figure 2.4 Excitation System in the chain of energy production [31]

2.5.1 Synchronous machine

Mathematical modelling of the synchronous machine has been investigated extensively in various literature [11], [14], [19] and therefore this aspect has not been included in this dissertation. However, in order to better understand the automatic regulation process of a synchronous machine, one needs to grasp the behaviour of the synchronous machine itself under all possible operating conditions. A regulated machine can be displayed in a simplified format in accordance with Figure 2.5.

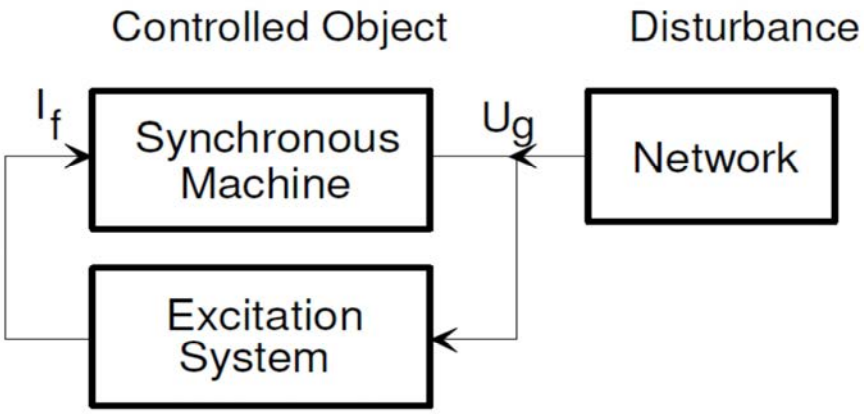

Figure 2.5 Regulating circuit diagram [31]

In the above Figure 2.5, I_f represents the field current and U_g represents the generator voltage. The synchronous machine is represented as the controlled object and all the other components form the regulator or excitation system. When the synchronous machine is coupled to the network, it has an effect on the closed loop regulating circuit, and it thus acts like an external interference variable [31].

The characteristics of the network and the synchronous machine are usually predetermined. The excitation is only able to correct the overall behaviour by means of optimisation techniques performed during commissioning [31]. This is achieved by adapting the corresponding regulating parameters. When one analyses the behaviour of synchronous machines, a distinction must be made between static, dynamic and transient behaviour. These behaviours are discussed below.

2.5.2 Static behaviour of a synchronous machine

The synchronous machine under static behaviour operates in three methods, namely [31]:

- no load operation where there is no load connected;
- machine operating in Island condition; and
- machine under load in parallel operation with the network.

The operating conditions related to no load conditions are the same for loaded conditions. The only difference between them would be that under no-load or island operation, the excitation predominately controls the voltage; while in network (loaded) operation the main source of control is reactive power which is controlled by the AVR and excitation [31].

2.5.3 Synchronous machines operating in no-load conditions

At no load operation, the terminal voltage of the generator is equal to the induced rotor voltage, while at constant rotational speed the terminal voltage depends entirely on the field current [31]. This having been stated, a linear relationship does exist between the field current and the generator terminal voltage as seen in Figure 2.6. When the generator voltage exceeds the nominal value, a saturation effect occurs, and, if the terminal voltage is required to be increased, the field current needs to be increased proportionally [31] .

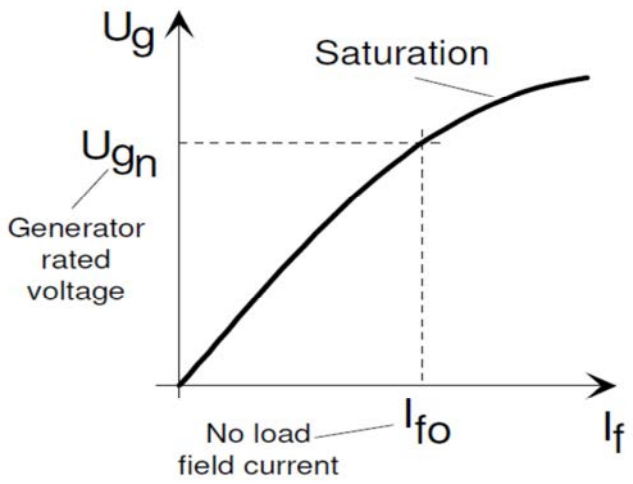

Figure 2.6 No-load characteristic [31]

2.5.4 Synchronous machine loaded

If the synchronous machine is loaded, a current is present in the stator windings, which creates a voltage drop, due to the synchronous reactance; and if the excitation current stays constant, the terminal voltage would be reduced [31]. This brings us back to the fundamental principle of an excitation system which has the function of increasing the terminal voltage by altering the excitation current.

Based on the aforementioned discussion, we are now able to develop a vector diagram based on the equivalent circuit diagram Figure 2.7. This vector diagram can be seen in Figure 2.8.

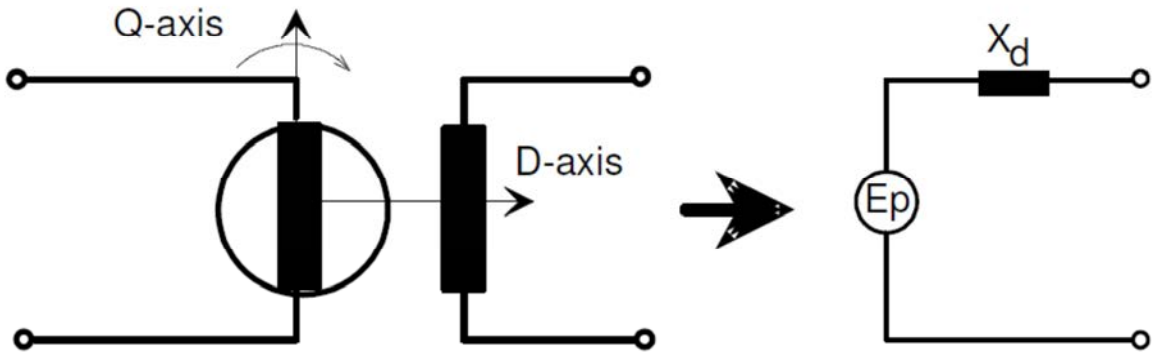

Figure 2.7 Equivalent-circuit diagram of the synchronous machine [31]

When referring to the Figure 2.7, assuming that the generator is lightly loaded with a purely resistive load, the generator current I_g is in phase with the generator voltage U_g. As a result of the synchronous reactance X_d, a voltage drop of $\Delta U = X_d.I_g$ is caused via the direct axis, which is perpendicular to the terminal voltage. This defines the magnitude and phase position of the induced rotor voltage E_p.

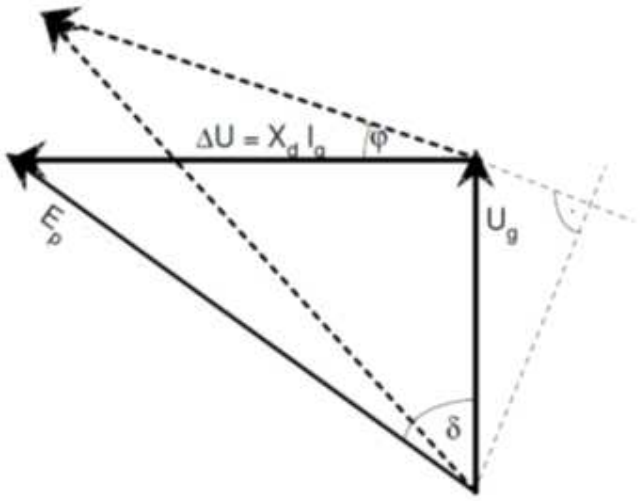

Figure 2.8 Vector diagram of the synchronous machine [31]

When referring to Figure 2.8 above, if the nature of the load is changed to a resistive-reactive circuit with the same magnitude as the resistive load discussed above, the magnitude of the current remains the same, but it lags the voltage by the phase angle φ [31]. In order to maintain the generator output voltage, a higher induced rotor voltage is required and this in turn produces a higher excitation current. The angle δ between the terminal voltage and induced rotor voltage describes the angular position of the rotor relative to the rotating field and the difference between the two is known as the load angle [31].

As illustrated in Figure 2.9 that follows, in order to better understand the dynamic between the synchronising torque and the load angle, a two-pole machine is used to illustrate this behaviour. An assumption is made that the rotating rotor field is in the same direction as the rotating stator field. Therefore, at rotor angle δ =0, the transmitted torque is equal to zero. When the load angle δ=45°, the mechanically driven rotor now pulls the stator field along by means of magnetic force. In stationary operation the mechanical drive is equal to the electrical torque. At load angle δ=90°, the electrical torque will reach its maximum. This however is impractical, as this operating point causes the machine to be unstable. At this point the rotor begins to slip in relation to the stator field which causes the generator to become asynchronous and "fall out of step" [31].

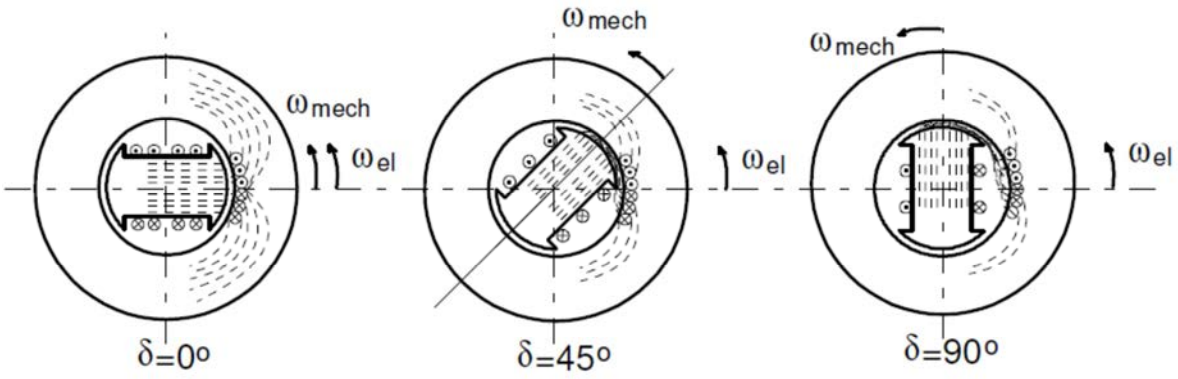

Figure 2.9 Synchronising torque and load angle [31]

The complete static operating conditions can be described in terms of a power diagram, and this is relatively easy when referring to the vector diagram found in Figure 2.8. To obtain the power diagram, the vector needs to be multiplied by a vector U_g/X_d, which converts the voltage vectors into power vectors [31]. From this, one is able to derive the power diagram that follows.

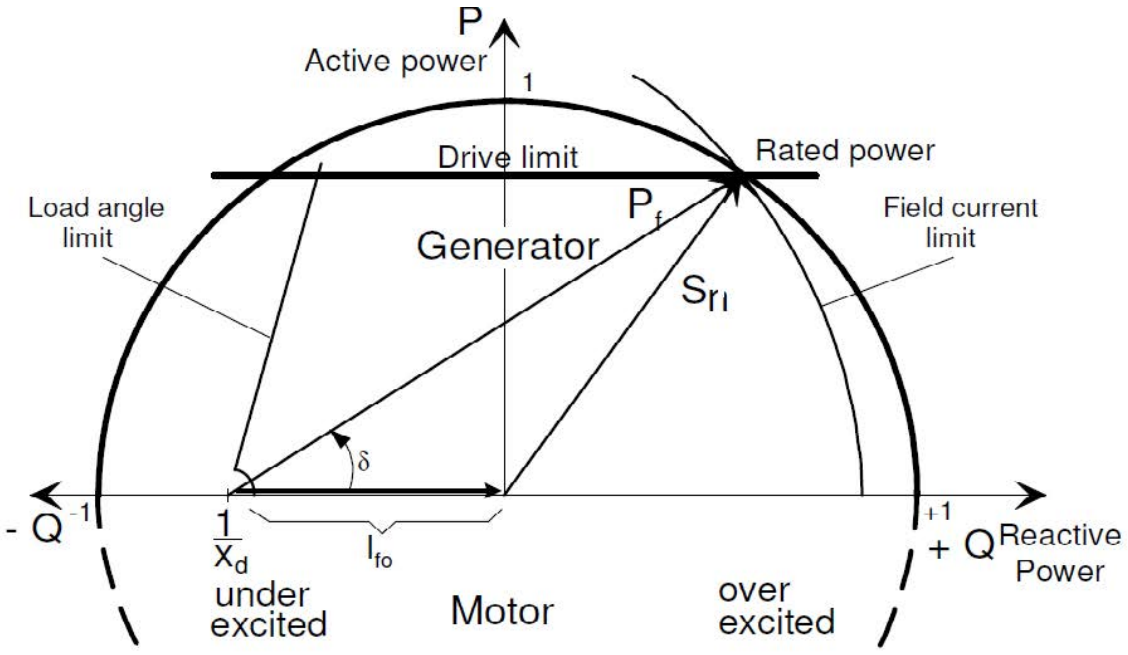

Figure 2.10 Power diagram of a synchronous machine [31]

When referring to Figure 2.10, usually the top half of the circle represents the generator operation, and the bottom half of the circle represents motor operation [31]. The circle around the co-ordinate centre point has a radius which corresponds to the nominal apparent power S_n. Here, the nominal apparent power is defined as the maximum permissible temperature rise of the stator winding, while the maximum generator operating

active power range is limited to the mechanical drive limit of the turbine. The reactive power limit is limited to the thermal design of the rotor winding (over-excited) and the stability limit (under-excited range). Here, the over-excited range limit is governed by the nominal excitation current. However, the main consideration when operating in the under-excited range is to maintain synchronism. The load angle δ for any working point can be read from the diagram between the reactive power axis and indicator for the excitation power P_f.

2.5.5 Dynamic behaviour of a synchronous machine

The dynamic responses of synchronous machines in operational conditions are very complex. Therefore, the behaviour of the machine during disturbances must be greatly simplified.
Typical changes that could be considered are as follows [31]:

- changes in the network voltage, frequency and load
- changes in torque from the prime mover; and
- faults due to load rejection and short-circuits which trigger excitation.

There are two main distinctions in physical variables, namely [31]:

- the electrical variables, which include voltage, reactive power and field current; and
- the mechanical variables such as rotational speed or frequency, active power torque and load angle.

An example would however best explain the aforementioned physical variable phenomenon. Here, once an idling generator has a load connected to it, the effect is dependent on whether there is a change in reactive power or active power. If an asynchronous motor is started and the active power is neglected initially, only the reactive power is influenced, and therefore the load angle δ will remain at 0. However, if the same process was followed for an active power load, the load angle δ is dependent on the active power. Under normal running conditions, the mechanical drive power of the turbine is equal to the electrical active power, ignoring losses. If the generator is then loaded with an additional active power load, the electrical power of the generator is immediately increased. However, the drive power of the turbine remains unchanged initially, and the balance which existed before between electrical power and mechanical drive power no longer exists. This electrical power increase is due to the kinetic energy of the rotating masses coupled to the shaft [31]. This means that the rotational speed is decreased until the rotational speed regulation circuit increases the shaft torque by adjusting steam, gas or water passing through the turbine [31].

For an unloaded generator, terminal voltage is equal to the induced rotor voltage [31]. After a load is added, a reactive current starts to flow immediately, causing a voltage drop through the generator reactance [31]. The original magnetic flux cannot change immediately from the stator to the rotor. The consequence would be that a reverse current is induced in the rotor circuit via the air gap, in order to compensate for the changes on the stator side and to maintain a balance. For the simplified circuit diagram in Figure 2.8, the direct axis

reactance X_d is replaced by transient reactance X_d', which is much smaller than the synchronous reactance [31].

2.5.6 Transient behaviour of the generator and network

When analysing transient behaviour, a distinction should be made between load changes and load dumping. A load change can typically go down to zero, but the generator circuit breaker usually stays closed [31]. However, for a load dump the generator circuit breaker is usually tripped, which disconnects the generator from operating in parallel mode to island mode [31].

A generator short-circuit is characterised by the electrical distance between the generator terminals and the location of the short-circuit [31]. On both sides of the generator and the network, a reactance limits the short-circuit current, and the most serious loading of the generator is caused by a terminal short-circuit [31]. A short-circuit near the power station usually leads to load dumping, which had to be triggered by protective devices. During load dumping, immediate reaction from the automatic voltage regulator is required. The way the generator changes voltage in time following the opening of a circuit breaker is an important quality characteristic of a voltage regulator or excitation system [31]. The short-circuit prevents the generator from exporting power, causing a rapid speed-up of the turbine. This rapid speed-up causes the load angle to increase rapidly against the rest of the network. It is important for the fault to be cleared before the out of synchronism condition becomes too large to recover from.

2.6 Pole slip or loss of synchronism protection

Generators connected in a power system usually remain in synchronism with one another. When severe faults occur which cause large loads to be disconnected from the network, the result is oscillations in the rotor angles of the generators [32]. These oscillations, if large enough, can cause the generators to pole slip and be disconnected from the network. When pole slipping occurs, the system and generator voltages slip past each other causing large pulsating current which, if analysed, could be much greater than a three-phase fault at the generator terminals [32]. It is imperative that the faulted generator be isolated from the network to prevent damage to the turbine, generator transformer and the generator itself. The effects of pole slipping will be explained below.

2.6.1 Damaging effects of a pole slip

During pole slip conditions, when the electrical centre moves from the network into the generator, large currents cause mechanical and thermal stress on the generator and generator transformer with each pole slip [32]. When calculating pole slip settings, the transient reactance (X_d') is generally used to represent the generator impedance. However, in some cases, when the generator transformer and system impedance are low, the current could exceed the sub-transient fault current at the generator terminals [33], [34]. During pole

slip conditions, a rotational speed difference exists between the rotor and the system. This speed difference between the rotor and the network induces currents into the rotor similar to when the stator currents are unbalanced. If the rotor is subjected to these currents for a long period, thermal damage to the rotor teeth, wedges, damper windings and rotor body could occur [32].

During each slip cycle, the turbine generator shaft is subjected to severe torque transients. The maximum stress is at the initial period of the pulsation, and this is usually when shaft damage occurs [32]. Each turbine generator shaft has a fatigue life. This can be greatly reduced after a few pole slip events. These severe stresses require protective devices to operate quickly to remove the electrical and mechanical transients [35], [36].

When we have a rotational difference between the rotor and the network, the diodes on the excitation system are exposed to high voltage, as they block reverse rotor currents. This overvoltage condition stresses the insulation of the diodes, and could result in insulation breakdown [34].

A loss of synchronism of one or more units causes fluctuations in the network frequency, affecting customer loads like induction and synchronous motors. The voltage fluctuations could cause auxiliary control equipment like contactors to drop out, removing supply to equipment and affecting productivity. This scenario of changing voltages could have a severe impact on nuclear power plants, as one of its main protection functions is to protect the reactor coolant pumps from under-voltage conditions [32]. Therefore, the network needs to be maintained at above 70% of the nominal voltage to ensure that the generator does not trip on an under-voltage condition due to low voltage on the reactor primary coolant pump [30].

2.6.2 Pole slip protection applications

Pole slip protection can be provided by various methods. The choice of method is usually dependent on the likelihood of a pole slip occurring and the significances should it occur. These methods are discussed below.

- **Pole slip protection using reverse power measuring element**

Pole slipping events have a period when active power flows in the reverse direction. Most generators are equipped with reverse power protection and this could be used to detect pole slipping, thus performing a dual protection function [32]. One major downside to this type of protection could be that it might reset during the forward pulsating power cycle. This could be overcome if the relay picks up and time delay is set short or the delay drop-off time is set suitably to prevent resetting of the relay.
The main drawback of this type of protection is the long time it takes to operate, coupled to the inability to control the load angle at which the command would be given to trip the generator circuit breaker.

- **Pole slip protection using an under-impedance element**

A loss of excitation under-impedance protection device could be employed to perform pole slip protection when the electrical centre of the power system sits "behind" the relaying point. It requires the drop-off timer of the larger diameter impedance to be set to prevent its reset during each pole slip cycle, until the trip time has expired. This type of protection might not be suitable for large machines where speedy operation is required during the first slip cycle and where the system control angle needs to initiate a breaker trip command.

With the additional impedance of the generator, transformer units may cause the system impedance to fall out of the under-impedance characteristic which is required for the loss of excitation. This protection thus becomes very dependent on the application.

- **Dedicated pole slip protection**

Dedicated pole slip protection is employed when large generator transformer units are coupled to the network. This type of protection allows for quick detection and disconnection using system angle tripping to open the breaker. It has characteristically or historically been based on ohm type impedance measurement characteristics.

- **Pole slipping protection by impedance measurement**

A change in impedance during pole slipping could be detected by an ohm type element characteristic. In some applications, a straight line ohm characteristic is more suitable. The protection principle is that two impedance zones are defined, and it detects the passing of the generator impedance through the characterised zone, as shown in Figure 2.11. The characteristic is defined into three zones A, B, and C. Zone A is the generator’s normal operating zone. When a disturbance occurs, the impedance moves through zones B and C, and tripping occurs when the impedance characteristic enters zone C [37].

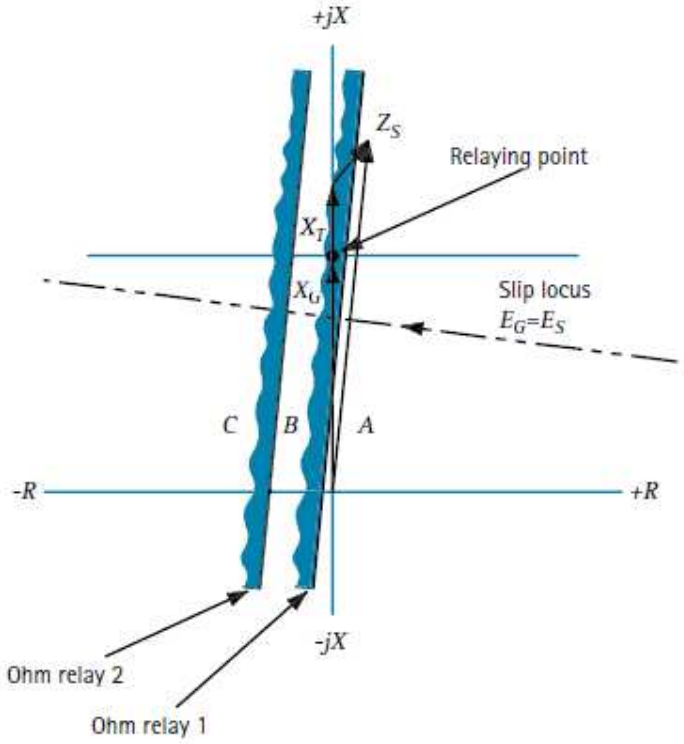

Figure 2.11 Pole slipping detection by ohm relays [37]

Tripping only occurs when all zones A-B-C are crossed consecutively. Network or power system faults should not cause tripping and should be cleared before the impedance reaches zone C. Enhancement in the security of the protection system is done by including a basic under-impedance control element (circle about the origin of the impedance diagram) that is set to prevent tripping for impedance trajectories for distant power system faults. The ohm elements should be set parallel to the total system impedance vector, and enclose it, as shown in the Figure 2.11 [37].

- **Lenticular characteristic to detect pole slip**

If a more sophisticated impedance protection system is required to measure the impedance of the generator, a lenticular impedance characteristic can be used to determine if pole slipping is taking place [37]. The lenticular characteristic can be seen in Figure 2.12. The lenticular characteristic is divided into two halves by a straight line, called the blinder.

The inclination, θ of the blinder and lens is determined by the angle of the total impedance of the system. The system and generator-transformer impedance determines the forward reach of lens Z_A and the transient reactance of the generator determines the reverse reach Z_B [37].

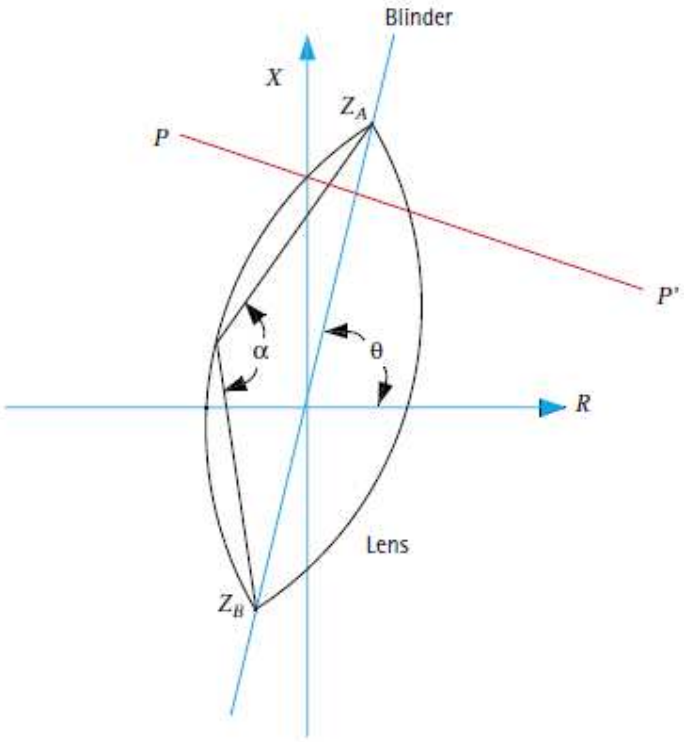

Figure 2.12 Pole-slip protection using lenticular characteristic and blinder [37]

The width of the lens is determined by the angle α. The line of PP', perpendicular to the axis of the lens determines the centre of the impedance swing and is located in the generator or the power system during a transient.

When one analyses a generator, the characteristic can be divided into four zones and two regions as seen in Figure 2.13 that follows. Normal operation occurs when the measured impedance is in zone R1. If pole slipping occurs, the impedance locus will move through zones R2, R3 and R4. When the impedance locus reaches zone R4, a trip signal is issued, provided that the impedance lies below the reactance line PP'. The locus of the swing lies within, or close to, the generator, which means that the generator is pole slipping with respect to the rest of the system.

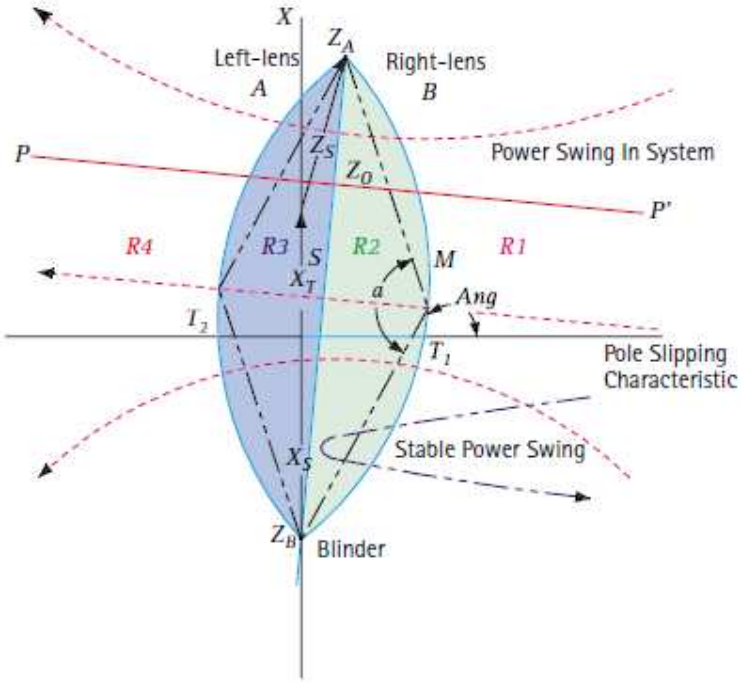

Figure 2.13 Definition of zones for lenticular characteristic [37]

If the impedance locus lies above the line PP', the fault is said to be further away from the generator and therefore the swing is far out of the generator. The generator is thus swinging against the rest of the network. Tripping may still occur if the swing is prolonged, which could initiate a complete network failure. Further checks are introduced by requiring that the impedance locus spends a minimum time within each zone for pole slipping to be valid. The trip signal may be delayed for a number of slips before it initiates, which provides validation of the pole slip condition and then allows for enough time for other relays to clear the fault if the fault lies somewhere in the power system. Tripping is blocked if the impedance swing is in a different sequence [37].

2.7 Nuclear plant protection philosophy

Tripping principles are determined by four factors. These are, in order of importance:

- the safety of personnel;
- the safety of the reactor;
- the safety of other plant; and
- plant availability.

The supply to the reactor auxiliaries is essential for reactor safety. Normally, the supply for the auxiliaries (normal and emergency) of the reactor, turbine, etc., will be from the generator via a unit auxiliary transformer. If this becomes unavailable, then the supply for the auxiliaries (normal and emergency) will be

from an alternative secure system. If the alternative supply becomes unavailable, then the supply for the emergency auxiliaries only will be from diesel generators. The generator protection shall select, according to the type of fault, a suitable combination of the following tripping functions:

A. generator circuit-breaker trip;
B. HV circuit-breaker trip;
C. field suppression;
D. unit board 1 incoming circuit-breaker trip (unit transformer 1, LV circuit-breaker);
E. unit board 2 incoming circuit-breaker trip (unit transformer 2, LV circuit-breaker);
F. Emergency Steam Valves (ESV) close (turbine trip);
G. transformer cooling (pumps and fans);
H. generator stator coolant; and
I. bus strip.

Firstly, the tripping sequences will be arranged to safeguard personnel, the reactor, the turbine, and the generating equipment. Secondly, the tripping sequences will ensure maximum plant availability without comprising safety, following the general principles indicated below:

- Faults in the generator (upstream of the generator circuit-breaker) require only the generator isolation and a turbine shutdown. The supply to the unit boards will be maintained from the HV system. (Tripping functions: A, C, F and H.)
- Faults between the generator circuit-breaker, the HV circuit-breaker and the unit board circuit-breakers require a unit shutdown. (Tripping functions: A, B, C, D, F and G.)
- Faults in the HV system that affect the machine only require the HV circuit-breaker to be opened, leaving the unit in a "house load" condition. (Tripping functions: B.)
- Faults that may be in the generating unit or in the HV system are initially assumed to be in the HV system and the HV circuit-breaker is opened. The unit is left in an islanded condition, and, if the fault persists after a further time delay, a unit shutdown is initiated. (Tripping functions: B, and if necessary A, B, C, D, E, F and in some cases G.)
- Faults that may be in one of the unit transformers or in its corresponding unit board system are initially assumed to be in the unit board system, and the respective incoming circuit breaker is opened. If the fault persists after a specific time delay, a unit shut-down is initiated. (The loss of one unit board requires a load reduction of the machine). (Tripping functions: D or E and if necessary A, B, C, D, E, F and G.)
- The following conditions (a)-(e) below require closing of the Emergency Steam Valves (ESV) (turbine shutdown), followed by tripping of the generator circuit-breaker when the machine is unloaded. This is referred to as a soft shutdown. (Tripping functions: A, B, C, D, E, F, G and H.):
    a. mechanical faults in the turbine or reactor;
    b. abnormal conditions that do not require immediate isolation of equipment;

c. operator shutdown;
d. tripping functions: F; and
e. a reverse power relay is used to detect when the power < 0 and then to operate A and C.

- If the generator breaker fails to open when required, the unit is shut down. (Tripping functions: A, B, C, D, E and F.)
- If the HV breaker fails to open when required, the adjacent HV breakers are tripped. (Tripping function: I.) Faults that may be in one of the unit transformers or in its corresponding unit board system, are initially assumed to be in the unit board system, and the respective incoming circuit breaker is opened. If the fault persists after a specific time delay, a unit shut-down is initiated.

2.7 Excitation system effect on transient stability

A typical excitation system comprises of two main elements, namely, the exciter and the voltage regulator [38]. Under normal conditions, the voltage in the power system is kept constant, but during transients the machine terminal voltage at the faulted end can be reduced to zero depending on the type of fault [38]. This makes power transfer difficult, as there is not sufficient synchronising power. This however gives us the confidence that a fast-acting excitation system will try to excite the machine more to keep the machine's terminal voltage high as long as possible. This allows for prolonged power transfer between the network and the affected machine and allows for faults to be cleared and stability to be maintained.

As discussed earlier, transient stability studies allow the system operator to prevent machines from losing synchronism with the rest of the network. In this dissertation, it is assumed that the mechanical power of the prime movers is constant. Here, the period of interest when discussing transient stability is usually short, during the first swing and usually completed in the first few seconds, depending on whether the AVR is installed.

Therefore, the effect the excitation system in maintaining the generator's terminal voltage has a major impact on the generators stability, mainly due to the excitation systems response during the first swing. Depending on the exciter and time response, it can have a major impact on the overall performance of the generator during transients.

3. Modelling

If one considers that modelling and analysis are required of all power stations, then the parameters used in modelling are equally important. The modelling of parameters or derivation of these fundamental equations like the swing equation, load flow calculations and equal area calculation, form the basis of all studies and require an in-depth knowledge or understanding. The various modelling and equations are discussed in this chapter.

3.1 Modelling for transient stability studies

To achieve synchronism in a power system with interconnected synchronous machines, the stator voltage and current of all the machines must have the same frequency [11]. Also, the rotor mechanical speed of each of the machines must be synchronised to this frequency. This stability also depends on the ability of the machines to maintain equilibrium between the electromagnetic torque and the mechanical torque [39]. The movement of the rotor is governed by Newton's second law of motion, given in equation (3.2) [22], [12].

Under equilibrium conditions, the relationship between the exchange of power and the rotor angles of interconnected synchronous machines in a power system is called the power versus angle relationship [11]. To illustrate this non-linear relationship, a power system with one motor connected to a generator is considered in Figure 3.1.

In Figure 3.1, the power transferred from the generator to the motor is a function of the rotor angular separation (δ) between the generator and the motor. This separation is caused by three factors, namely the generator internal angle (δ_G), the angular difference between the terminal voltages of the generator and the motor, and the internal angle of the motor (δ_M). For steady state analysis, the synchronous reactance is used with the assumption that the internal voltage is equal to the excitation voltage [11].

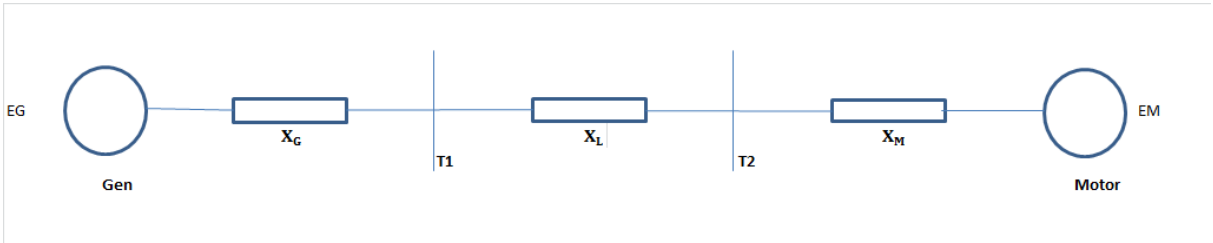

Figure 3.1 Two machine Model of the power system [12]

The power transferred from the generator to the motor is expressed by equation (3.1)

$$P=\frac{E_G E_M}{X_T}\sin\delta \qquad (3.1)$$

where:

$X_T = X_G + X_L + X_M$

- E_G: generator internal voltage
- E_M: motor internal voltage
- $\delta = \delta_G - \delta_M$
- X_T is the total reactance, X_G is the reactance of the generator, X_L is the transmission line inductive reactance and X_M is the reactance of the motor.
- δ_G is the generator internal angle (angle by which the generator rotor angle leads the stator angle)
- δ_M is the motor internal angle (angle by which the motor rotor angle leads the stator angle)

The phasor diagram showing the relationship between the generator and the motor voltages is given in Figure 3.2.

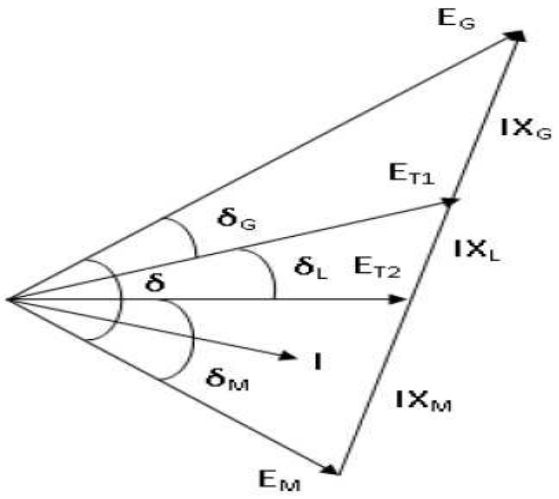

Figure 3.2 Phasor diagram of generator and motor voltages [12]

- E_{T_1} is the voltage at terminal at bus $T1$ and E_{T_2} is the voltage at terminal at bus $T2$
- δ_L is the angular separation between voltage at E_{T_1} and E_{T_2}
- I is the current.

The corresponding power-angle relationship is shown in Figure 3.3. The representation in Figure 3.3 is that of an idealised model. The power transfer varies as the sine of the angle. When the effects of controllers such as Automatic Voltage Regulators (AVRs) and Power System Stabilizers (PSS) are taken into account, the shape of the curve in Figure 3.3 will vary slightly.

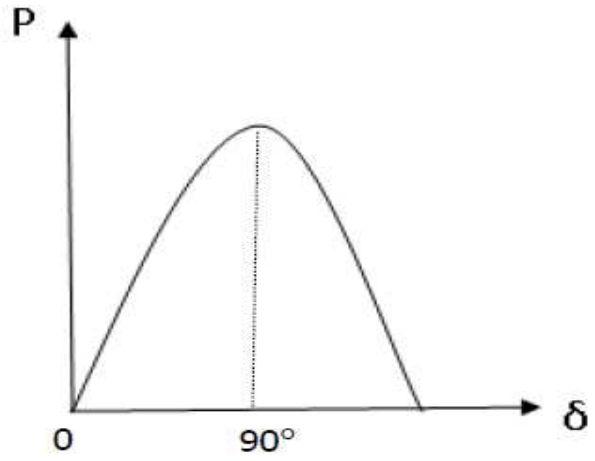

Figure 3.3 Power-angle curve [12]

In Figure 3.3, when the angle is zero, there is no power transferred. As the angle increases from zero to 90°, the amount of power transferred reaches its maximum. Any further increase of the angle will lead to a decrease in the amount of power transmitted. Similarly, in a multi-machine power system, the relative rotor angular displacement affects the interchange of power as well as the complex relationship between the load distribution and the power generation [11].

3.1.1 The swing equations

The critical equations in power system stability analysis are the rotational inertia equations describing the effect of imbalance between the electromagnetic torque and the mechanical torque of machines, if one considers a prime mover and its phase synchronous generator.

- Generator is running at synchronous speed and is developing electrical torque T_e
- Prime mover is producing mechanical torque or driving torque T_m

Then under steady state conditions T_m=T_e

However, following a disturbance an acceleration or deceleration torque T_a will be induced on the rotor. This torque can be expressed as*:*

T_a=T_m -T_e

The rotor motion is determined by Newton's second law, given by:

$$J\alpha_m = J\frac{d\omega_m}{dt} = J\frac{d^2\theta_m}{dt^2} = T_m - T_e = T_a \quad (3.2)$$

where:

J = total movement of inertia of the rotating masses, kgm^2

$\propto_m$= rotor angular acceleration, rad/s^2

ω_m= rotor angular velocity, *rad/s*

θ_m= rotor angle position with respect to a stationary reference axis on the stator, *rad*

t = time, *sec.*

In a steady state T_a = 0, resulting in a constant rotor angular velocity called synchronous speed. When the mechanical torque exceeds the electrical torque, the acceleration torque is greater than zero, which increases the rotor speed. Conversely, if the electrical torque exceeds the mechanical torque the acceleration torque is less than zero causing the rotor to decrease in speed.

It is convenient to measure rotor angular position with respect to a synchronously rotating reference axis instead of a stationary axis. Accordingly we define:

$$\theta_m = \omega_{0m} t + \delta_m \tag{3.3}$$

Where:

ω_{0m} = synchronous angular velocity of the rotor, *rad/s.*

δ_m = mechanical torque angular position with respect to the synchronously rotating reference, *rad.*

Derivative of equation (3.3) gives the rotor angular velocity, expressed in the form:

$$\omega_m = \frac{d\theta_m}{dt} = \omega_{0m} + \frac{d\delta_m}{dt} \tag{3.4}$$

The rotor acceleration is $\frac{d^2\theta_m}{dt^2} = \frac{d^2\delta_m}{dt^2}$.

Substituting the above equation into equation (3.2), we have:

$$J\frac{d^2\theta_m}{dt^2} = J\frac{d^2\delta_m}{dt^2} = T_m - T_e = T_a \tag{3.5}$$

For simplicity of calculations it makes sense to calculate in power rather than torque, and to work in per-unit rather than work with the actual units. The equation in (3.5) can be reduced to equation (3.6) by multiplying equation (3.5) by $\omega_m$and divide by S_B.

$$\frac{J\omega_m}{S_B}\frac{d^2\delta_m}{dt^2} = P_m - P_e = P_a \tag{3.6}$$

It is convenient to work with a normalized inertia constant called *H* constant rather than the moment of inertia *J*. An inertia constant *H* is defined as the stored kinetic electrical energy divided by the generator volt-

ampere (VA) rating. This constant quantifies the electrical energy of the rotor at rated speed (synchronous speed) in terms of seconds that it would take to provide an equivalent amount of electrical energy when operating at power output levels equal to its VA rating. An advantage of using *H* is that it has a very narrow range, which makes computing easy when compared to Joules (*J*)

$$H = \frac{1}{2}\frac{J{\omega^2}_{0m}}{S_B}\ (seconds) \qquad (3.7-a)$$

$$\text{Or } 2H = M = \frac{J{\omega^2 0}_m}{S_B} \qquad (3.7-b)$$

From (3.7-a), solving for *J* we have:

$$J = \frac{2HS_B}{{\omega^2}_{0m}}$$

Replacing *J* in the equation (3.6) we have

$$2H\frac{\omega_m}{{\omega^2}_{0m}}\frac{d^2\delta_m}{dt^2} = P_{m^*} - P_{e^*} = P_{a^*} \qquad (3.8)$$

Defining per-unit rotor angular velocity as

$$\omega_{m^*} = \frac{\omega_m}{\omega_{0m}} \qquad (3.9)$$

Equation (3.8) becomes

$$\frac{2H}{\omega_{0m}}\omega_{m^*}\frac{d^2\delta_m}{dt^2} = P_{m^*} - P_{e^*} = P_{a^*} \qquad (3.10)$$

We can now write the swing equation (3.10) in terms of electrical radian frequency ω and electrical power angle δ.

If P is the number of poles of a synchronous generator, the relationship between mechanical and electrical quantities are expressed in the following forms:

$$\alpha = \frac{P}{2}\alpha_m \qquad (3.11)$$

$$\omega = \frac{P}{2}\omega_m\ , \omega_0 = \frac{P}{2}\omega_{0m} \qquad (3.12)$$

$$\delta = \frac{P}{2}\,\delta_m \tag{3.13}$$

The swing equation in terms of electrical quantities is given by:

$$\frac{2H}{\omega_0}\,\omega_*\,\frac{d^2\delta}{dt^2} = P_{m^*} - P_{e^*} = P_{a^*} \tag{3.14}$$

In practice $\omega \approx 1$ and can be ignored in equation (3.14) to give:

$$\frac{2H}{\omega_0}\,\frac{d^2\delta}{dt^2} = P_{m^*} - P_{e^*} = P_{a^*} \tag{3.15}$$

This equation is called the per-unit swing equation. It is the non-linear equation which determines the rotor dynamics in transient stability studies.

If δ is the angular position of the rotor in electrical radians with respect to a synchronously rotating reference and $\delta_0$is its value at t=0,

$$\delta = \omega t - \omega_0 t + \delta_0 \tag{3.16}$$

Taking the derivative with respect to time we have:

$$\frac{d\delta}{dt} = \omega - \omega_0 = \Delta\,\omega \tag{3.17}$$

Since equation (3.15) is a second order differential equation, it can be written as two first order differential equations as follows:

$$\frac{d\delta}{dt} = \omega - \omega_0 \tag{3.18}$$

$$\frac{2H}{\omega_0}\,\frac{d\omega}{dt} = P_{m^*} - P_{e^*} = P_{a^*} \tag{3.19}$$

3.1.2 Equal area criterion

Simpler and quicker calculations can give one insight into the network for verification of critical clearing times. One simple method that can be used is the equal area criterion. This can only be done by reducing the network to a simple infinite bus and single generator network. It allows for quick computation to assess stability without the need for expensive computer-based software. Its simplicity allows network reduction with fairly quick assessments.

From the swing equation it can be seen that there is a relationship between the rotor angle and the accelerating power, which is expressed as follows (From now on, it is assumed that P_m and P_e are expressed in per unit, and therefore the symbol "*"will be dropped.):

$$\frac{d^2\delta}{dt^2} = \frac{\omega_0}{2H}\,(P_m - P_e) \tag{3.21}$$

P_e is a non-linear function of δ, and therefore the equation cannot be solved directly. If both sides are multiplied by 2dδ/dt then:

$$2\frac{d\delta}{dt}\,\frac{d^2\delta}{dt^2} = \frac{\omega_0\,(P_m - P_e)}{H}\,\frac{d\delta}{dt}$$

Or

$$\frac{d}{dt}\left[\frac{d\delta}{dt}\right]^2 = \frac{\omega_0\,(P_m - P_e)}{H}\,\frac{d\delta}{dt} \tag{3.22}$$

Integrating gives

$$\left[\frac{d\delta}{dt}\right]^2 = \int \frac{\omega_0\,(P_m - P_e)}{H}\,d\delta \tag{3.23}$$

Initially the speed deviation dδ/dt is zero. It changes as a result of a disturbance. For stable operation, the deviation of angle δ must be bounded, reaching a maximum value and then changing direction. This leads to the conclusion that the speed variation dδ/dt becomes zero at some point. Therefore, equation (3.22) as a criterion of stability can be written as

$$\int_{\delta_o}^{\delta_m} \frac{\omega_0}{H}(\,P_m - P_e\,)d\delta = 0 \tag{3.24}$$

Where, δ_0 is the initial rotor angle and δ_m is the maximum rotor angle, as illustrated in Figure 3.4. Thus, the area under the function P_m-P_e plotted against δ must be zero if the system is stable. This statement is true when area A_1 is equal to area A_2. Kinetic energy is gained by the rotor during acceleration when δ changes from δ_0 to δ_1. The energy gained is expressed as follows:

$$E_1 = \int_{\delta_o}^{\delta_1} \frac{\omega_0}{H}(\,P_m - P_e\,)d\delta = area\ A_1 \tag{3.25}$$

Energy lost during deceleration when δ changes from δ_1 to δ_m.is expressed as follows:

$$E_2 = \int_{\delta_1}^{\delta_m} \frac{\omega_0}{H} (P_m - P_e) d\delta = area\ A_2 \quad (3.26)$$

As we have not considered any losses, the energy gained equals the energy lost and therefore the area A_1 equal to the area A_2. This forms the basis of the equal area criterion concept.

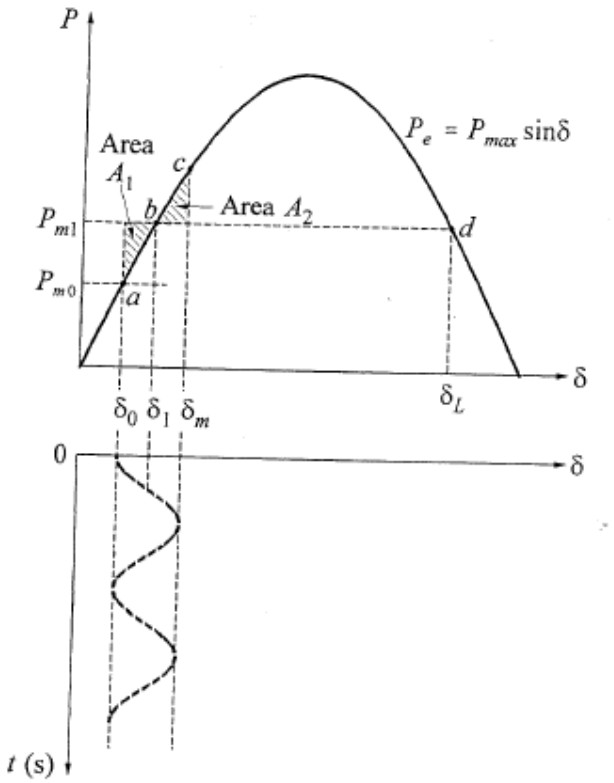

Figure 3.4 Power angle curves in relation to rotor angle time response [11]

When analysing the equal area criterion graphically in Figure 3.4, a step-by-step approach is used to better explain the phenomenon [40]:

- at steady state $P_{m0} = P_{e0}$ point a;
- a sudden change in mechanical power from P_{mo} to P_{m1} occurs from point a to point c; and
- δ increases from δ_0 to δ_1.and later to δ_m.(maximum angle value).

As the operating point moves from δ_0 to δ_1.and later to δ_m two areas are created [11]:

- Area A_1, known as the accelerating area (excess stored energy in the rotor), as the mechanical power is greater than the electrical power.
- Area A_2, known as the decelerating area (energy removed from the rotor), as the electrical power is greater than mechanical power.

The equal area criterion states that, for a system to be stable, the acceleration area should be at least equal to the deceleration area. That means that A_1=A_2. For stability to be maintained, the critical clearing time must

be calculated. The critical clearing time, denoted t_{cr}, is defined as being the longest fault duration before the generator falls out of step with the rest of the network.

If it is assumed that the electrical power P_e in equation (3.15) drop to zero during a fault, one could calculate the critical clearing angle δ_{cr} from equations (3.25) and (3.26). Then the critical clearing time t_{cr}, is obtained by integrating equation (3.15) twice with initial condition $\delta(0) = \delta_0$ and $\frac{d\delta(0)}{dt} = 0$.

$$\frac{d\delta(t)}{dt} = \frac{\omega_{0\,P_m}}{2H}t + 0 \tag{3.27}$$

$$\delta(t) = \frac{\omega_{0\,P_m}}{4H}t^2 + \delta_0 \tag{3.28}$$

To determine the critical clearing time $t_{cr,}$ $\delta(t)$ in equation (3.29-a) is replaced with δ_{cr} so as to obtain equation (3.29-b).

$$t = \sqrt{\frac{4H}{\omega_{0\,P_m}}(\delta(t) - \delta_0)\}} \tag{3.29-a}$$

$$t_{cr} = \sqrt{\frac{4H}{\omega_{0\,P_m}}(\delta cr - \delta_0)} \tag{3.29-b}$$

3.2 Numerical integration methods

Although the equal area approach is used as a quick assessment, it has a few shortcomings. The critical clearing time remains unknown if the output power is not zero during the fault. Also, it cannot be used for multi-machine stability studies and therefore more complex techniques should be applied.

It becomes apparent that numerical integration techniques are needed to solve the swing equations. One such method is known as the Euler method, which is the simplest of the numerical integration techniques and will be discussed below.

3.1.2 Euler method

Consider a first-order non-linear differential equation.

$$\frac{dx}{dt} = f(x, t) \tag{3.30}$$

Where, x is the state vector of n dependant variables and t is the independent variable (time).

The main objective is to solve for x as a function of t, with the initial values of $x = x_0$ and $t = t_0$ respectively. Figure 3.5 illustrates the principle of applying the Euler method. The integration step size is denoted as Δt. At $x = x_{0,}$ $t = t_{0,}$ we can approximate the curve representing the true solution by its tangent having a slope.

$$\left.\frac{dx}{dt}\right|_{x=x_0} = f(x_{0,}t_0) \tag{3.31}$$

Therefore, the increment Δx is expressed as follows:

$$\left.\frac{dx}{dt}\right|_{x=x_0} . \Delta t = \Delta x \tag{3.32}$$

The value of x at $t = t_1 = t_0 + \Delta t$ is given by

$$x_0 + \left.\frac{dx}{dt}\right|_{x=x_0} . \Delta t = x_0 + \Delta x = x_1 \tag{3.33}$$

After using the Euler technique for determining $x = x_1$, corresponding to $t = t_1$, we can make another short time step Δt and determine x_2 corresponding to $t_2 = t_1 + \Delta t$ as follows:

$$x_1 + \left.\frac{dx}{dt}\right|_{x=x_1} . \Delta t = x_2 \tag{3.34}$$

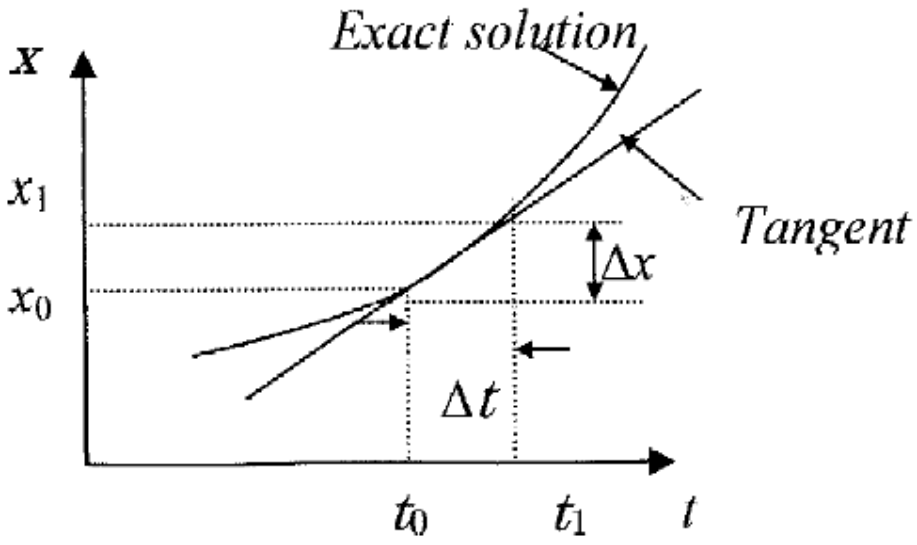

Figure 3.5 Euler's method [11]

By applying this technique successively, values of *x* can be determined corresponding to values of *t*. As shown in Figure 3.5, the Euler method assumes that the slope is uniform over the entire interval. Since this method only uses the first derivative of *x*, it is known as a first-order method. To give utmost accuracy in each step, Δt needs to be small. This will increase round-off errors, and the computational effort required will be very high [40] .

It is apparent that by applying numerical integration methods, the propagation of error is likely to magnify later if the errors were made early in the calculation. If the errors do not cause significant errors later, the method is said to be numerically stable; however, if the mistake is continuous and causes significant errors, it is said to be numerically unstable. To deal with inaccuracies, a modified Euler method is described next.

3.2.2 Modified Euler method

The conventional Euler method results have inaccuracies, as it uses the derivative at the beginning of the interval as though it is applied throughout the interval. The modified Euler method is an adaption of this method by calculating the slope at the beginning and end of the interval, and then uses the average of the slopes .The modified Euler method consists of two steps [40]:

1. Predictor step, which uses the derivative at the beginning of the step and which allows for the prediction of the value at the end of the step.

$$x_1^p = x_0 + \left.\frac{dx}{dt}\right|_{x=x_0} . \Delta t \tag{3.35}$$

2. Corrector step, which uses the predicted value of $x^p{}_1$ to compute the derivative at the end of the step. The average of this derivative and the derivative at the beginning of the step is used to find the correct value.

$$x_1^c = x_0 + \frac{1}{2}\left(\left.\frac{dx}{dt}\right|_{x=x_0} + \left.\frac{dx}{dt}\right|_{x=x_1^p}\right)\Delta t \tag{3.36}$$

A more accurate value of the derivative at the end of the step can be calculated using $x = x^c{}_1$. This derivative can be used to calculate a more accurate value of the derivative, which in turn is used to apply the corrector step again. This process can be used repetitively until successive steps converge with the desired accuracy.

The modified Euler method is the simplest of the predictor-corrector methods. For this dissertation, a Microsoft Excel Spreadsheet was developed for the modified Euler method. Excel spreadsheets are widely available and do not require significant programming; and spreadsheets offer a convenient environment for tracking convergence of solutions and exploring “what-if” questions for sensitivity analysis. In addition, spreadsheets lend themselves to a very transparent implementation of the step-by-step procedures encountered in transient stability analysis, without obscuring the inner workings of the numerical methods employed in such studies [41]. The parameters were adapted to reflect the nuclear power plant connected to the grid in–feed and would be used to confirm simulation and calculated results.

3.3 Simulation protocols in DIgSILENT

As power networks increase their capacity, the need to perform more and more simulations/permutations is vital for understanding network conditions under various configurations. Networks are expanding and the need to evaluate complex networks and future expansion has become extremely vital. This allows for analysis of the present network as well as future expansion networks for years of operation. All major components of the network can be simulated and used to determine response during normal operation or faulted operation. Power system simulation packages compute all electrical parameters, including voltage magnitudes, current magnitudes, phase angles and power flows in the network [12]. These simulation packages include load flow, stability, short-circuit, transient programmes, etc. Computer-based simulations have allowed system operators to perform complex simulations. Advances in technology have allowed for better computational speed and improved component modelling. There are many simulation packages available with various qualities, like time domain and frequency simulation packages that can be used for various applications. This reduces the time spent doing lengthy hand calculations and allows more time for verifying and validating models. The simulation package used in this dissertation is DIgSILENT. This software package is widely used and accepted by network operators to perform simulation and validation of networks currently in operation. Any future changes of the network can be verified before implementation to ensure that any amendments/modifications to the network do not have an adverse effect on the behaviour of the power system.

The name DIgSILENT stands for "**DIg**ital **SI**mu**L**ation and **E**lectrical **N**e**T**work calculation program". DIgSILENT Version 7 was the world's first power system analysis software with an integrated graphical one-line interface. That interactive one-line diagram includes drawing functions, editing capabilities and all relevant static and dynamic calculation features [20], [42].

The DIgSILENT package was designed and developed by qualified engineers and programmers with many years of experience in both electrical power system analysis and programming fields. The accuracy and validity of the results obtained with this package have been confirmed in a large number of implementations for organisations involved in planning and operation of power systems [20], [42].

In order to meet today's power system analysis requirements, the DIgSILENT power system calculation package was designed as an integrated engineering tool which provides a complete "walk-around" technique through all available functions, rather than a collection of different software modules. DIgSILENT is able to perform load flow analysis, harmonic analysis, and transient stability studies, to name a few. This software was used to determine the load flow of the nuclear power station, and the method it uses to determine load flow is detailed in section 3.3.1 and the Newton-Raphson method is detailed in section 3.3.2. It also has the ability to perform time domain analysis, which is used for transient stability studies and is detailed in section 3.3.3.

3.3.1 Load flow analysis

Load flow (power flow) analysis can be defined as a process which is aimed at ascertaining the voltage magnitude, voltage angle, active power and reactive power at various nodes in a power system operating under steady-state conditions. This analysis assists system engineers to determine the stress on the power system in terms of its loading and its operation with respect to normal conditions. Furthermore, load flow analysis gives an indication of areas in the power system that may need capacity expansion owing to increase in load demand. Several methods have been developed to analyse the load flow condition on power systems which includes Gauss-Seidel, Newton-Raphson, Decoupled and the Fast Decoupled load flow methods. These methods are mainly deployed on high voltage alternating current (HVAC) [43], [44] .

There are three fundamental bus type classifications in load flow analysis. The first bus type is the swing bus, which is also referred to as the reference or slack bus, where the voltage magnitude and the phase angle are specified [43]. The second bus type is the PV bus, also known as the generator or voltage controlled bus, where the voltage magnitude and the active power are specified [43]. The third bus type is the PQ bus, also known as the load bus and at this bus, the active and reactive powers are specified [43].

- **Newton-Raphson method in HVAC load flow analysis**

In this section, the Newton-Raphson load flow method will be used to determine the HVAC load flow. This method, which is also adopted by DIgSILENT, uses an iterative technique for solving a set of simultaneous non-linear equations. In doing this, rectangular or polar co-ordinates can be used in defining the bus voltages and line admittances. In this dissertation, the polar coordinates will be used.

Assuming a power system with bus 1, 2, 3……n

The net complex power S_k injected at bus k is given as

$$S_k^* = P_k - jQ_k = V_k^* I_k = |V_k| \angle -\delta_k \quad \sum_{i=1}^{N} |Y_{ki}V_i| \angle (\theta_{ki} + \delta_i) \tag{3.37}$$

where,

θ_{ki} is the angle of the admittance Y_{ki}.

δ_i and δ_k are the phase angles of the bus voltages V_i and V_k , respectively.

P_k is the active power at bus k, and Q_k is the reactive power at bus k

When separating the real and imaginary parts of equation (3.37), we get

$$P_k = \sum_{i=1}^{N} |Y_{ki}V_iV_k| \cos(\theta_{ki} + \delta_i - \delta_k) \tag{3.38}$$

$$= \left|V_k^2\, Y_{kk}\right| \cos(\theta_{kk}) + \sum_{i \neq k}^{N} |Y_{ki} V_i V_k| \cos(\theta_{ki} + \delta_i - \delta_k)\; k = 2,3 \ldots\ldots, N \tag{3.39}$$

$$Q_k = -\sum_{i=1}^{N} |Y_{ki} V_i V_k| \sin(\theta_{ki} + \delta_i - \delta_k) \tag{3.40}$$

$$= -\left|V_k^2\, Y_{kk}\right| \sin(\theta_{kk}) + \sum_{i \neq k}^{N} |Y_{ki} V_i V_k| \sin(\theta_{ki} + \delta_i - \delta_k)\; k = 2,3 \ldots\ldots, N \tag{3.41}$$

Equations (3.39) and (3.41) give a set of non-linear algebraic equations in terms of the voltage magnitude in *pu* and phase angle in radians which are all independent variables. Assuming that all system busbars are PQ bus, except the slack bus, the active and reactive power at each bus is specified. This means that each of the other buses, with the exception of the slack bus, has two variables δ_k and $|V|_k$ to be calculated in the load flow solution.

Therefore, the power mismatches $\Delta P_k^{(i)}$ and $\Delta Q_k^{(i)}$ are the difference between the scheduled and calculated values of the active and reactive power, respectively at bus *k* in the i^{th} iteration. This is given by equations (3.42) and (3.43).

$$\Delta P_k^{(i)} = P_k^{sch} - P_k^{(i)} \tag{3.42}$$

$$\Delta Q_k^{(i)} = Q_k^{sch} - Q_k^{(i)} \tag{3.43}$$

For the load bus, if the load is inductive:

$P_k^{sch} < 0$
and
$Q_k^{sch} < 0$

if the load is capacitive:
$P_k^{sch} < 0$
and
$Q_k^{sch} > 0$

For each load bus, we have two of these equations given by equations (3.39) and (3.41), and expanding equations (3.39) and (3.41) in Taylor's series about the initial estimate and neglecting all higher order terms will result in equation (3.44).

$$\begin{bmatrix} \Delta P_2^{(i)} \\ \cdots \\ \Delta P_N^{(i)} \\ \Delta Q_2^{(i)} \\ \cdots \\ \Delta Q_N^{(i)} \end{bmatrix} = \begin{bmatrix} \frac{\partial P_2^{(i)}}{\partial \delta_2} & \cdots & \frac{\partial P_2^{(i)}}{\partial \delta_N} & \frac{\partial P_2^{(i)}}{\partial |V_2|} & \frac{\partial P_2^{(i)}}{\partial |V_N|} \\ \cdots & \cdots & \cdots & \cdots & \cdots \\ \frac{\partial P_N^{(i)}}{\partial \delta_2} & \cdots & \frac{\partial P_N^{(i)}}{\partial \delta_N} & \frac{\partial P_N^{(i)}}{\partial |V_2|} & \frac{\partial P_N^{(i)}}{\partial |V_N|} \\ \frac{\partial Q_2^{(i)}}{\partial \delta_2} & \cdots & \frac{\partial Q_2^{(i)}}{\partial \delta_N} & \frac{\partial Q_2^{(i)}}{\partial |V_2|} & \frac{\partial Q_2^{(i)}}{\partial |V_N|} \\ \cdots & \cdots & \cdots & \cdots & \cdots \\ \frac{\partial Q_N^{(i)}}{\partial \delta_2} & \cdots & \frac{\partial Q_N^{(i)}}{\partial \delta_N} & \frac{\partial Q_N^{(i)}}{\partial |V_2|} & \frac{\partial Q_N^{(i)}}{\partial |V_N|} \end{bmatrix} \begin{bmatrix} \Delta \delta_2^{(i)} \\ \cdots \\ \Delta \delta_N^{(i)} \\ \Delta \left| V_2^{(i)} \right| \\ \cdots \\ \Delta \left| V_N^{(i)} \right| \end{bmatrix} \tag{3.44}$$

In equation (3.44), bus 1 is excluded in the matrix, because it is assumed to be the swing bus.
We can summarise equation (3.44) above, as written in equation (3.45) below.

$$\begin{bmatrix} \Delta P \\ \Delta Q \end{bmatrix} = \begin{bmatrix} J_1 & J_2 \\ J_3 & J_4 \end{bmatrix} \begin{bmatrix} \Delta \delta \\ \Delta |V| \end{bmatrix} \tag{3.45}$$

Matrix *J* is called the Jacobian matrix whose elements are partial derivatives of equations (3.39) and (3.41) with respect to $\delta_k^{(i)}$ and $\left| V_k^{(i)} \right|$. The Jacobian matrix gives the linearised relationship between changes in voltage angle and voltage magnitude with the small changes in the real and reactive power [11] , [43].

For voltage controlled (PV) bus, the voltage magnitudes are known. Therefore, if *m* buses of the system are voltage-controlled, *m* equations involving $\Delta \boldsymbol{Q}$ and $\Delta \boldsymbol{V}$ and corresponding columns of the Jacobian matrix are eliminated. Accordingly, there are *n-1* real power constraints and *n-1-m* reactive power constraints, and the Jacobian matrix is of the order (2*n*-2-*m*) x (2*n*-2-*m).*

The diagonal and off-diagonal elements of J_1 are

$$\frac{\partial P_k}{\partial \delta_k} = \sum_{j=1, j \neq k}^{N} \left| Y_{kj} V_k V_j \right| \sin(\theta_{kj} + \delta_j - \delta_k) \tag{3.46}$$

$$\frac{\partial P_k}{\partial \delta_j} = - \left| Y_{kj} V_k V_j \right| \sin(\theta_{kj} + \delta_j - \delta_k) \qquad j \neq k \tag{3.47}$$

The diagonal and off-diagonal elements of J_2 are

$$\frac{\partial P_k}{\partial |V_k|} = 2|V_k Y_{kk}| \cos(\theta_{kk}) + \sum_{j=1, j \neq k}^{N} \left| Y_{kj} V_j \right| \sin(\theta_{kj} + \delta_j - \delta_k) \tag{3.48}$$

$$\frac{\partial P_k}{\partial |V_j|} = \left| Y_{kj} V_k \right| \cos(\theta_{kj} + \delta_j - \delta_k) \qquad j \neq k \tag{3.49}$$

The diagonal and off-diagonal elements of J_3 are

$$\frac{\partial Q_k}{\partial \delta_k} = \sum_{j=1, j\neq k}^{N} \left|Y_{kj} V_k V_j\right| \cos(\theta_{kj} + \delta_j - \delta_k) \tag{3.50}$$

$$\frac{\partial Q_k}{\partial \delta_j} = -\left|Y_{kj} V_k V_j\right| \cos(\theta_{kj} + \delta_j - \delta_k) \qquad j \neq k \tag{3.51}$$

The diagonal and off-diagonal elements of J_4 are

$$\frac{\partial Q_k}{\partial |V_k|} = -2|V_k Y_{kk}| \sin(\theta_{kk}) - \sum_{j=1, j\neq k}^{N} \left|Y_{kj} V_j\right| \sin(\theta_{kj} + \delta_j - \delta_k) \tag{3.52}$$

$$\frac{\partial P_k}{\partial |V_j|} = -\left|Y_{kj} V_k\right| sin(\theta_{kj} + \delta_j - \delta_k) \qquad j \neq k \tag{3.53}$$

Once the Jacobian Matrix *J* has been calculated, the new estimates for bus voltage magnitude and angle are given by:

$$\delta_k^{(i+1)} = \delta_k^{(i)} + \Delta\delta_k^{(i)}$$

$$\left|V_k^{(i+1)}\right| = \left|V_k^{(i)}\right| + \Delta\left|V_k^{(i)}\right| \tag{3.54}$$

In case of PV bus, there are some limits imposed on the reactive power.

The next step will be to re-evaluate equations (3.38) to (3.54) using the new values obtained in equation (3.54) as the initial condition for the next iteration. This will be repeated until the power mismatches given in equation (3.42) and (3.43) are less than the specified tolerance, which is usually $\varepsilon \cong 10^{-5}$.

3.3.2 Short-circuit calculation in DIgSILENT

DIgSILENT's fault calculation is based on international standards. The software programme uses the IEC 60909, VDE 0102/010, IEEE 141/ANSI e 37.5, G 74 and IEC 61363 fault calculation standards. The following features are available for all fault analysis methods [45]:

- calculation of short circuits at the busbar, along a section of line/cable and includes all branch contributions and busbar voltages;
- fault impedance defined by the user;
- specially designed graphs and diagrams required by the protection engineer;

- busbar and line thermal overload highlights in the graphic;
- Thevenin's equivalent calculation as seen from the faulty node; and
- calculation of apparent phase impedances at any point along a transmission line/cable or busbar.

The short-circuit function of DIgSILENT is able to calculate the initial symmetrical peak current, short-circuit power, peak short-circuit current, symmetrical short-circuit breaking current and the thermal equivalent current. Both minimum and maximum currents can be calculated based on the network voltage c-factors. The software is capable of calculating all types of faults including three-phase, two-phase, two-phase ground and single-phase to ground.

The Complete Method employed by DIgSILENT allows protection engineers to perform multiple fault analysis which occurs simultaneously in the system without considering the simplifications or assumptions typically made in conventional fault analysis. An example of this type of analysis would be the precise evaluation of the fault current in a specific situation, so that the engineer could determine if there was a malfunction of the protection device or improper settings on the relay itself.

3.3.3 DIgSILENT method in computing transient studies

These tools support simulations with full electromagnetic transient models (EMT), providing instantaneous values of voltages and currents in the grid, combined with the ability to build dynamic models for generator movers. Besides the EMT simulations, DIgSILENT provides the ability to make the so-called RMS simulations. These simulations are also referred to as (dynamic) stability simulations, and they correspond to standard models in other power system stability simulation tools, e.g. PSS/E. The advantage of using RMS simulations is that the simulation speed can be increased significantly, but the simulations omit the fast electromagnetic transients. The RMS simulations can be done with the symmetrical component only or with the unsymmetrical components as well. The stator transients in the induction generator models are omitted in the RMS simulations, thus, the order of the induction generator model is reduced. A graphical representation of the DIgSILENT's methods in performing analysis can be seen in Figure 3.6.

Time-domain simulations in PowerFactory are initialized by a valid load flow, and PowerFactory functions determine the initial conditions for all power system elements, including all controller units and mechanical components. These initial conditions represent the steady-state operating point at the beginning of the simulation, fulfilling the requirements that the derivatives of all state variables of loads, machines, controllers, etc., are zero [45].

Before the start of the simulation process, it is also determined the following, namely: what type of network representation must be used for further analysis; what step sizes to use; which events to handle; and where to store the results. The simulation uses an iterative procedure to solve AC and DC load flows, and the dynamic model state variable integrals simultaneously. Highly accurate non-linear system models result in exact solutions, including during high-amplitude transients. Various numerical integration routines are used for the

electro-mechanical systems (including voltage regulators and power system stabilizer) and also for the hydro-mechanical or thermo-mechanical models.

The process of performing a transient simulation typically involves [45] :

1. calculation of initial values, including a load flow calculation;
2. definition of result variables and/or simulation events;
3. optional definition of result graphs and/or other virtual instruments;
4. execution of simulation;
5. creating additional result graphs or virtual instruments, or editing existing ones;
6. changing settings, repeating calculations; and
7. printing results.

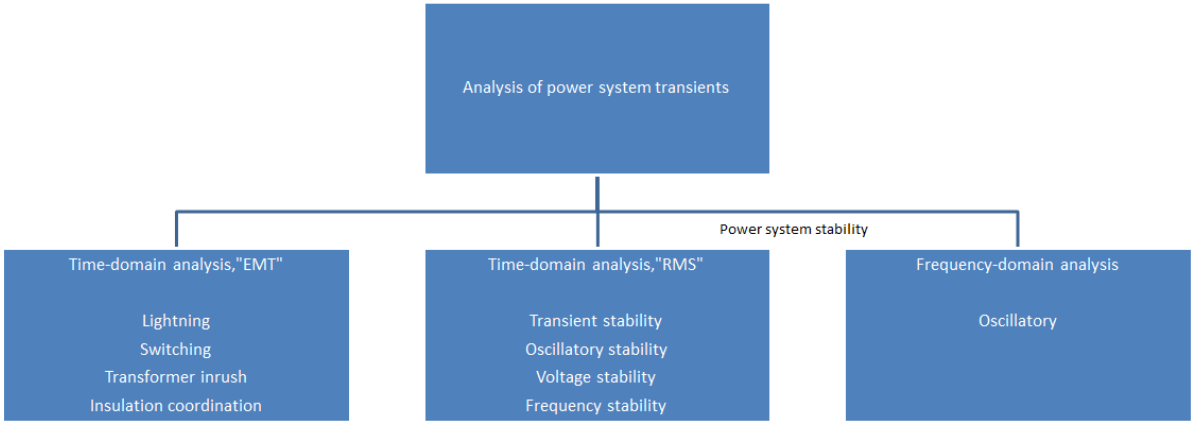

Figure 3.6 DIgSILENT analysis of power systems [45]

The built-in synchronous machine models of DIgSILENT PowerFactory are of the 8th order (one differential equation for the field winding, one for the damper winding in the d-axis, two for the damper windings in the q-axis, two for the stator flux transients and two for the shaft). In DIgSILENT PowerFactory, the model is reduced automatically to 6th-order (by neglecting the stator flux transients). It executes a time-domain simulation of the 'RMS' type. The generator model includes core saturation.

4. Simplified Network Response to Grid Transients

The South African electrical network, like any other electric network, is made up of many components such as generators, overhead power lines, power transformers, static VAr compensators, capacitor banks, loads and busbars. To model all these components would take a long time to develop and therefore, simplified models are essential in order to perform a quick analysis. The ability to perform quick analysis allows the plant engineer to assess if further investigations are required and whether support from national control system operators is required. This section deals with the reduced South African network including the Western Cape grid which is represented by a grid in-feed with equivalent fault levels for the network at the HV bus of the nuclear plant.

4.1 Reduced network load flow analysis

The complete South African 400kV transmission system was reduced to grid in-feed connected to the HV busbar closest to the power station for simplicity. The entire network is made up of thousands of components and would take many years to develop. Not all the data is available for the entire network and hence a reduced network is used with all available parameters. The reduction of the network depends on the location of the study and the results required. The 400kV network is used to perform the studies, as the South African transmission system uses 400kV as the main voltage level to transfer electricity from one source to another (although the 765 kV also exists). It may be stepped up or stepped down from 400kV as required by load centres.

Figure 4.1 shows the model built in DIgSILENT. It comprises of 19 busbars, 12 loads, 2 step-up transformers, 2 unit transformers, 2 main 24kV generators and 4 emergency diesel generators. If the model was compared to Figure 2.2 and 2.3 the generators G1 and G2 is reflected as the Koeberg generator and the rest of the network is represented in the model as a grid infeed. The busbars LGA to LHA is a representation of the plants internal 6,6kV network and the lumped loads are reflected on each associated busbar.

Although various 6,6kV switchboards have many loads connected to them, an equivalent PQ load was modelled in the software to reduce modelling time and to ensure simplicity. The lumped loads can be seen in Appendix A.

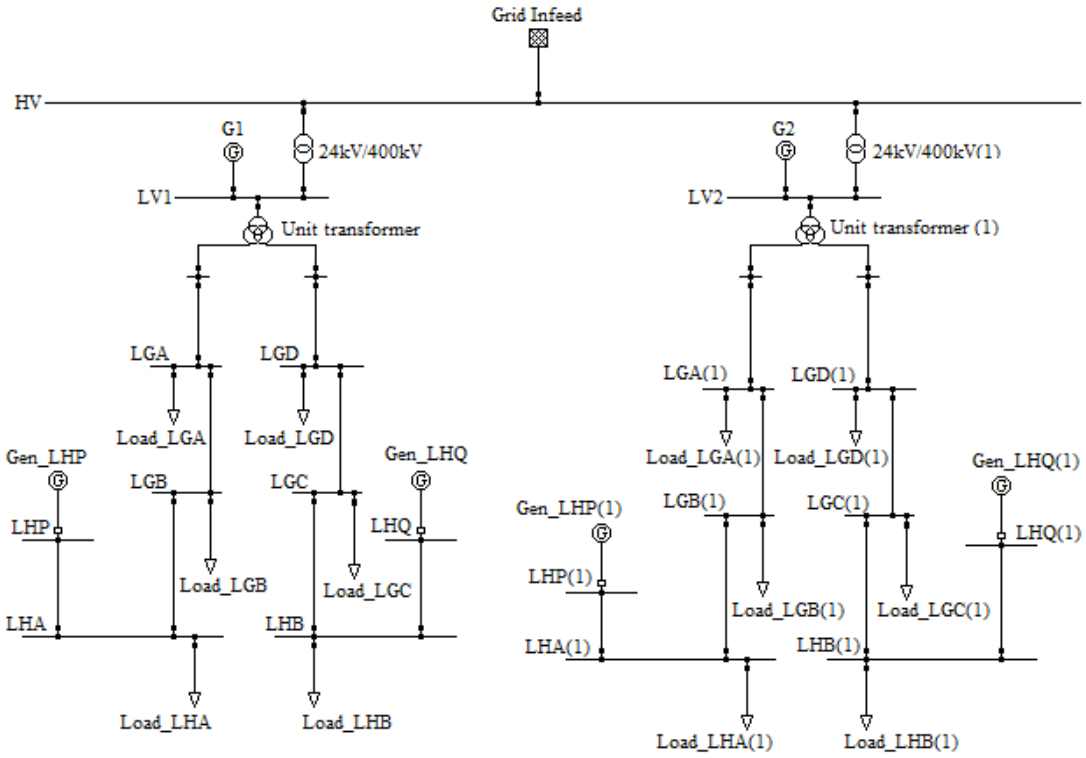

Figure 4.1 Reduced network topology built in DIgSILENT

Load flow analysis, as explained in Chapter 3, forms the foundation of any network analysis. The first process was to input all the plant data into DIgSILENT software. This data include all line parameters, transformer data, load data and generator parameters. System operators often perform simulations on reduced networks, and compare results with known network behaviour, where they have available data to compare results.

A load flow was initiated on DIgSILENT and then compared to the original load currents of the plant. This can be seen in Table 4.1.

Table 4.1 Comparison between DIgSILENT results and original plant load flow current data

6.6kV Switchboard	DIgSILENT simulated load current	Original load current	Relative Error Percentage %
LGA	2128A	2090A	1.78%
LGB	105A	103A	1.9%
LHA	430A	435A	1.15%
LGD	1547A	1517A	1.62%
LGC	297A	290A	2.36%
LHB	352A	348A	1.13%

As illustrated in Table 4.1, the relative error between the original load flow current and the simulated DIgSILENT current was found to be less than 2.5%. This gives great confidence in the load model and ensures that all the plant components have been simulated correctly and that a short circuit and transient stability study can be performed using this reduced model.

4.2 Short-circuit study

To ensure that the results were comparable, a short-circuit study was performed to confirm that the simulated plant data was correct. Short-circuit studies have been used for years to determine correct protection parameters, but they also aid with modifications verification to ensure plant reliability and component limitations [45]. When simulated results are compared to original calculations, it gives confirmation that the data simulated is correct. It thus allows for a verification of modifications that have been completed to ensure plant parameters are still within its design parameters. The method used for the simulation was to apply a short-circuit on each 6.6kV switchboard and to compare it to the existing short-circuit data of the plant as indicated in the original design documents of the plant.

When the results were analysed, a difference between the simulated results and the plant data was noted. This difference could be attributed to the fact that individual motor loads were lumped as PQ loads in the simulation. When loads are simulated as motors, they feed into the fault current during short circuit conditions. From Table 4.2 it can be seen that the differences between the original data and the DIgSILENT simulated values are between 2- 4.2%, which is acceptable for this study.

The significance of performing the load flow study and short-circuit analysis is that when changes are made to the plant, it can be verified using the DIgSILENT software tool to perform quick, short-circuit analysis. Load flow studies and short-circuit analysis form the basis of all power system analysis.

Table 4.2 Relative error between simulated DIgSILENT and original plant data short circuit results

6.6kV Switchboard	Simulated DIgSILENT in kA	Original Data in kA	Relative Error in Percentage
LGA	27.6	28.1	2%
LGB	26.98	27.5	2%
LGC	26.01	27.2	3.60%
LGD	26.3	27.47	4.20%
LHA	26.5	27.1	1.40%
LHB	25.7	26.8	4.10%

4.3 Critical clearing times assessment

Critical clearing time presents the maximum time within which the fault must be cleared to maintain synchronism. Should the fault be cleared after $t_{cr,}$ the system will lose synchronism [14]. The network is such

that it can be reduced to a two machine feeding into an infinite bus; hence the ability to perform simple assessments of critical clearing times using three methods. These methods are discussed below.

The first technique required performing an equal area criterion calculation to determine the critical clearing time. All plant data was collated and calculated using the equal area calculation. This calculation was performed with only one generator connected to the infinite bus at first. The calculated time was 0.264 seconds. The calculation was repeated using two generators connected to the infinite bus. To complete the equal area calculation, we included two generators swinging together, which were reduced to a single machine. All the calculations can be found in Appendix B. The results of the two generators coupled to the infinite bus reduced the critical clearing time to 0.235 seconds from 0.264 seconds. The two generator scenario reduces the clearing time by 29 milliseconds mainly due to the reduction of the two generators into one large generator.

The second technique used to confirm the critical clearing time was the modified Euler technique. As discussed in earlier chapters, the modified Euler was an alternative to the equal area criterion assessment. This technique and all its calculation techniques were adapted in a Microsoft Excel programme. All the network parameters were input into the Excel spreadsheet. These parameters can be seen in Appendix C. The result for the critical clearing time of a single generator feeding into an infinite bus using the modified Euler method, was 0.27 seconds. The results for a single generator fed into an infinite bus using the modified Euler method was about 2% higher than the results attained using the equal area criterion calculation. The Excel spreadsheet calculation for the modified Euler only allowed for two decimal places after comma.

As with the equal area criterion calculation, a second assessment was completed combining the two generators to perform as one coherent machine. The critical clearing time was found to be 0.24 seconds. Again the critical clearing time is reduced by 30 milliseconds, which gives confidence in both techniques.

The third and final technique or assessment was the main focus of this chapter. It reduces the network to a simplified network to perform stability studies. DIgSILENT was used to perform the transient stability assessment. The parameters used in DIgSILENT can be found in Appendix D. The critical clearing time when using DIgSILENT varied due to different parameters allowable in the software package, such as the generator reactive power limits and the grid in feed short-circuit value to name a few. The critical clearing time was based only on one generator connected to the infinite bus and was found to be 0.251 seconds. This result required the reactive power limits to be removed from the generator parameters and the plant reticulation connected to the generator via the unit auxiliary transformer to be disconnected and the AVR switched off. When parameters like reactive power limits and various other parameters were used in the DIgSILENT, it changed the critical clearing time to 0.201 sec. which prevented a comparison between the simulated results and the calculated results completed earlier. Similarly, when both generators were connected to the infinite bus, the simulated values and the calculated values were comparable. The critical

clearing time using DIgSILENT was found to be 0.231 seconds. A comparison between the three different techniques can be found in Table 4.3. It can be seen that the results obtained using equal area criteria and DIgSILENT are very close compared to those obtained using the modified Euler method.

Table 4.3 Critical clearing time using various techniques

Techniques	Critical clearing time for a single generator coupled to infinite bus	Critical clearing for two generators coupled to infinite bus
Equal area	0.264s	0.235s
Modified Euler	0.270s	0.240s
DIgSILENT	0.251s	0.231s

Figures 4.2 and 4.3 typically display the machine power angle and machine speed during instability, as displayed using the modified Euler method in Excel format. This is typical behaviour when one deals with transient stability. The figures below are taken from the Microsoft Excel spreadsheet and reflect a single machine connected to an infinite bus with no AVR connected.

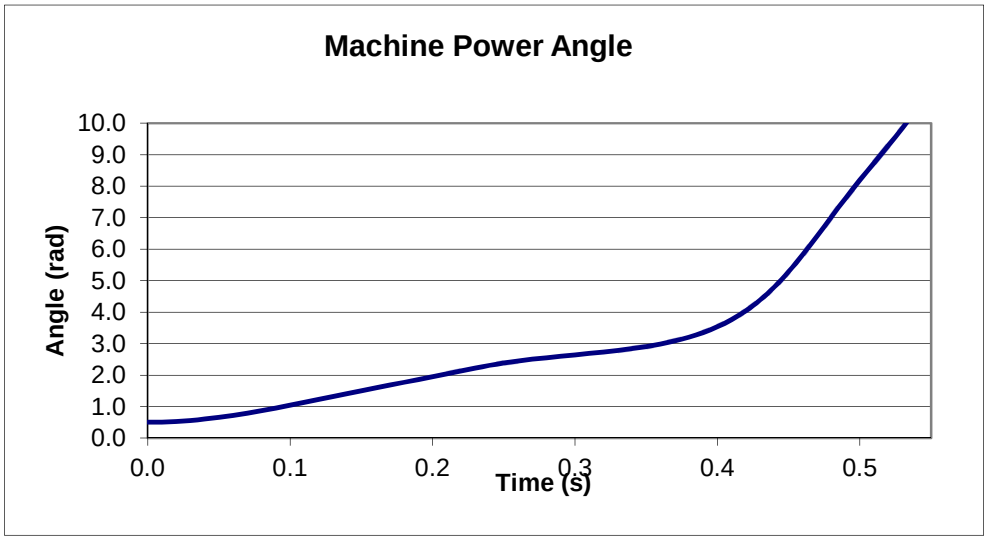

Figure 4.2 Machine power angle results at instability using modified Euler method

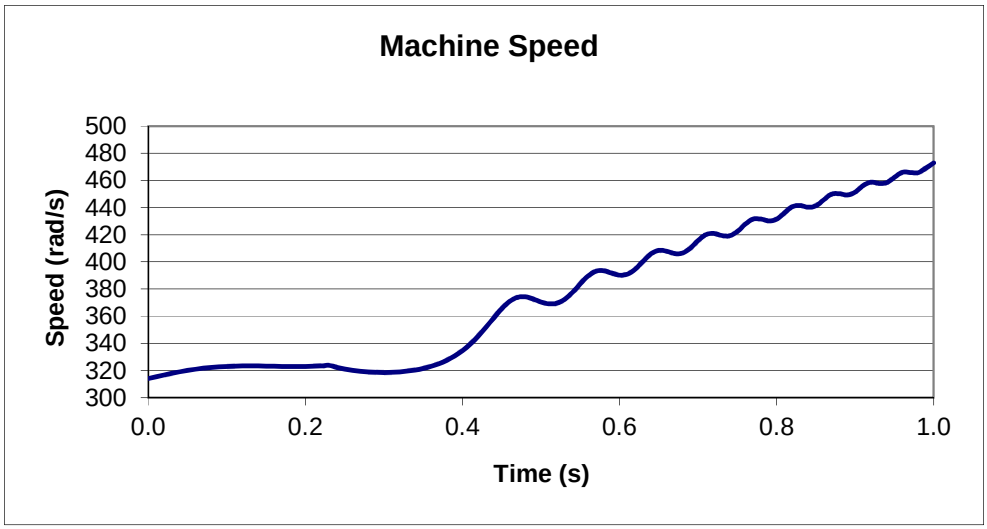

Figure 4.3 Machine speed results in instability using modified Euler method

4.4 Automatic voltage regulators

Automatic Voltage Regulators are commonly used to regulate the terminal voltage of generators. They also help with reactive power flow.

There are two main types of excitation systems, namely [40]:

- excitation fed through slip rings via brushes (older system); and
- brushless excitation systems.

The synchronous generator keeps the terminal voltage magnitude at a pre-set value. A simplified control loop can be seen in Figure 4.4.

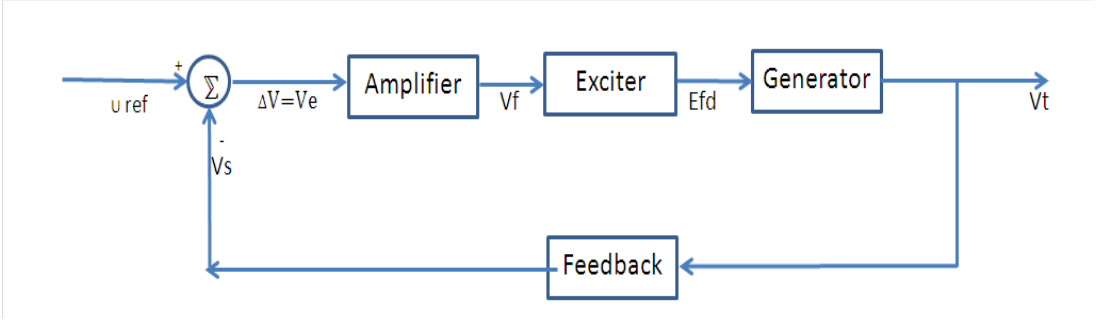

Figure 4.4 AVR block diagram [40]

If the terminal voltage of the generator in Figure 4.4 drops, the control loop sensors detect a change in voltage compared to the reference voltage and increase the excitation to maintain generator output voltage at a desired value [40]. Exciter models differ depending on the type of design used. Fast-acting static exciters

respond much faster than rotating exciters. The inertia response time of the rotating equipment severely impacts on the excitation voltage response to large transients when compared to a static controlled excitation system, which responds almost immediately to maintain output voltage [46].

The Koeberg Nuclear Power Station has a rotating exciter. As a result, the controlled excitation voltage energises the field of the main exciter. The main exciter's output is then rectified via rotating diodes and then routed to the field winding of the synchronous machine. The AVR and exciter model used for the simulation was the IEEE ST5B type AVR and exciter. This model emulates the AVR installed on the plant. The IEEE defines the ST5B as a variation of the Type ST1A model, with alternative over-excitation and under-excitation inputs and additional limits. An illustration of this can be seen in Figure 4.5.

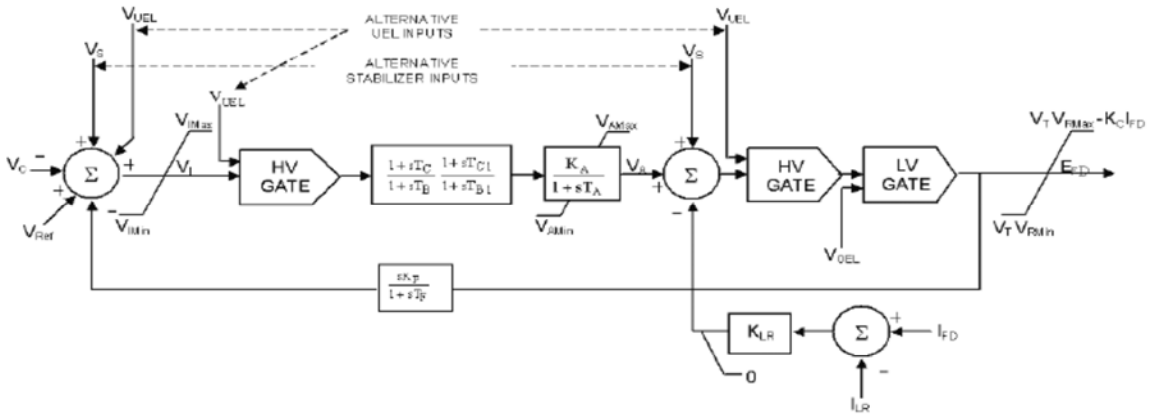

Figure 4.5 IEEE ST5B AVR model [47]

The excitation control system at the nuclear power plant consists of three independent control loops. The normal operating condition of the excitation system consists of two channels (Channel 1 and Channel 2) and is supplied by the shunt-connected excitation transformers [48]. Each channel consists of an automatic voltage regulator (AVR) and a field current regulator.

The emergency channel (Channel 3) is fed via a separate excitation transformer. Channel 3 has a dual function. It acts as an emergency channel under abnormal/operational conditions, i.e., it will take over excitation if neither Channel 1 nor Channel 2 can control the required excitation current to the machine. Its second function is exclusively used for testing purposes while it is selected to open loop control [48]. The parameters of the generator are shown in the Appendix D. The block diagram of the AVR can be seen in Appendix E.

4.5 AVR model validation

Computer-based stability analysis is an important component of power systems' operations and planning. As a result, it is crucial that the models and parameters of the generators and associated excitation systems are as accurate as possible to ensure that results are representative of the real power system. Hence, the validation

of the AVR model using the plant parameters and DIgSILENT software was critical during simulations relating to transient stability studies of the nuclear power plant.

4.5.1 Generator open-circuit saturation curve

The open-circuit saturation test is done to derive the generator's open-circuit saturation curve [48]. The open-circuit saturation curve (OCS curve) is obtained by driving the generator being tested at rated speed, open-circuited, and recording its stator voltage and exciter field current [48]. Koeberg Nuclear Power Station units employ rotating non-controlled rectifiers, and, as a result, it is difficult to measure the field (rotor) current directly. Table 4.4 provides the open-circuit saturation test for the nuclear power plant's exciter current and output terminal voltage.

Table 4.4 Koeberg unit open-circuit saturation test

Stator Voltage (V)	Exciter Field Current (A)
120	0
2640	11.28
4867.2	21.056
7329.6	30.832
9705.6	40.608
11904	50.008
14640	61.664
16857.6	72.192
19248	83.0584
20208	87.232
21600	94.4512
22824	101.52
24000	**109.04**
25284	118.064
26376	125.208

Saturation parameters S1.0 and S1.2 as illustrated in Figure 4.6 can be derived from the open-circuit saturation curve.

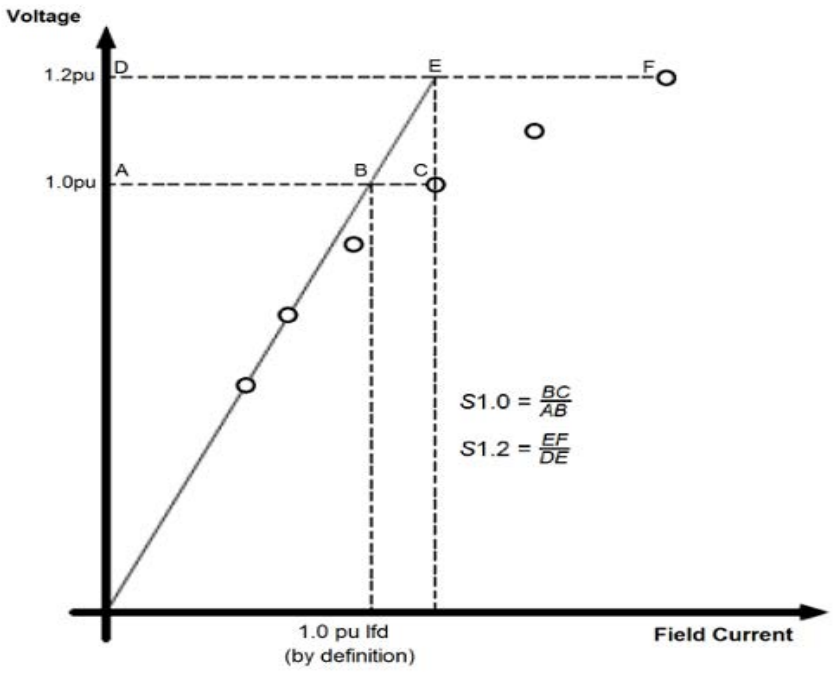

Figure 4.6 Typical open-circuit saturation characteristics [48]

The measured residual flux in this case is 120V, which is less than 1%. Thus, subtracting this out and extrapolating the curve, the open-circuit saturation curve can be drawn. Figure 4.6 shows the open-circuit saturation characteristic for a typical unit at Koeberg Nuclear Power Station. This is at low voltage, and hence low levels of flux, where the major reluctance (magnetic resistance) of the magnetic circuit is the air-gap. In the linear portion of the open-circuit curve, the terminal voltage and flux are proportional to the exciter field current. This linear portion of the open-circuit saturation curve is called the air-gap line [48]. At higher voltages, as the flux increases, the stator iron saturates, and additional exciter field current is required to drive magnetic flux through the iron. This is due to the apparent higher reluctance of the magnetic circuit. Hence, the upper part of the curve bends away from the air-gap line.

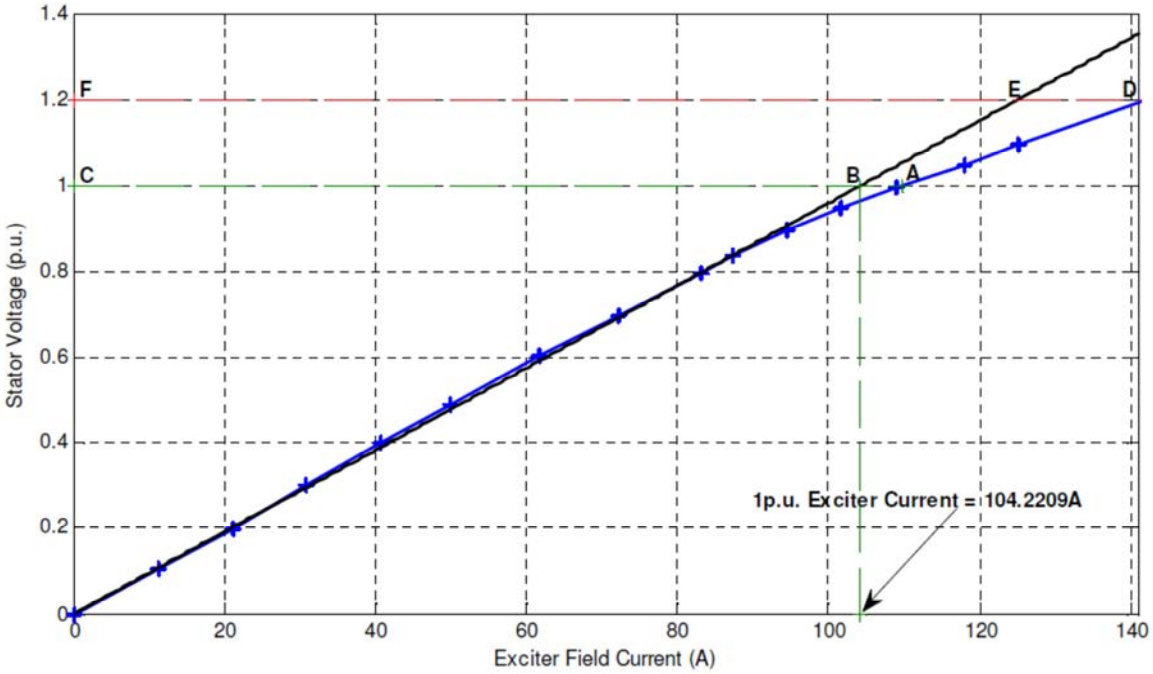

Figure 4.7 Koeberg open-circuit saturation curve [48]

Based on Figure 4.7 above, the generator saturation parameters were calculated as follows (By definition: 1 p.u. Exciter Field Current = 104.2209 A):

Saturation Parameters

$S_{1.0} = \frac{1325-1072}{1072} = 0.236$

$S_{1.2} = \frac{2525-1287.5}{1287.5} = 0.9611$

4.5.2 Automatic Voltage Regulator (AVR) Step Response Test – Offline

The automatic voltage regulator of the Original Equipment Manufacturer (OEM) AVR was validated utilising data recorded during the open-circuit step response test. The open-circuit (voltage reference) step response test is done by injecting a small percentage step into the reference of the automatic voltage regulator. These response test results are used to estimate the parameters for the automatic voltage regulator and the exciter system. The open-circuit voltage reference step response test can be performed with the unit either on-line or off-line. Figure 4.8 and Figure 4.9 show the off-line open-circuit step response test results for a voltage reference step of approximately 9% for model utilising OEM parameters and estimated model parameters, respectively. The figures have two sets of plots – stator voltages (Vab, Vbc & Vca) plot (which is the top waveform) and exciter field voltage (Vefd) plot (which is the waveform at the bottom) for both measured quantities and simulated quantities (Vslm). In Figure 4.8 stator voltage graph, only one measured phase Vca is displayed and compared to the simulated waveform displayed in black. The excitation voltage displayed in Figure 4.8 has the red waveform representing the exciter field voltage and the black waveform displaying the simulated waveform. From Figure 4.8 it can be seen that there are differences between the measured quantities and the model's response with OEM parameters. Figure 4.9 shows that the estimated model parameters (black waveform) closely match the measured quantities (green in the stator voltage

waveform and red in the exciter field voltage) and display a better fit than the given OEM parameters, with the greatest error being less than 1% between measurements and model. Figure 4.8 and Figure 4.9 show the off-line open-circuit step response test results – comparison of the two shows a better close match for the model with estimated parameters. Table 4.4 provides the parameter list and settings for the recommended model for a typical unit at Koeberg plant.

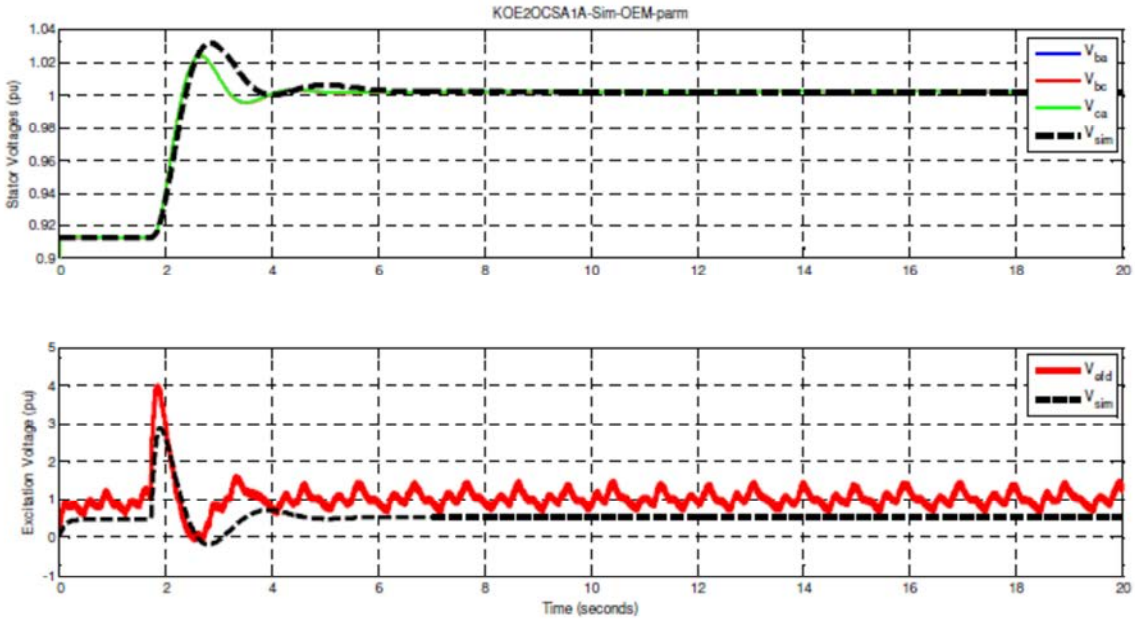

Figure 4.8 AVR step response OEM parameter results [48]

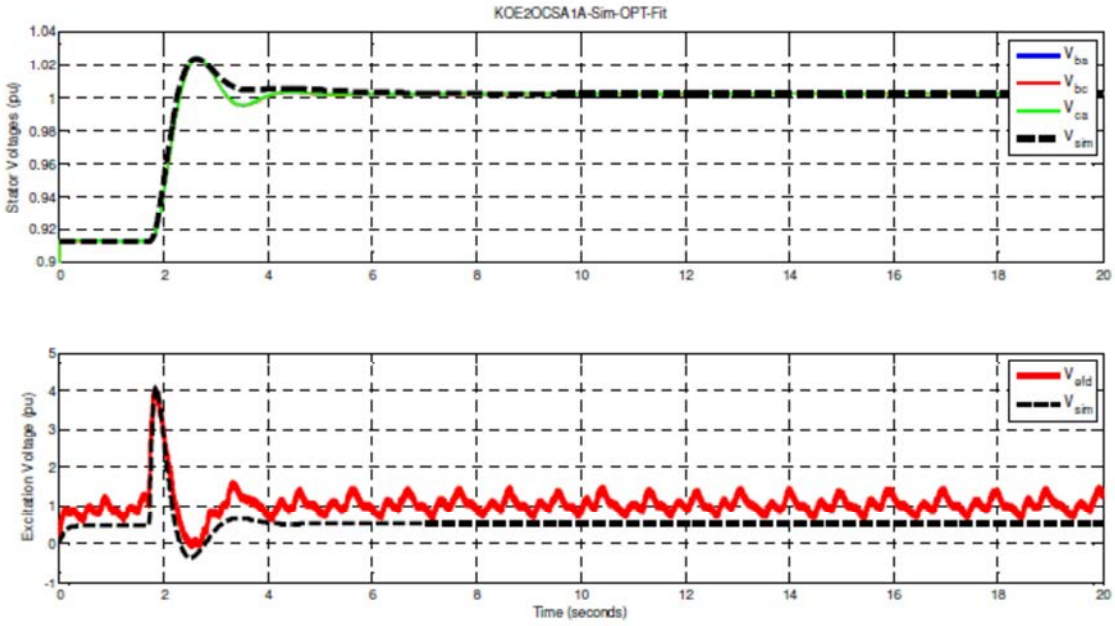

Figure 4.9 AVR step response adapted results [48]

4.5.3 AVR effect on transient stability

AVR's primary function is to maintain the generator output voltage to within an acceptable range. Occasionally, disturbances occur and require the AVR to perform its function. The AVR boosts excitation voltage, which in turn increases excitation current that changes the reactive power flow of the generator. In the case studies, the effect of the AVR on transient stability was investigated in a nuclear power station, namely, Koeberg Nuclear Power Station.

A three-phase short-circuit was applied to the HV busbar, seen in Figure 4.10, to confirm the critical clearing time before the associated generator pole slipped. The analysis of having the AVR installed and removed when one nuclear generator was connected to infinite bus, are as follows:

- AVR was de-activated and removed from service in DIgSILENT, and the critical clearing time was found to be 0.251 sec.
- AVR was activated in DIgSILENT, and the critical clearing time was found to be 0.256 sec.

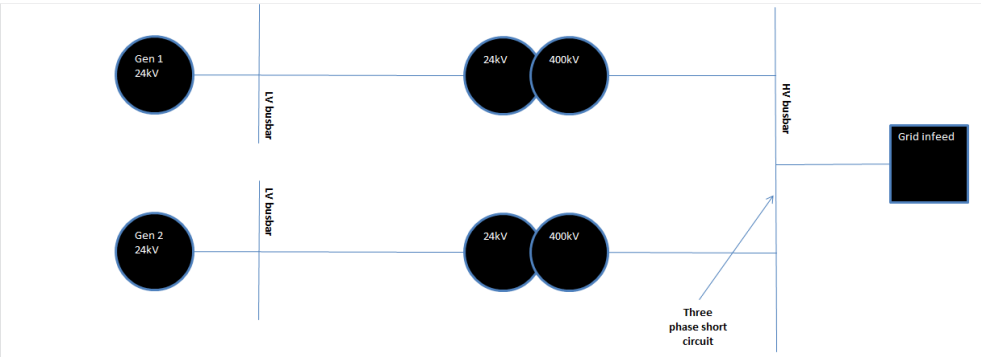

Figure 4.10 Three-phase fault placed at the HV busbar

Analyses of the results above show that there is only a 0.005 sec. improvement in critical clearing time when the AVR was installed compared to when the AVR removed from the simulation. The main contributor to this small improvement is due to the slow response of the excitation system. If one has to analyse the slow response of the AVR, it would be greatly attributed to the slow response of the excitation voltage and current. In Figure 4.12 the excitation voltage took more than 0.7 sec. to get to full excitation voltage. To better understand the response of the exciter, the type of exciter should be analysed. The model in the software used is an IEEE ST5B type exciter and can been seen in Appendix F. The main contributor to the response is the rotary type exciter of which the parameters have been included in the ST5B AVR parameters found in Table 4.5.

Table 4.5 IEEE ST5B parameters in DIgSILENT

Parameter & Description	Unit	Actual setting
Tr Regulator input filter time constant	[s]	0.02
TB1 lag time constant of 1st lead-lag block (avr channel)	[s]	57.5
TC1 lead time constant of 1st lead-lag block (avr channel)	[s]	2.3
Kr Voltage regulator gain	[pu]	500
TB2 Saturation ratio at 75% of maximum field voltage	[s]	0.16
TC2 lead time constant of 2nd lead-lag block (avr channel)	[s]	0.4
TUB1 lag time constant of 1st lead-lag block (uel channel)	[s]	75
TUC1 lead time constant of 1st lead-lag block (uel channel)	[s]	3
TUB2 lag time constant of 2nd lead-lag block (uel channel)	[s]	0.1
TUC2 lead time constant of 2nd lead-lag block (uel channel)	[s]	0.25
TOB1 lag time constant of 1st lead-lag block (oel channel)	[s]	5.75
TOC1 lead time constant of 1st lead-lag block (oel channel)	[s]	0.23
TOB2 lag time constant of 2nd lead-lag block (oel channel)	[s]	0.092
TOC2 Saturation ratio at 75% of maximum field voltage	[s]	0.23
Kc Current compensation factor	[pu]	0
T1 Voltage regulator time constant	[s]	0.004
Kterm_fed Terminal fed flag	[1/0]	1
Ke Exciter self-excitation factor	[pu]	0.4
Te Exciter time constant	[s]	0.5
E1 Maximum field voltage	[pu]	3.63
SE1 Saturation ratio at maximum field voltage	[pu]	0.78
E2 75% of maximum field voltage	[pu]	2.72
SE2 Saturation ratio at 75% of maximum field voltage	[pu]	0.179

During the simulation a fast-acting AVR was used to analyse critical clearing time, and the IEEE AC4 type AVR model was used to illustrate the major difference in response. A step response of 3% was analysed to see the differences in response. Figure 4.11 shows the 3% step response of the IEEE ST5B type AVR model (slow acting) and Figure 4.12 shows the 3% step response of the IEEE AC4 type AVR model (fast acting). It can be seen that the IEEE AC4 exciter excitation voltage peaks immediately, while the ST5B takes a few seconds to respond.

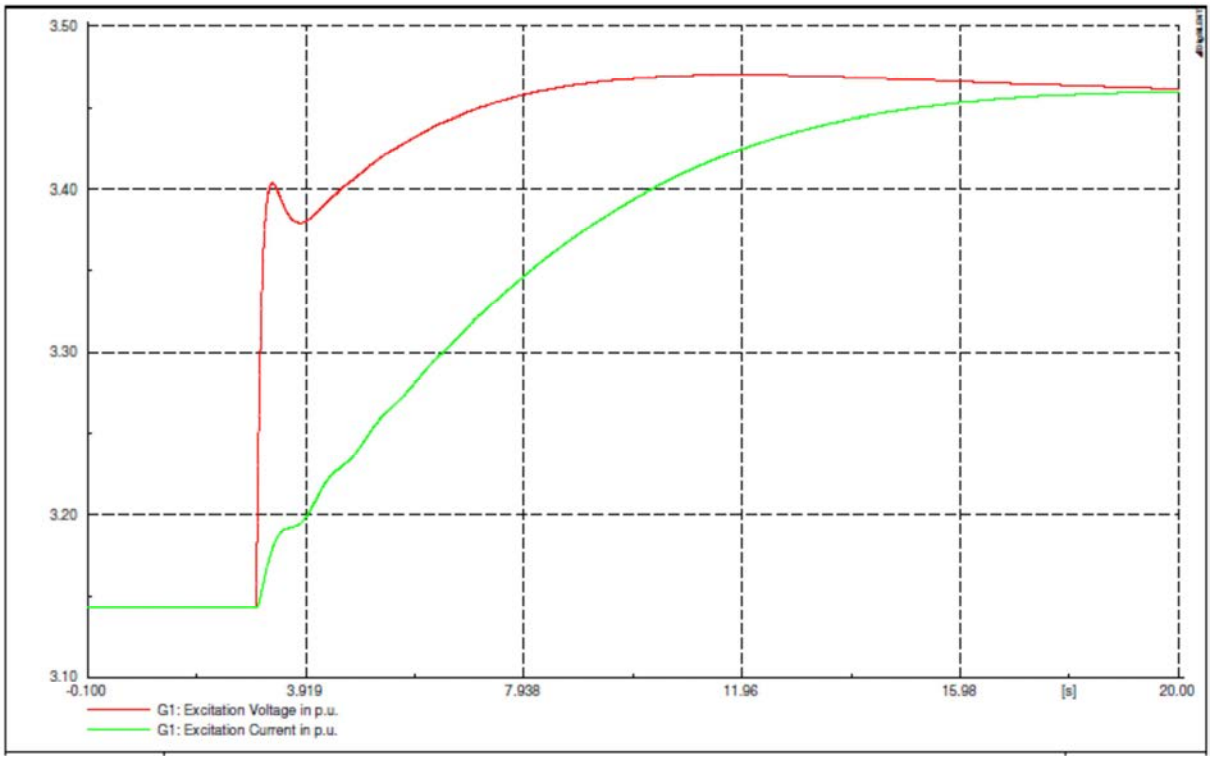

Figure 4.11 ST5B type AVR response to a 3% step

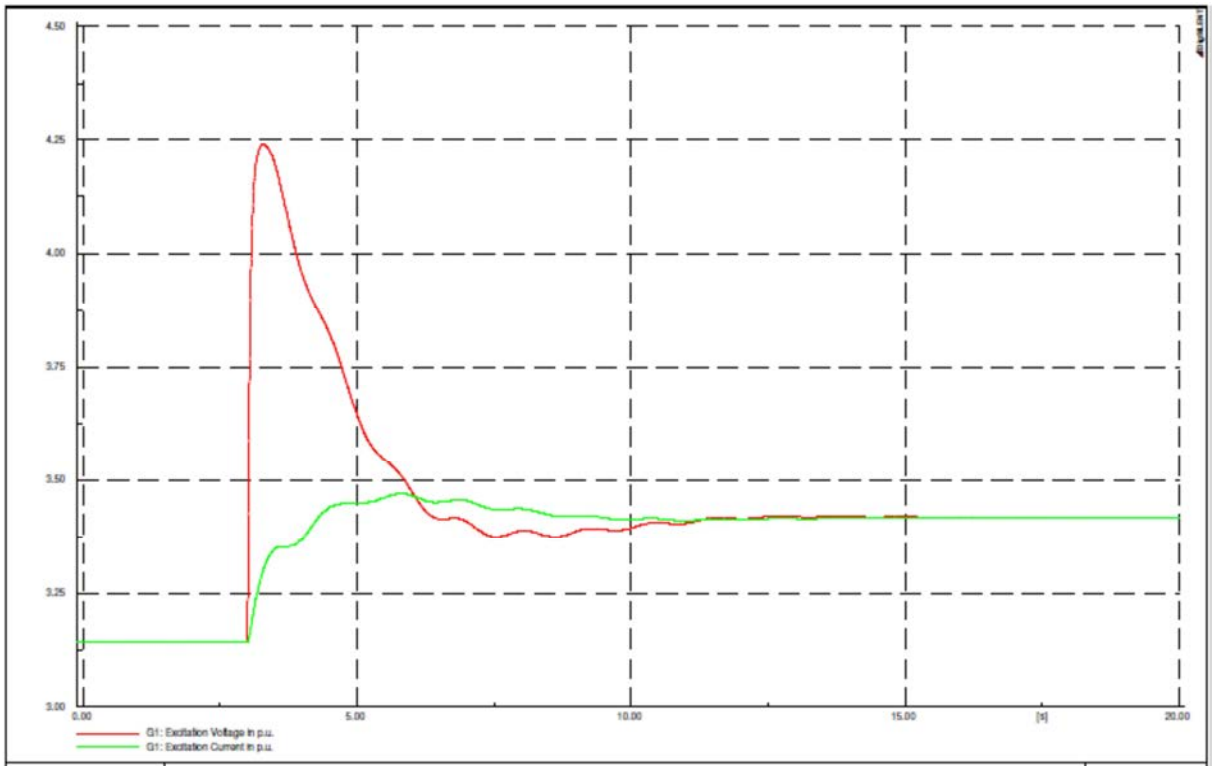

Figure 4.12 IEEE AC4 type AVR response to a 3% step

When the IEEE AC4 type AVR is used, the critical clearing time increased from 0.256 sec. to 0.277 sec. when compared to the IEEE ST5B type AVR. The AC4 type AVR increased the clearing time by 0.021 sec.

when compared to the ST5B AVR. This increase in clearing time could improve transient stability for the nuclear power station by one cycle.

Table 4.6 IEEE AC4 AVR parameters in DIgSILENT

Parameter & Description	Unit	Actual Setting
Tr Measurement Delay	[s]	0.02
Tb Filter Delay Time	[s]	12
Tc Filter Derivative Time Constant	[s]	1
Ka Controller Gain	[pu]	400
Ta Controller Time Constant	[s]	0.04
Kc Exciter Current Compensation Factor	[pu]	0.2
Vimin Controller Minimum Input	[pu]	-0.2
Vrmin Exciter Minimum Output	[pu]	-8
Vimin Controller Maximum Input	[pu]	0.2
Vrmax Exciter Maximum Output	[pu]	8

When the IEEE AC4 parameters in Table 4.6 are compared to the IEEE ST5B AVR parameters, it is clear why the AVRs respond differently. In the ST5B AVR parameters, provision is made for the response of the rotating exciter. The exciter time response is 0.5 sec. , which explains the slow response of the excitation voltage and current.

4.6 Increased generation effect on transient stability

To extend the life of the Koeberg Nuclear Power Station by about 20 years, a decision was made to replace the steam generators [15]. These steam generators are the source of steam to the turbines and play an integral part in the production of electrical power by the nuclear reactor. To increase the power output of a reactor, typically, a utility will refuel a reactor with either slightly more enriched uranium fuel or a higher percentage of new fuel. This enables the reactor to produce more thermal energy and therefore more steam, driving a turbine generator to produce electricity.

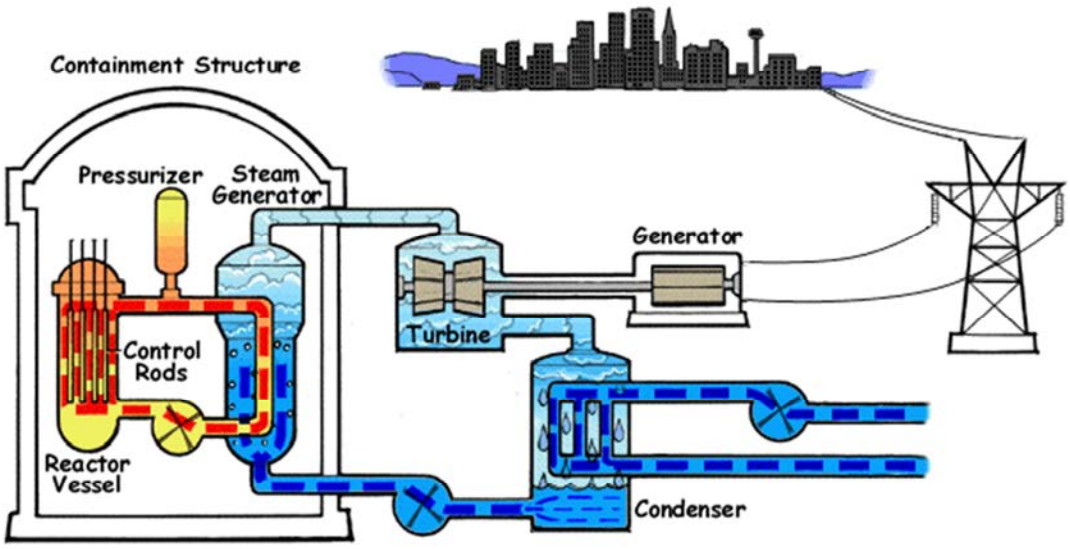

Figure 4.13 Nuclear electrical production [49]

The nuclear power plant is planning to increase the mechanical output (thermal output) from 2833MW to 3100MW, which roughly translates to an increase of electrical output from 970MWe to 1100MWe [15]. An intensive study is required to ensure that all electrical parameters are adequately rated for this upgrade. However, some components, like the generator and generator transformers, have been upgraded in anticipation of this modification and further analysis of the network needs to be confirmed. Hence, the transient stability study is required and the effect on the critical clearing time should be studied.

Once again, a short circuit was applied on the HV busbar closest to the power plant. DIgSILENT was used to determine the critical clearing time. The network in DIgSILENT was adapted for real plant parameters, like the load connected to the generator and the generator's reactive power limits set. The critical clearing time for two generators coupled to the HV busbar was found to be 0.201 sec. In the simulation package, the generator parameters were adapted to 1100MW. A critical clearing time of 0.166 seconds was obtained, and, when compared to the critical clearing time previously recorded, a significant change can be seen. This fault clearing time puts both generators into a "Pole Slip Condition." The standard clearing times in the HV transmission plant never exceeds 0.1 sec., thus confirming that "no protection" setting requires adjustment and new operating parameters can be established. However, the 0.066 sec. margin is close to the transmission clearing time of 0.1 sec. and should be noted in the planning of the upgrade.

In this section, results from three case studies are presented to give better insight into the behaviour of the nuclear power plant's stability when a three-phase short-circuit is applied to a HV busbar close to the generator at a nuclear power station. Analysis of these results will help evaluate vital parameters to ensure correct operation of a nuclear power plant when changes are made.

All previous simulations were completed only with one generator in service. However, the nuclear power plant has two generators coupled to a common busbar. This common coupling confirms that both generators will see the fault and their rotor angles will swing together. Although most studies use the N-1 criterion as the worst case analysis, the two machines swinging together gives reduced clearing times when connected together. This is largely due to the impedance change and the combined powers of the two generators connected to the common coupling busbar. All three-phase faults were placed at the common HV busbar, and a comparison of the three methods used to determine the critical clearing times can be seen in Table 4.7. Critical clearing times reduce by approximately 20-30 milliseconds, which equates to a 10% reduction in critical clearing times when both generators are coupled to the common busbar as compared to a single generator coupled to the busbar. Although discussed earlier, this needs to be re-iterated again.

Table 4.7 Comparison of different methods to determine critical clearing times

Equal Area criterion		**Modified Euler**		**DIgSILENT**	
1 Generator	2 Generators	1 Generator	2 Generators	1 Generator	2 Generators
0.264	0.235	0.270	0.240	0.251	0.231

This 10% decrease in critical clearing time when compared to a single generator coupled to the common coupling busbar has a negative effect on the transient stability of the nuclear power plant. One could argue that the main reason for the reduction in critical clearing time could be attributed to the increase in power when the two generators are coupled to the infinite bus and not solely due to two generators coupled to the common busbar. The clearing time margin is reduced dramatically to the transmission network limit of 0.1 sec. Analysis of the two generators coupled to a common busbar gives insight into the reduction of clearing times when both nuclear units are in service. This places a huge risk on the network, as it poses a risk of losing both generators via pole slipping, which could possibly lead to widespread power losses and prolonged generating source repairs.

As discussed earlier, the South African grid has not been subjected to cascading unit trips; however, this still remains a possibility. Studies like these give insight into how a nuclear plant having two generators would react when a disturbance/fault is placed close to the power plant. Although the likelihood of a three-phase fault at the HV busbar is small owing to the busbar configurations which are independent and insulated from each busbar. This type of fault would only be a certainty if a portable or motorised earth was placed for maintenance and was left on when the circuit was re-energised. This brings in the human element, which is the cause of many grid disturbances that have occurred and are detailed in Appendix G.

The details of Appendix G are taken from the nuclear power plant's internal problem notification system. In reality the nuclear power plant is most at risk when both generators are operating and the fault is close to the power plant. Thus, all activities planned for the HV switchyard require a thorough review which details all the risks to the plant, as the situation might cause significant power losses in the Western Cape Grid.

System operators are required to set-up the grid to prevent widespread power outages and possible generator damage owing to pole slipping when a disturbance is caused by a fault close to the power station. Mitigation plans by the system operator can prevent further power loss if the network is adapted. A relationship between the system operator and the plant operators is required before any changes are made to ensure that the nuclear plant will be able to withstand network faults. A working group was established at the nuclear power plant to discuss this very issue, and the group convenes on a monthly basis, so that both parties can discuss all issues and evaluate the risks [50].

5. Emergency Diesel Generator Response to Grid Disturbances During 100% Load Testing

Nuclear power plants require dedicated off-site diesel supplies and on-site emergency diesel generators in the event of a power system failure. These systems form part of the licencing agreement between the National Nuclear Regulator and the power plant, and play a vital role in nuclear safety. Without sufficient electrical supply to essential equipment used to cool the reactor during a unit trip and loss of grid supply, there would be a catastrophe. Therefore, the nuclear power plant requires a reliable back-up supply, to ensure that critical components are available and accessible during a loss of electrical supply.

The emergency power supply system consists of the two emergency trains referred to as A and B. Each train consists of an emergency switchboard LHA and LHB with an emergency diesel generator connected to it, namely, Gen_LHP and Gen_LHQ (see Figure 4.1). In the event of a total loss of off-site electric supply (400kV and 132kV) and if attempt to fall back to house mode (24kV plant generator, G1 and G2 in Figure 4.1) fails, then back-up is provided automatically by two emergency diesel generator sets (one for each train).

These emergency diesel generators automatically start up on an under-voltage signal and are connected 10 seconds after their respective emergency switchboards have been de-energised. This is done after opening the normal incomer breakers on LHA and LHB switchboard. As mentioned earlier, the emergency diesel generators are started either by a special under-voltage signal originating on switchboards LGA and LGD or in case of an accident by a specific signal coming from the reactor protection system (safety injection or containment high pressure). If a prolonged under-voltage signal persists on the LHA or LHB switchboards, the switchboard loads are tripped, the diesel generator is connected, and the loads are reconnected in a pre-determined sequence. This re-connection of the electrical supply on the essential switchboards is vital to nuclear safety to ensure that the equipment used during a nuclear incident is supplied to bring the plant down safely.

5.1 Transient behaviour of the on-site emergency diesel generator following thermal power upgrade

The Fukushima nuclear power plant incident proved that diesel generators are imperative for nuclear safety and are the most vital pieces of back-up equipment, along with the plant DC back-up system. Here, the loss of off-site supply coupled to the diesel generator electrical switchboards flooding caused the reactor to melt

owing to the lack of core cooling as a result of the lack of electrical supply essential to the operation of the pumps [51].

As previously discussed, these types of studies have become more and more critical to the safeguarding of nuclear power plants. Therefore, all associated generators are to be verified to withstand a transient or able to protect themselves from damage. Many small generators however, including the emergency diesel generator (EDG), are not equipped with pole slip protection, and therefore verification of their clearing times is important in determining system health or availability of vital supplies during transient disturbances. The diesel generator operation, diesel engine and generator explanation are discussed next.

5.1.1 Diesel generator operation

The diesel generators fulfil an extremely important function at Koeberg Nuclear Power Station. In the event of the loss of external power supplies, they supply the necessary power to bring the reactor to a safe state (cold shutdown) and maintain that condition.

Emergency power supply is provided by two generator sets per unit, each with a generator power rating of 4800kW at 0,8 power factor. One diesel generator supplies the 6,6kV ac LHA busbars; while the other diesel generator supplies the 6,6kV ac LHB busbars. Both LHA and LHB, as shown in Figure 5.1, supply the safeguard auxiliaries that are systematically redundant. It is sufficient to have only one of the two diesel generators operational for the safe shutdown of the unit.

Each diesel generator is installed in its own building, which provides independence and isolation between the generators of the two safety systems and the generators of the adjoining unit. The diesel generator buildings are located such that 1 LHP and 2 LHQ are located on the north side of the station, while 1 LHQ, 2 LHP and 9 LHS are located on the south side. This arrangement ensures that no single significant event can affect both generators and ultimately both safety trains of the same unit.

The auxiliaries associated with the diesel generator are supplied under normal operation in the same manner as other auxiliaries, i.e. the network supply. When the generator is connected to its associated safeguard board, it supplies its own auxiliaries. The total power required from the diesel generators by the connected motors during the restarting of the auxiliaries cannot be provided as a single step load. For this reason, a tripping and reloading programme is provided. Loss of supply to the 6,6kV ac switchboards is detected by the “loss of voltage” signal at the safeguard busbar level, which initiates the switchover to the generator set that then provides the electrical supplies to ensure an automatic and safe shutdown of the unit.

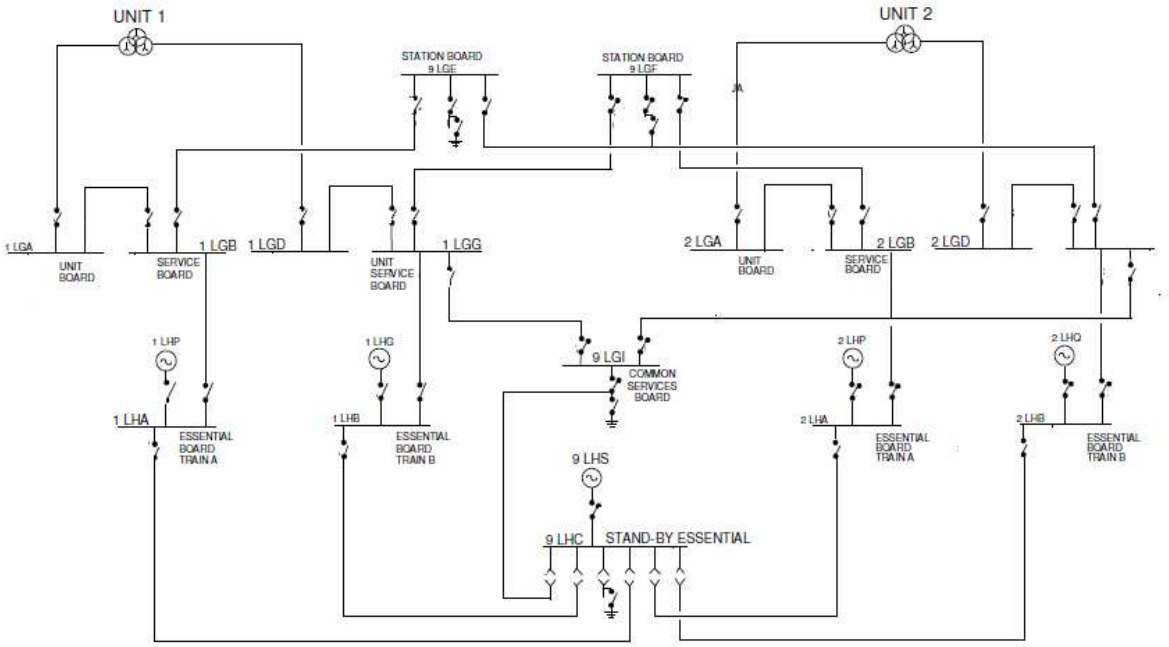

Figure 5.1 Koeberg electrical distribution system

5.1.2 Diesel engine and generator

The diesel engine is an 18 PA GV 280 engine, which is a single-acting, 4-stroke, 18-cylinder engine, turbocharger boosted, with cooled air, mechanical fuel injection and compressed air starting. The nominal operational speed of the engine is 1000rpm.

The generator terminal voltage is 6.6kV and is rated to supply 4800kW at 0,8 power factor. It is provided with a ringless, brushless excitation system consisting of the main exciter LHj 002 AP and a rotating diode bridge. The brushless exciter is mounted on the end of the rotor shaft and, when rotated at 1000rpm, produces direct current (dc) supply which produces the rotor's excitation current. This current produces an electromagnetic field in the rotor. The rotating electromagnetic field induces a three-phase 6,6kV 50Hz alternating current (ac) in the star windings of the stator. This can be seen in Figure 5.2.

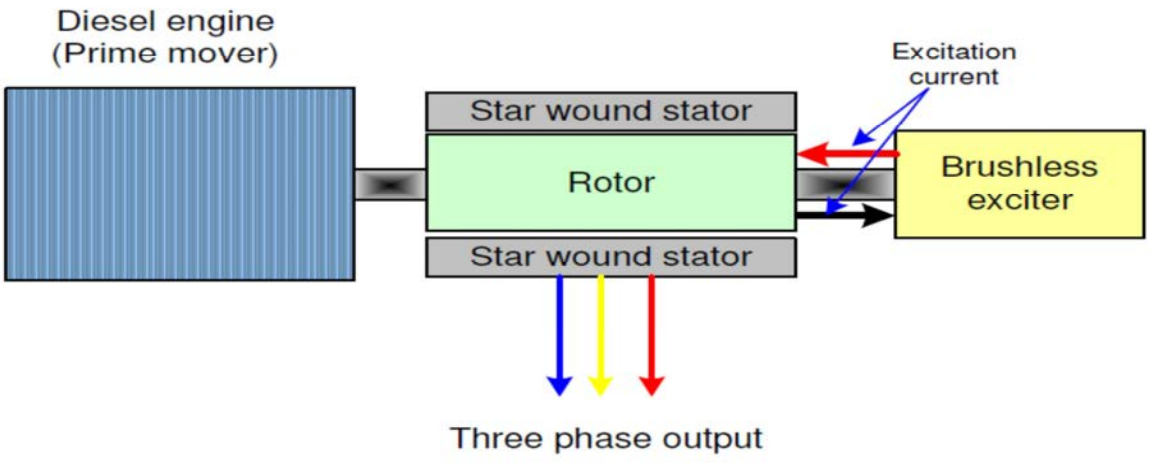

Figure 5.2 Integrated diesel generator system

As the dissertation examines the topic of transient stability within a nuclear plant, it is vital to perform a study on all on-site supplies, as they form the basis of nuclear power plant integrity. There is a need to ensure that, during an off-site disturbance, no damage occurs to the essential back-up supply (during these transients).

The risk however only exists when the routine testing is carried out on the EDG. These are usually performed periodically as the engine is required to run at 100% load, as determined by the Original Equipment Manufacturer (OEM), to prolong life and prevent build up in the exhaust stack. The diesel generator is synchronised to the network via the diesel circuit breaker, while the network breaker remains closed. The operator increases the MW by increasing the speed reference of the engine, which in turn increases the output power, and the MVArs are increased to a predetermined value via the voltage regulator. This synchronised load test poses the most risk, as any network disturbance would affect the diesel generator. In essence, the risk is reduced owing to redundancy, as each nuclear generator has two electrical trains with identical equipment both backed up by an emergency diesel generator. However, the effect of grid disturbances on emergency back-up equipment should still be verified.

5.2 Emergency diesel generator critical clearing time

The effect of a three-phase fault on the diesel generator was investigated using the critical clearing time to determine the point of instability. The network was configured as before with a grid in-feed used to simplify the national grid, and all the plant's internal plant parameters were simulated up to the 6.6kV network with all the loads lumped as PQ loads. The network was configured both with the single generator and both generators connected to the HV busbar, the first being the N-1 contingency with one nuclear power plant unit shut down for routine maintenance. The previous chapter validated the simulated information with plant data for the correct simulation. However, for this simulation, the network was configured with reactive power limits and the AVR installed.

The simulation results in DIgSILENT for the critical clearing time of the emergency diesel generator Gen_LHP or Gen_LHQ was found to be 0.271 sec when a fault was applied externally to the plant. This is around 0.07 sec. more than the main generators G1 and G2 whose critical clearing time was 0.201 sec. Further analysis of the critical clearing time for three-phase faults at the plants 24kV internal generator terminal was found to be 0.207 sec at the diesel generator. The simulation results indicate that once the main generator pole slips, the relevant diesel generators will pole slip as well.

The emergency diesel generator however has an under-voltage protection two out of two logic, which trips the diesel breaker if it detects a 30% under-voltage, and both relays have to detect the under-voltage to initiate a diesel breaker trip. This protects the emergency diesel generator during network transients by opening the diesel breaker. However, based on historical events, protective devices occasionally fail to operate, which leads to cascading tripping. In the case of the diesel generator, this could have an adverse effect on the plants safeguard system. This fact gives insight and risk recognition when the EDG is connected to the grid as depicted in Figure 5.3. The 100% load test configuration would have 001JA (network breaker) closed and 002JA closed (diesel breaker).

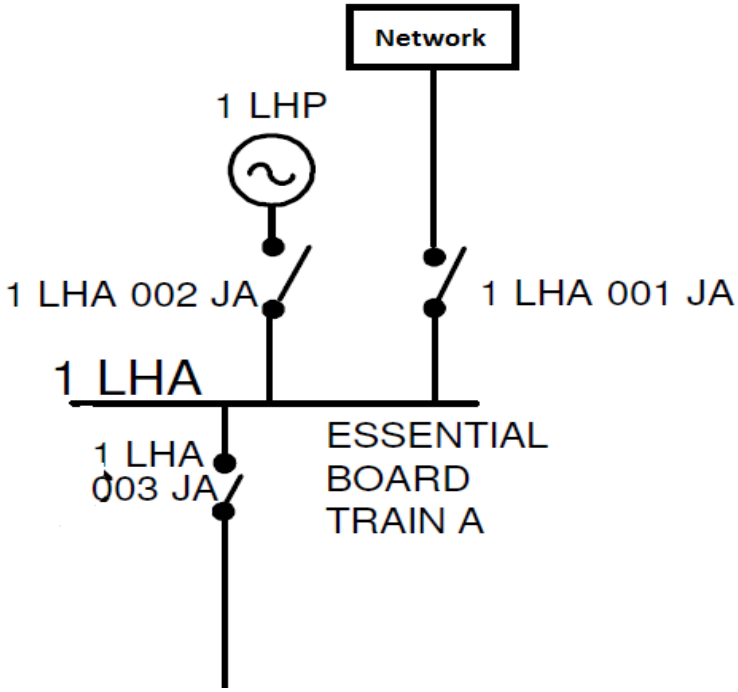

Figure 5.3 Network and diesel breaker configuration

The EDG is most vulnerable to grid disturbances during this period. The current under-voltage protection scheme could possibly not operate as designed for various reasons, which could cause the diesel generator to pole slip while connected to the network. Figures 5.4 and 5.5 provide the DIgSILENT plots for rotor angle and speed of the diesel generator during a three-phase fault applied on the HV busbar closest to the nuclear power. The fault was cleared by the protection in 0.160 sec. with the emergency diesel generator transiently

stable following the disturbance. Further DIgSILENT plots for the emergency diesel generator can be found in Appendix H.

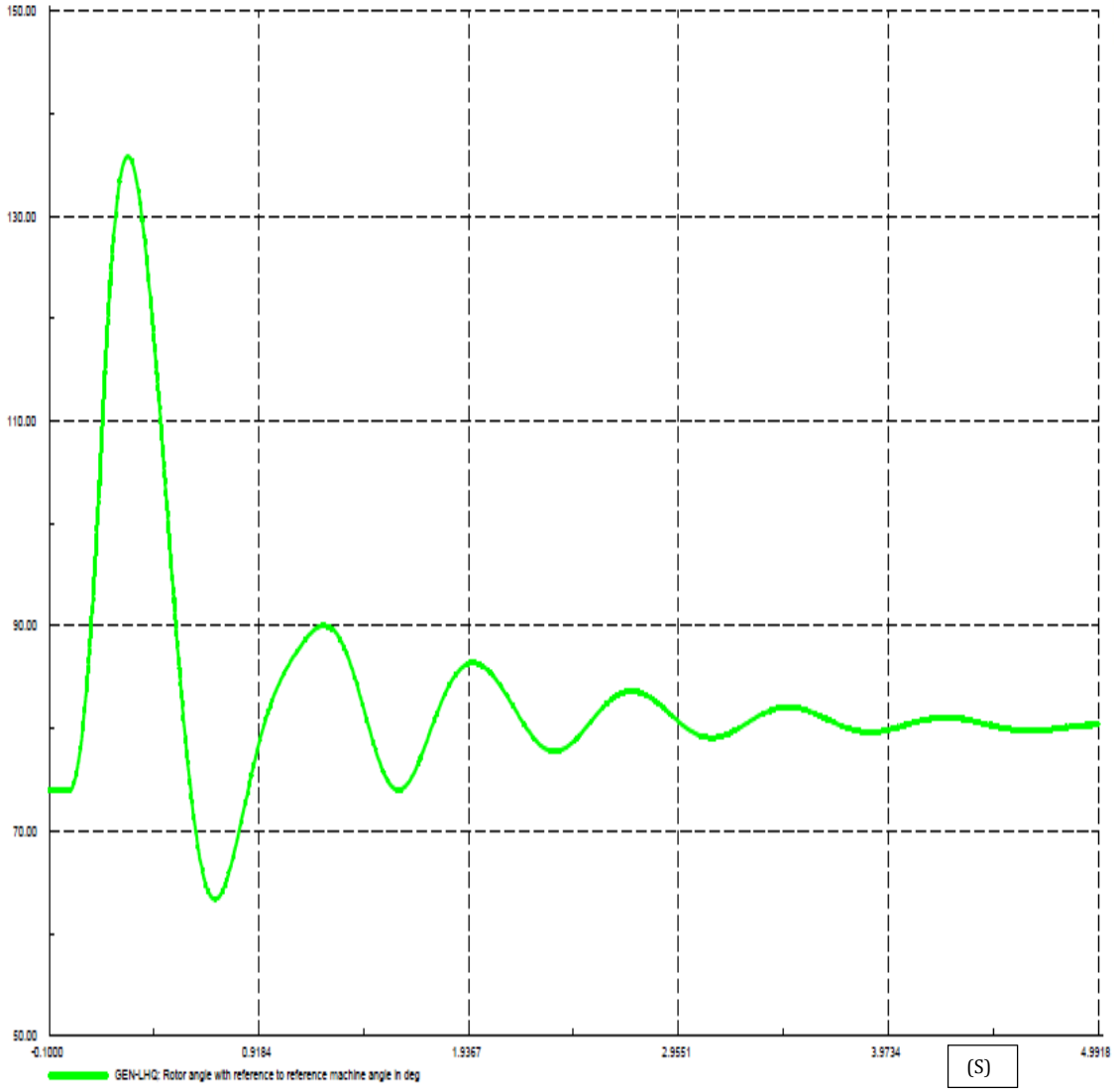

Figure 5.4 Emergency diesel generator rotor angle plot in DIgSILENT

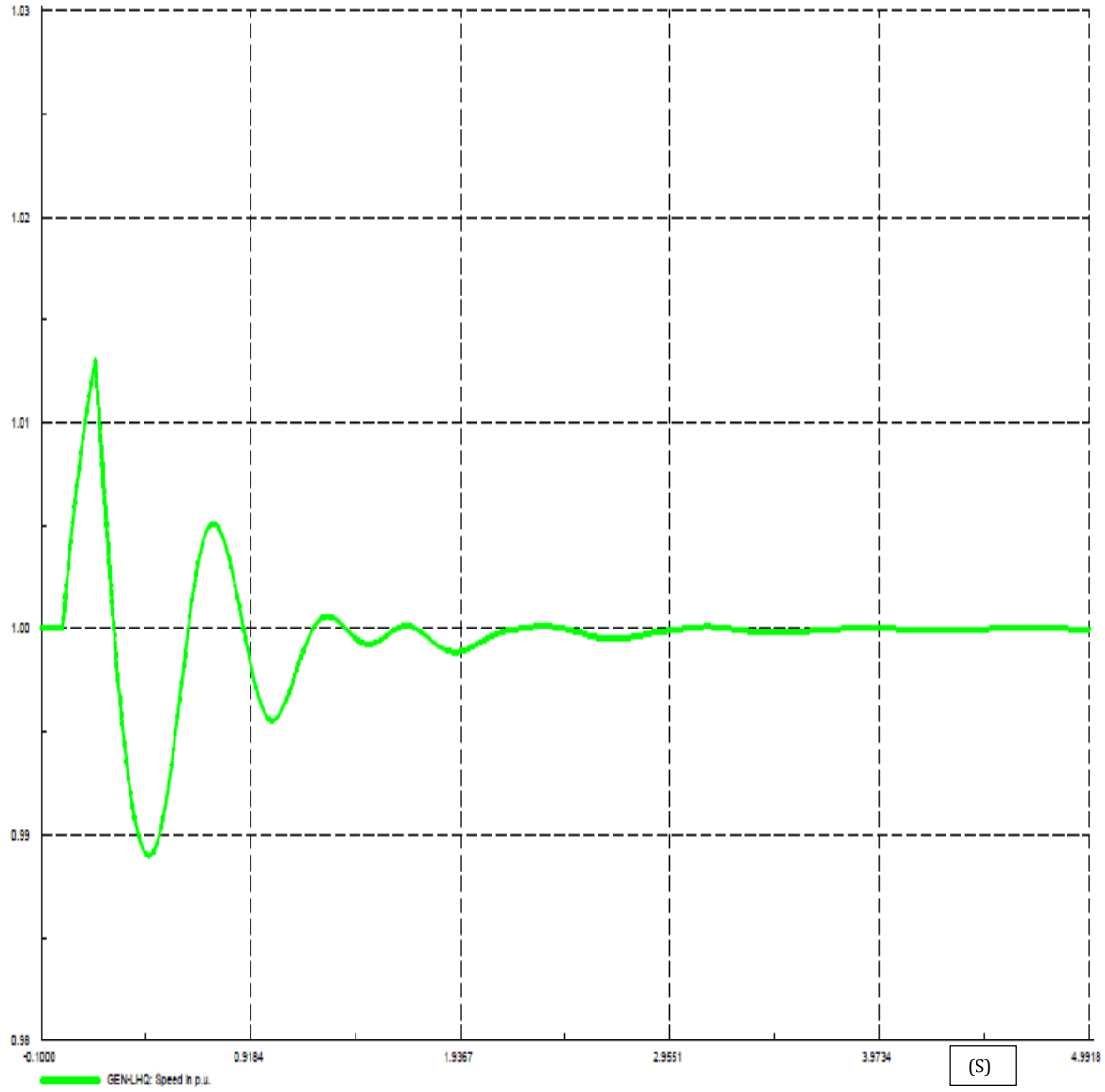

Figure 5.5 Emergency diesel generator speed plot in DIgSILENT

6. Western Cape 400kV Network Response to Transients

The nuclear power plant is not an isolated generating unit. It forms part of a very delicate network or electrical grid whose topology can be seen in Appendix I. The nuclear power plant is the only base generating supply for the Western Cape and is aided by peaking stations for power during high loading situations. The grid is characterised as having long lines between strong generating sources in the north, with a much smaller generating source in the south. This characteristic lends itself to instability, as power transferred over long distances requires reactive power to ensure grid stability. The Western Cape grid is separated from the mass generating pool by a connecting corridor called Hydra [4]. It isolates the Western Cape grid from the rest of the network during faults, thus making the Western Cape grid a small grid on its own. This places huge emphasis on maintaining the supply of the two nuclear power generators as it forms an integral part of the grid and ensures stability to the Western Cape grid.

Plant ageing, climate changes and human factors have caused considerable decrease in reliability of generating plants worldwide. The examples given in sections 2.2 and 2.3 have been linked to ageing equipment, high loading and protection malfunction. These factors have caused widespread power outages, which not only affect customers but also affect the economy negatively, as production is halted.

Although a reduced network allows for quick computation, a more comprehensive network is required to determine if the nuclear plant would be stable under different dynamic conditions. The latter allows for dynamic simulation which has more validity. A more advanced network gives insight into the effect a three - phase short-circuit close to the nuclear power plant has on the rest of a network and what the effect would be on other generators in and around the nuclear power plant.

Unfortunately, networks are not made up of a single/double machine connected to an infinite bus. Network loading changes continuously depending on peak or non-peak times. Network parameters were configured for different scenarios to determine critical clearing times under various fault conditions. The nuclear plant design is such that it has a dedicated off-site supply other than the grid supply. However, the network sometimes requires reactive power support and starts these plants up to ensure system stability during high loading. At some point back-up supplies are periodically tested. Changes in network frequency and voltage could have an adverse effect on dedicated safety systems.

Again, multiple scenarios are required to identify possible short-comings in ensuring a reduction of risk to the plant. A typical example would be the testing of the emergency diesel generator for 100% load, with the

back-up gas turbines used as an alternative supply if the grid supply is unavailable. All these scenarios were tested using the complete DIgSILENT network and internal plant parameters.

A generator may pole-slip, or fall out of synchronism with the power system, for a number of reasons. The principal causes are prolonged clearance of a heavy fault on the power system, when the generator is operating at a high load angle close to the stability limit, or partial or complete loss of excitation. Weak transmission links between the generator and the bulk of the power system aggravate the situation. It can also occur with embedded generators running in parallel with a strong utility network if the time for a fault clearance on the network is slow, perhaps because only IDMT relays are provided. Pole slipping is characterised by large and rapid oscillations in active and reactive power. Rapid disconnection of the generator from the network is required to ensure that damage to the generator is avoided and that loads supplied by the network are not affected for very long. Protection can be provided using several methods. The choice of method will depend on the probability of pole slipping occurring and on the consequences should it occur [37].

Scenarios based on the entire Western Cape grid were divided into two categories, namely:

- faults close to the nuclear power plant; and
- faults at other power station busbars further away (i.e., 800km away).

These faults are predominantly three-phase faults, but an assessment of a single phase to ground fault was also completed. Based on the simulated data, the critical clearing times did not change much when a single phase to earth fault was subjected to the HV busbar. This type of fault seems to be the most realistic, as the busbars are encapsulated by individual busbar chambers filled with SF6 gas. The likelihood of a single phase to ground fault is also more realistic as these faults are more common and can usually propagate over time before widespread trips occur.

6.1 Faults close to the nuclear plant

The 400kV Western Cape network, including all generators, is shown in Figure 6.1. The first fault was applied at the busbar closest to the nuclear power station, with a comparison in critical clearing times for all the required assessments detailed above. Again, taking into consideration that network configurations can vary, the network was configured to have all generators in service.

The critical clearing time for the nuclear power plant for a fault close to the nuclear plant was 0.201 sec. If compared to the reduced network with the AVR switched on, reactive power limits of the generator was set and the loads connected the critical clearing time was 0.201 sec. The critical clearing time of the reduced network was found to be the same as the complete network for faults close to the nuclear power plant. One major observation when performing the study was that all the generators in the Western Cape would pole slip once the nuclear plant pole slipped. It caused a cascading trip on all the generators within the Western Cape network. Hence, the prevention of pole slip is critical to the safeguard of the nuclear power plant.

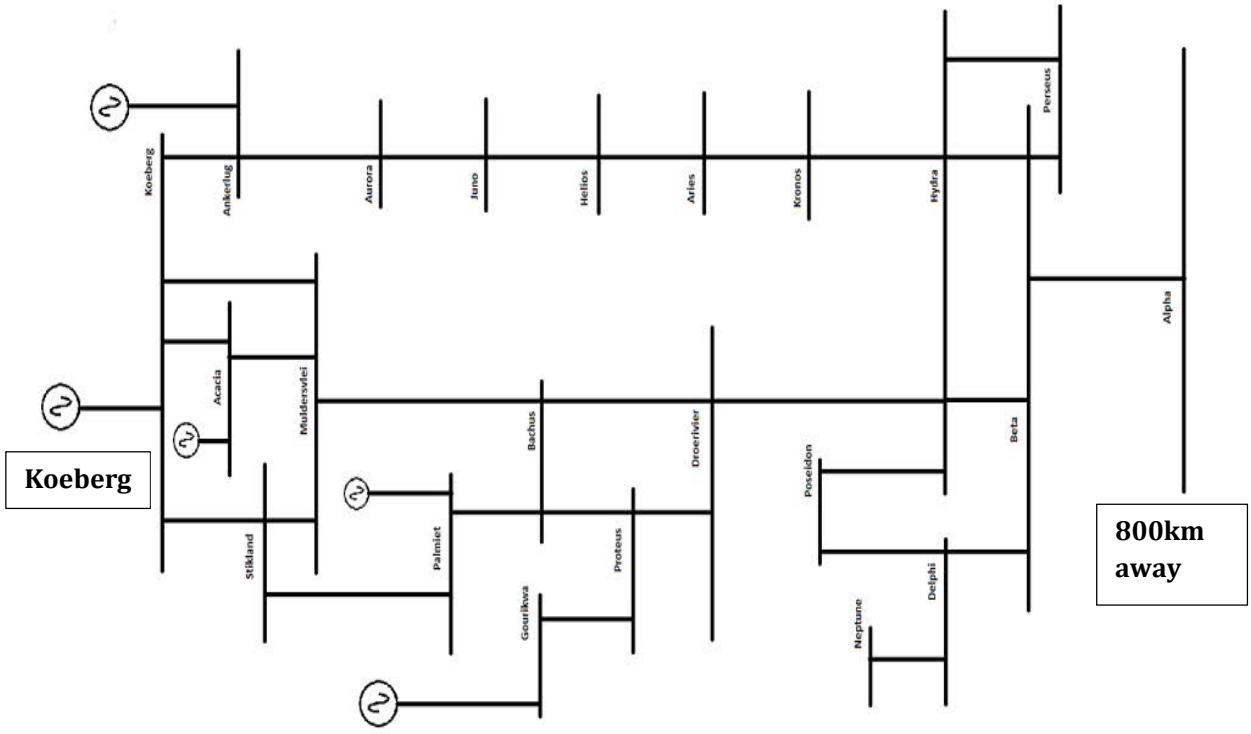

Figure 6.1 400kV network including all generators

6.2 Faults further from the nuclear plant

Although the worst fault would be a fault close to the power station, one should not rule out the likelihood of a fault occurring further away from the power plant. The network topography of the South African electricity grid illustrates that the power stations have long lines between them and are far away from one another. Analysis of faults further away from the power station is as critical as faults close to the power station.

The case study placed a three-phase short-circuit fault 800km away from the power station. In this case the critical clearing time for the nuclear power station was increased. The critical clearing time was found to be 0.278 sec. compared to the clearing time of 0.201 sec. for faults close to the power plants busbar. Although the critical clearing time increased, there was an effect on the power plant, which means that no plant acts in isolation when a fault occurs. All the generators on the network swing together, but their magnitudes vary depending on the fault. Figure 6.2 displays the speed plots of all the generators in the Western Cape grid during a 200 millisecond fault at 800km from the nuclear power station.

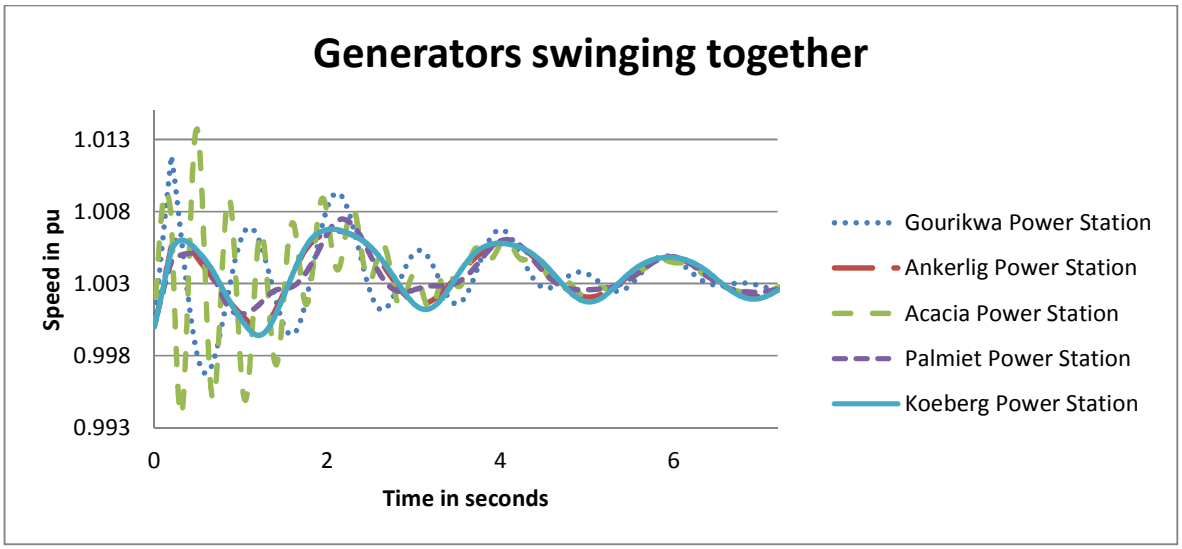

Figure 6.2 Western Cape generators swinging during a fault

In all scenarios the generators in the Western Cape grid would pole slip causing cascading tripping when determining the critical clearing time for faults at the nuclear power plant based on the DIgSILENT simulation package. When analysing the previous issues relating to black-outs, cascading tripping has always been the common outcome. The analysis proved that faults further away from the nuclear plant have a lesser effect on the critical clearing time of the nuclear power plant. However, network operators and protection schemes are required to ensure that the network is kept stable. Figure 6.3 displays the speed plots of all the generators in the Western Cape when an instability condition occurred.

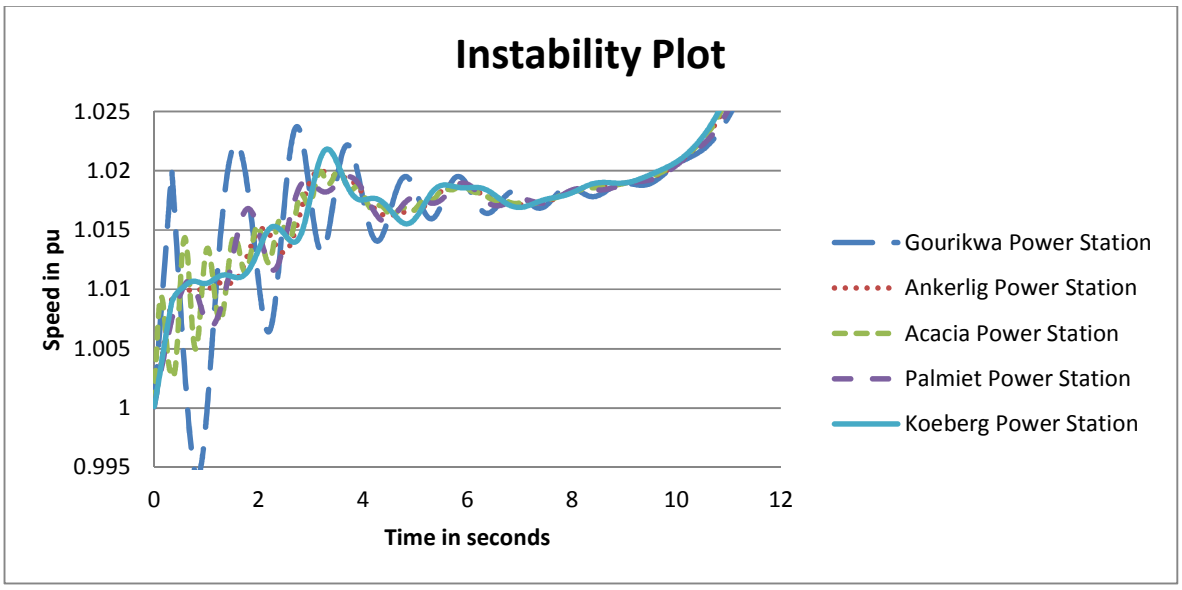

Figure 6.3 Speed plot displaying the speed of the generators in the Western Cape during an instability incident

A comparison in rotor angle relationship between faults close to the power station and faults further away can been seen in Figure 6.4. The generator's maximum rotor angle for a fault close to the power station for a three-cycle fault is 166.43°. The generator's maximum rotor angle for faults 800km away was 154.48°. This is approximately 12° variance in rotor angle for the different fault locations.

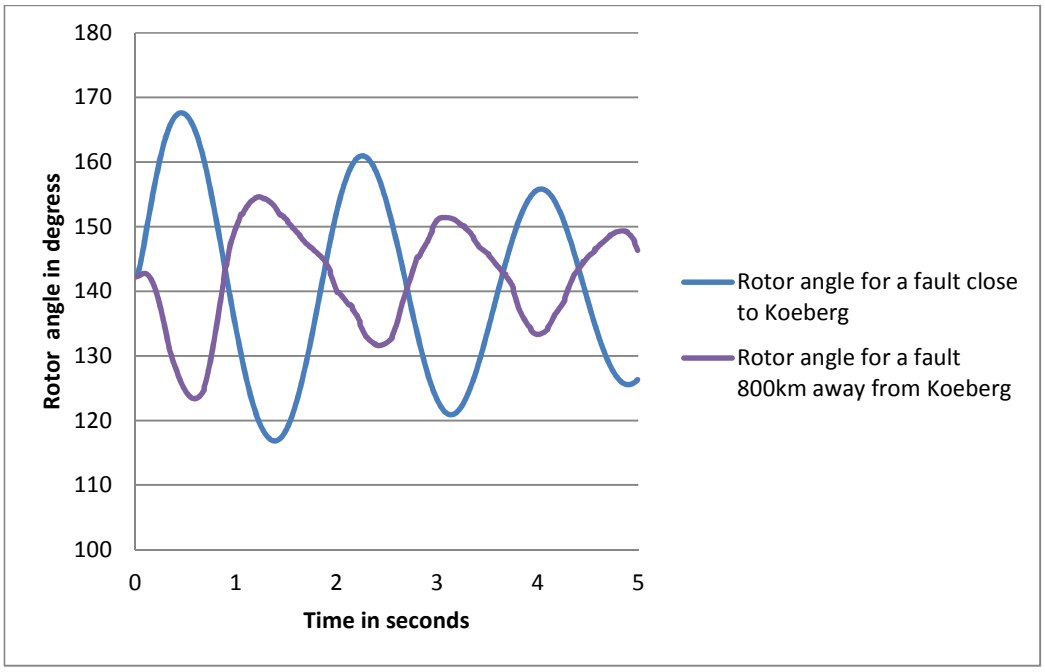

Figure 6.4 Rotor angle comparison for a 3 cycle fault close to Koeberg compared to a fault 800km away.

6.3 Pole slip protection assessment

Protection settings shall be such that protection equipment shall not operate unnecessarily as protection trips impose stress on the reactor, shutdown plant and cause a loss of revenue. This is to ensure maximum availability of generating units while providing adequate protection against faults and abnormal conditions.
Pole slipping of generators, with respect to the system, can be caused by a number of conditions leading to an increase in rotor angular position beyond the generator's transient stability limits. Some of the causes of pole slipping are:

a. large network disturbances;
b. faults on the electrical network close to the generator;
c. weak ties between the network and the generator (tripping of transmission lines);
d. loss of generator field (field winding or excitation supply failure); and
e. operating the generator in an excessive under-excited mode.

There are different types of pole slipping relays. The nuclear power plant uses a combination approach to pole slip protection. The first relay detects the internal angle of the generator by measuring the rotor angle position relative to the stator terminal voltage. The second function combines a reverse power function to the internal angle measurement. This is to detect the power inversions that occur during asynchronous operation.

Slip counting is employed before a trip signal is issued. The reverse power relay measures current and voltage on the generator terminals. The relays are set to operate for reverse directional power.

The reverse power setting currently is set to 5% of the active power. It is currently set to 48.5MW, which is 5% of the 970MW the power plant produces. Hence, with the thermal power upgrade, the settings will change to 55MW. This is not a significant change and requires a dial-setting change on the relay to adapt.

The internal angle protection relay is currently set to 150°. The equal area calculation for $\delta max/\delta_3$, which can be seen in the equal area calculation in Appendix A, was calculated and found to be 151.25° for a single generator coupled to an infinite bus. The DIgSILENT simulation plot for the internal (rotor) angle can be seen in Figure 6.5, with the generator stable when the rotor angle was above 150°. Even if the output of the generator is increased following the thermal power upgrade, the current relay setting does not need to be changed as all the critical clearing angles are above 150°, making it a more conservative setting.

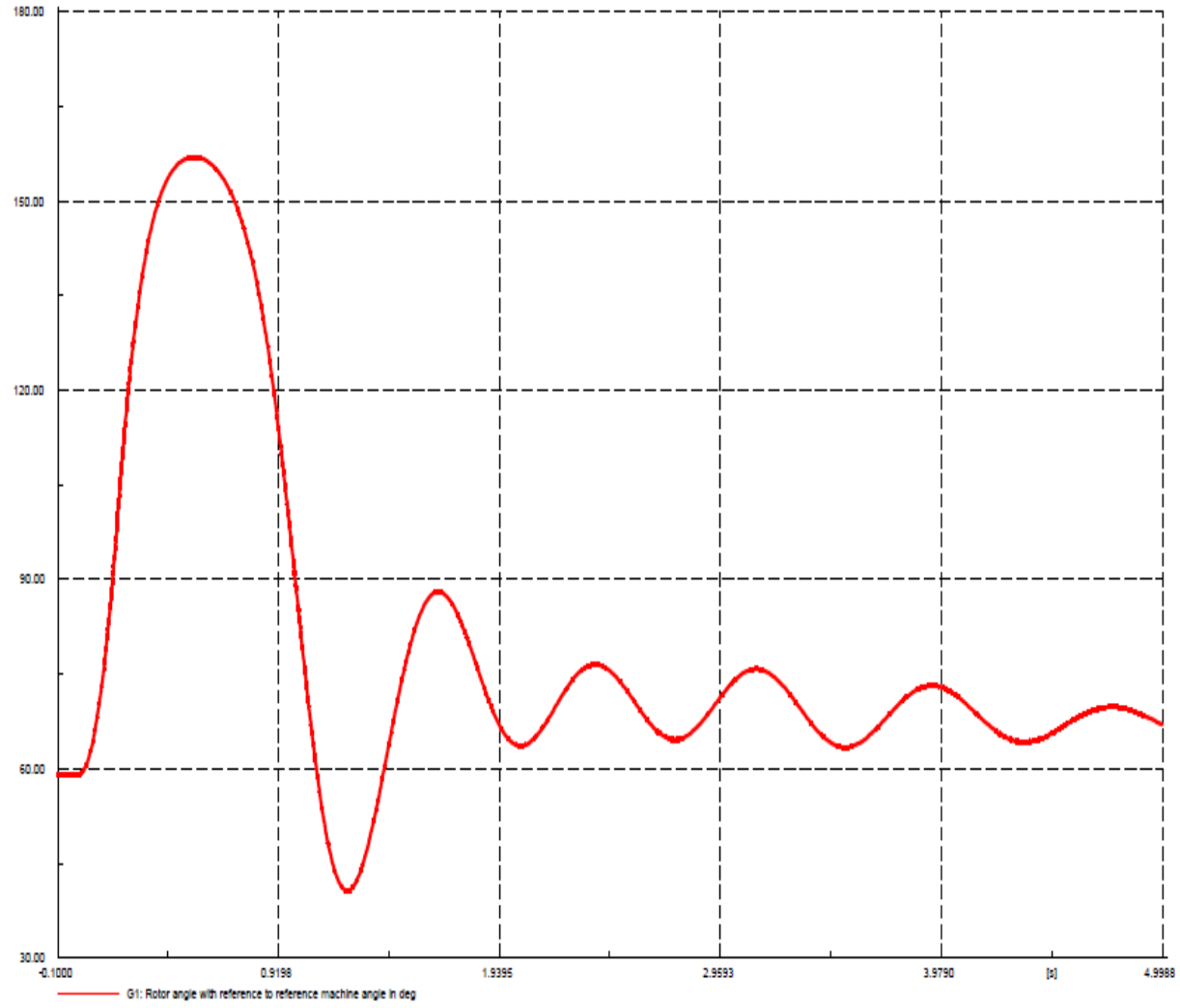

Figure 6.5 Rotor angle plot of unit 1 generator in DIgSILENT

7. Conclusions and Recommendations

7.1 Conclusions

This thesis studied and validated the nuclear power plant DIgSILENT model against known parameters, analysed the plant response with the Automatic Voltage Regulator (AVR) with respect to future capacity expansion plans under various plant configurations, investigated the network response to transients emanating from switchyard faults close and far away from the nuclear plant. The reaction of the Western Cape grid during these disturbances post thermal power upgrade and the transient behaviour of the on-site emergency generators during faults on the 400kV transmission network with an increase in generation at the nuclear power plant was also studied. To this end, the following conclusion where reached.

- Although the plant measured data are different to the simulated results, they are comparable when analysed. The load flow results given by DIgSILENT are a worst case scenario, which takes all the equipment in service into consideration. Hence, the load flow for this analysis is deemed acceptable and comparable and can be used for future work.

- The short-circuit study provided a valuable confirmation of studies completed 34 years ago. The anomaly noted with the line parameter only yielded a 2-4.2% difference between the original documentation and the simulated short-circuit results. A great level of confidence is given when the data simulated is comparable to the original documentation. This was achieved and understood in the dissertation with an update and recent computer-based model that could be used for further research into protection analysis and possibly arc flash calculations, which are a major plant safety focus currently.

- Data collated from the load flow and the short-circuit study were used to allow for the next step in the process, which confirms critical clearing times using different methods. The first method used to calculate the critical clearing time was the equal area criterion calculation. Here, the plant data was used to calculate the critical clearing time for a single generator or a double generator connected to an infinite bus. The results from the calculation were found to be 0.264 sec. for a single generator and 0.235 sec. for both nuclear plant generators connected to the common busbar. The second method was used to validate the equal area criterion calculation. For this method, called the modified Euler method, Microsoft Excel programme was used to solve the critical clearing times. Critical clearing time results obtained were found to be 0.27 sec. for a single generator and 0.24 sec. for two generators feeding into the infinite bus. The final assessment used a computer-based simulation tool, DIgSILENT, to perform critical clearing time calculations by placing a short circuit at the HV busbar and iteratively checking the critical clearing time before the generator pole slips. The results for a single generator were 0.251 sec. and 0.231 sec. for the two generators.

- The simplified network simulation results yielded similar results when compared to the calculation completed using the equal area criterion and the modified Euler method to determine the critical clearing times under various conditions. The results, when analysed, are all less than 1% of each other, which give great confidence in the calculation and simulation. The simplified network also gives a platform for future upgrades and designs to enable plant engineers to perform simulations before implementing modifications. The study confirms that this approach has been effective, based on the results obtained.

- The simulation results indicate that the use of a slow acting AVR has no substantial impact on the critical clearing time of the power station. This is predominately due to the rotating exciter installed on the plant, which was modelled in DIgSILENT to be a reflection of the plant's response during faults. As discussed in the results, when the exciter type was changed to a faster responding exciter, it produced better results and improved the critical clearing time by 10 milliseconds.

- With the nuclear power plant's plan to increase generation, the effect on critical clearing times is the most profound. An increase in generation by 12% reduces the critical clearing time by 17%. The new critical clearing time of 0.166 sec. is very close to the boundaries of the 0.1sec. maximum operating time of the protection scheme and auxiliaries. Therefore, this should be considered in the design of the thermal power upgrade project.

- The effect that increased generation has on the emergency diesel generators has also been analysed. The Fukushima nuclear incident has caused a greater appreciation of the emergency diesel generators in accident conditions [51]. Having performed the analysis, we found that the emergency diesel generators are most at risk when the generator is connected to the network during its 100% load test. Based on the studies performed, we further found that the diesel generators would be stable if the fault is cleared within the 0.271 sec. clearing time. There was no information relating to the critical clearing times of the emergency diesel generator, and these studies have contributed significantly to our knowledge of the behaviour of the generators under network transient behaviour.

- The entire Western grid network was analysed for critical clearing times for faults close to the nuclear power station and faults 800 km away. When using the detailed network, faults close to the power station have similar clearing times to the clearing times obtained using the reduced network. Faults some 800km away, will still have an adverse effect on the nuclear power plant, based on the simulation results obtained.

- All the completed studies give confidence in the system model and the effect that different parameters have on the nuclear power station. The study ensures that nuclear integrity is maintained and that the plant will not trip unnecessarily for faults at the HV busbar closest to the power plant.

This caters for generator house loading after a transient fault without causing a “Pole Slip” event.

7.2 Recommendations

The studies recommend that the reduced network be used for future plant modifications as an initial response to the changes being made. It will allow plant engineers and design engineers the ability to verify parameter changes and plant response before the implementation of the changes takes place. Any major changes to the parameters of the generator or the network need careful studies to be performed. The studies performed in this dissertation proved that an increase in generator output capacity decreases the critical clearing time of the nuclear power plant.

Based on the studies conducted, it would be an added benefit to perform similar studies once the PSS and the turbine governor model have been completed. Although the AVR did not improve the critical clearing time significantly, further studies could prove that the AVR with the PSS and the turbine control system will improve the critical clearing time. Once the PSS has been modelled and validated, future work on small signal stability would be able to be performed. A recommendation based on this dissertation is that the rotating exciter installed on the plant be replaced by a more modern fast-acting static rectifier system to improve system response during a network disturbance. Again, extensive studies need to be completed to ensure that the nuclear plant will be transiently stable following a network disturbance.

Future work could include a protection study of the network to prevent cascading tripping owing to large power excursions following a network disturbance or fault. Studies must also be performed to understand the various generators’ behaviour in the network to allow the faulted area to be isolated and to prevent the fault from causing major power loss as experienced by many transmission systems.

8 List of References

[1] Eskom Holdings Ltd, "www.eskom.co.za," 19 January 2015. [Online]. Available: http://www.eskom.co.za/OurCompany/CompanyInformation/Pages/Company_Information.aspx. [Accessed 19 January 2015].

[2] Generation Communication, "Eskom's generation plant mix," Eskom, South Africa, 2011.

[3] Eskom Holdings Ltd, "Eskom Heritage" History of Salt River Power Station"," Eskom, 01 November 2010. [Online]. Available: http://heritage.eskom.co.za/heritage/saltriver ps/saltriver ps.htm. [Accessed 01 November 2010].

[4] G. Atkinson-Hope and P. Emmanuel, "Maximum Power Transfer, With An Increase In Generation In The Western Cape," in *B-Tech Conference*, Cape Town, 2010.

[5] Eskom, "Environmental Impact Assessment for the Proposed Eskom Nuclear Power Station and Infrastructure," Cape Town, August 2007.

[6] Government, "National Response to South Africa's Electricity Shortage," January 2008. [Online]. Available: http://www.ilovemycarbondioxide.com/archives/National_Response_sa_electricity.pdf. [Accessed 27 August 2015].

[7] J. Ansie van Wyk, "South Africa's Nuclear Future," in *SAIIA Occasional paper 150*, South Africa, June 2013.

[8] R. J. Thomas, D. Gan and R. D. Zimmerman, "A Transient Stability Constrained Optimal Power Flow," in *Bulk Power System Dynamics and Control IV – Restructuring Santorini*, Santorini, Greece, August 1998.

[9] K. Moloankoa, "The Impact of Wind Generators on a Power System's Transient Stability," University Of Cape Town, Cape Town, 2009.

[10] P. W. Sauer and M. A. Pai, Power System Dynamics and Stability, Upper Saddle River, New Jersey: Prentice-Hall, 1998.

[11] P. Kundur, Power System Stability and Control, Tata McGraw-Hill, 1994.

[12] D. T. OYEDOKUN, "Power flow and rotor angle stability studies of HVAC - HVDC power system interconnections using DIgSILENT," UCT, Cape Town, 2010.

[13] J. Smith, "High voltage direct current strategy solving power delivery shortages to localised area of national grid," Cape Peninsula University of Technology , Cape Town, June 2009.

[14] P. K. Iyambo, "Transient Stability Analysis of Power System," Cape Peninsula University of Technology(CPUT), Cape Town, December 2007 .

[15] Eskom, "Koeberg Units Upgrade Assessment-Steady State Studies," Eskom, South Africa, June, 2011.

[16] P. Lilje, "Stabilising an island nuclear power plant with a high-energy resistor," University Of Cape Town (UCT), Cape Town, 2009.

[17] S. Davies, "What now for nuclear?," *Engineering & Technology* , vol. 6, no. 4, pp. 39-43, 2011.

[18] A. Bartylak, "Protection Settings For Transmission and Sub-Transmission Grids," Eskom, June 2009.

[19] J. J. Granger and W. D. Stevenson, Power System Analysis, McGraw-Hill Publishing, 1994.

[20] DIgSILENT GmbH, *PowerFactory Manual Version 13,* Gomaringen Germany, 2007.

[21] Organisation for economic co-operation and development, "Defence in Depth of Electrical Systems and Grid Interaction," Organisation for economic co-operation and developement (OECD), 2009.

[22] P. Kundur, J. Paserba, V. Ajjiarapu, G. Andersson, C. Canizares, N. Hatziargyriou, D. Hill, A. Stankovic, C. Taylor, T. Van Cutsem and V. Vittal, "Definition and classification of power system stability IEEE/CIGRE Joint Task Force on Stability Terms and Definitions," *IEEE Trans. on Power Systems,* Vols. 19,, no. 2, pp. pp. 1381 -1397, May, 2004.

[23] P. Kundur, "Power System Security in the New Industry Environment: Challenges and Solutions," Toronto, October 2003.

[24] D. N. Ewart and F. P. deMello, "A Digital Computer Program for the Automatic Determination of Dynamic Stability Limits," *IEEE Trans,* Vols. PAS-86, pp. 867-875, July 1965.

[25] H. Editor and M. Rustebakke, Electric Utility Systems and Practices, John Wiley & Sons, 1983.

[26] CIGRE, "Tentative Classification and Terminologies Relating to Stability Problems of Power Systems," Electra No 56, 1978.

[27] IEEE Task Force, "Proposed Terms and Definitions for Power Systems Stability," *IEEE Trans,* Vols. PAS-101, pp. 1894-1898, July 1982.

[28] B. Gao, G. K. Morison and P. Kundur, "Voltage Stability Evaluation Using Modal Analysis," *IEEE Trans,* Vols. PWRS-7, no. 4, pp. 1529-1542, November 1992.

[29] National Energy Regulator of South Africa (NERSA), "Investigation into the electricity outages in the Western Cape for the period November 2005 to March 2006," Government, 2006.

[30] Eskom Holdings Ltd, "System Operations & Planning Report," Michelle Anthony, May 2010.

[31] ABB Switzerland Ltd, *UNITROL 5000 User's Manual,* 2007.

[32] S. de Freitas Goncalves, "Investigating the dynamic performance of generator-pole-slip protection," University of Kwazulu Natal (UKZN), October 2013.

[33] D. Reimert, "Protection relaying for power generation systems," CRC Press, New York, 2006.

[34] M. Checksfield and M. Redfern, "A study into a new solution for the problems experienced with pole slipping protection," *IEEE Transactions on Power Delivery,* vol. 13, no. 2, April 1998.

[35] IEEE/PES Power System Relaying Committe, "Out-of-step relaying for generators and systems-IEEE Working Group," *IEEE Transaction on power apparatus,* Vols. Vol. Pas-96, no. 5, pp. 1556-1564, September/October 1977.

[36] D. W. Smaha, "Out-of-step relay protection of generators," Power system relaying committee,, 1995.

[37] Alstom , Network Protection & Automation Guide, Alstom Grid, May 2011.

[38] P. M. Anderson and A. A. Fouad, Power System Control and Stability, IOWA: The IOWA State University Press, 1977.

[39] K. R. Padiyar, Analysis of subsynchronous resonance in power systems, Boston, 1999.

[40] K. A. Folly, *Transient Stability, EEE 4090F notes,* University of Cape Town, 2012.

[41] M. A. Lau and S. P. Kuruganty , "A Spreadsheet Illustration of the Transient," *Spreadsheets in Education (eJSiE),* vol. 3, no. 3, p. Article 6, 2010.

[42] DIgSILENT, Technical Reference DIgSILENT PowerFactory version 13.1, Gormaringen, Germany: DIgSILENT PowerFactory, 2004.

[43] A. Husain, Electrical Power Systems, 5th Edition, New Delh: CBS Publishers & Distributors, 2007.

[44] B. Smith and J. Arrillaga, "AC - DC power system analysis," *IEE Power and Energy,* vol. Series 27,

pp. 51-125, 1998.

[45] D. GmbH, *PowerFactory Manual Version 15,* Gomaringen Germany, April 2013.

[46] H. Saadat, Power System Analysis, New Delhi, Sixteenth Reprint: Tata McGraw-Hill Publishing Comp.Ltd , 2009.

[47] Institute of Electrical and Electronic Engineers, IEEE recommended practice for excitation system models for power system stability studies, New York, 21 April 2006.

[48] M. B. Siavhe and F. D. Modau, "Koeberg Power Station _ABB UNITROL5000 Voltage Regulator Model Validation," Eskom, October 2011.

[49] U. S. N. R. C. "The Pressurised Water Reactor," [Online]. Available: http://www.nrc.gov/reading-rm/basic-ref/students/animated-pwr.html. [Accessed 06 11 2015].

[50] T.Carolin, "Managing a network for optimization and safety," *Energize magazine,* pp. pp 30-32., March 2008.

[51] EPRI, "Fukushima Daiichi Accident-Technical Causal Factor Analysis," EPRI, Palo Alto, CA, 2012.

Appendix A: Lumped load data

LGA

System	Designation	P input (kW)	Q input (kVAr)
RCP	Reactor coolant pump 1	5442,62	1975,4
CEX	Condensate pump 1	3263,82	1672,1
CEX	Condensate pump 2	3263,82	1672,1
CRF	Circulating water pump 1	2988,37	3178,3
CRF	Circulating water pump 2	2988,37	3178,3
LKA	MV/LV transformers	540,0	261,5
	Total	18487	11937,77

LGB

System	Designation	P input (kW)	Q input (kVAr)
GGR	Turbine turning gear	82,5	543,78
LKD	MV/LV transformers	540,0	261,5
LKE	MV/LV transformers	540,0	261,5
	Total	1162,5	1066,78

LGC

System	Designation	P input (kW)	Q input (kVAr)
SAP	Main compressor	376,3	277,4
LKF	MV/LV transformers	540,0	261,5
LKG	MV/LV transformers	540,0	261,5
LKH	MV/LV transformers	540,0	261,5
LKJ	MV/LV transformers	540,0	261,5
LKS	MV/LV transformers	540,0	261,5
	Total	3076,3	1584,9

LGD

System	Designation	P input (kW)	Q input (kVAr)
RCP	Reactor coolant pump 2	5442,62	1975,4
RCP	Reactor coolant pump 3	5442,62	1975,4
ACO	Forward drain pump 1	2940,56	1424,2
ACO	Forward drain pump 2	2940,56	1424,2
ATE	Condensate recovery pump 1	490,5	291,0
ATE	Condensate recovery pump 2	490,5	291,0
ATE	Condensate recovery pump 3	490,5	291,0
LKB	MV/LV transformers	540,0	261,5
LKC	MV/LV transformers	540,0	261,5
	Total	19317,86	8167,2

LHA

System	Designation	P input (kW)	Q input (kVAr)
RCV	Charging pump or HHSI 1	461,0	261,2
RIS	Low Pressure injection pump 1	129,6	87,1
EAS	Containment spray pump 1	470,9	228,1
ASG	Aux. feed water pump 1	339,1	144,4
RRA	Residual heat removal pump 1	366,3	179,5
RRI	Component cooling pump 1	433,9	213,8
RRI	Component cooling pump 3	433,9	213,8
SEC	Essential service water pump 1	227,0	140,7
SEC	Essential service water pump. 3	227,0	140,7
DEG	Reactor refrigeration set 2	410,0	203,2
DEG	Reactor refrigeration set 2	410,0	203,2
LLA	MV/LV transformers	540,0	261,5
LLC	MV/LV transformers	540,0	261,5
LLE	MV/LV transformers	540,0	261,5
LLI	MV/LV transformers	540,0	261,5
	Total	6068,7	2800,2

LHB

System	Designation	P input (kW)	Q input (kVAr)
RCV	Charging pump or HHSI 2	461,0	261,2
RIS	Low head injection pump 2	129,6	87,1
EAS	Containment spray pump 2	470,9	228,1
ASG	Aux. feed water pump 2	339,1	144,4
RRA	Residual heat removal pump 2	284,5	157,4
RRI	Component cooling pump 2	433,9	213,8
RRI	Component cooling pump 4	433,9	213,8
SEC	Essential services water pump 2	227,0	140,7
SEC	Essential services water pump 4	227,0	140,7
DEG	Reactor refrigeration set 1	410,0	203,2
DEG	Reactor refrigeration set 3	410,0	203,2
LLB	MV/LV transformers	540,0	261,5
LLD	MV/LV transformers	540,0	261,5
LLJ	MV/LV transformers	540,0	261,5
	Total	5446,9	2778,1

Appendix B: Critical clearing time calculation using the equal area criterion method

Critical clearing time using the equal area criterion calculation for a single generator feeding into an infinite bus:

The current feeding in to the infinite bus was calculated where P_e and V is equivalent to 1 per unit.

$$I = \frac{Pe}{V*(pf)} \angle -cos^{-1}(pf) \quad \text{(B. 1)}$$

$$I = \frac{1}{1*0.9} \angle -cos^{-1}(0.9)$$

$$I = 1.111 \angle -25.8419° \quad pu$$

The machine internal angle

$$E' / \underline{\delta = V_{bus}} + jX_{eq} I \quad \text{(B.2)}$$

$$= 1/\underline{0}° + (j0.747)(1.111/-25.8419°)$$

$$=1.553 \underline{/28.745°} \text{ per unit}$$

$$P_e = \frac{|1.553|\times|1|}{0.747} \sin\delta$$

$$= 2.079\sin\delta$$

where

$\delta = 28.745°$, hence δ_0 28.745°

Maximum angle δ_3 = 180°-28.745°

= 151.25° or 2.639 rad

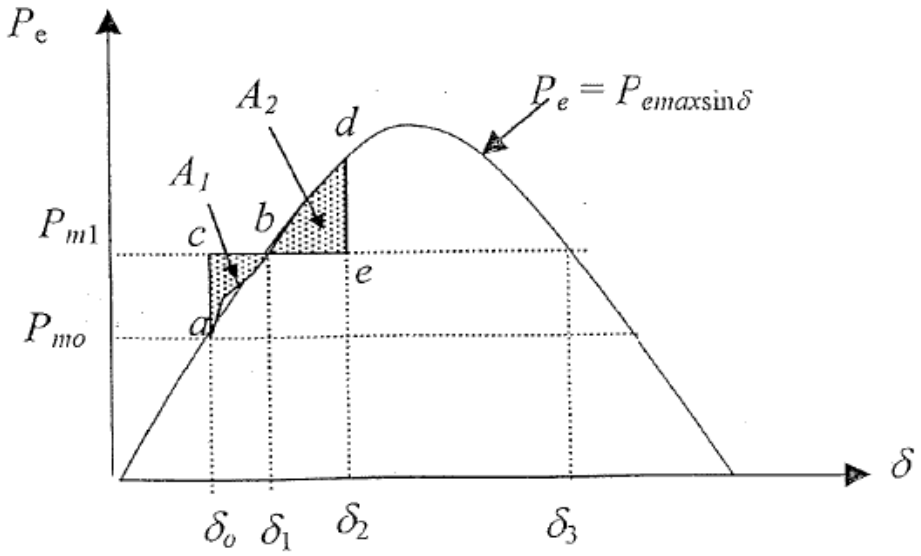

Figure B.1 Equal area criterion displayed on an electrical power P_e vs power angle δ [40]

Using the equal area criterion calculation and equating the accelerating and decelerating areas:

$$A_1 = \int_{\delta_0}^{\delta_{cr}} P_m \, d\delta = A_2 = \int_{\delta_{cr}}^{\delta_3} (P_{max} \sin\delta - P_m) d\delta \quad \text{(B.3)}$$

$$A_1 = \int_{0.5017}^{\delta_{cr}} 1 \, d\delta = A_2 = \int_{\delta_{cr}}^{2.639} (2.079 \sin\delta - 1) d\delta$$

(δ_{cr} -0.5017) = 2.079 {cosδ_{cr} -cos(2.639)}-{2.639-δ_{cr}}

δ_{cr} - 0.5017 = 2.079cosδ_{cr} + 1.822-2.639+ δ_{cr}
-2.079cosδ_{cr}= -0.3153
δ_{cr}= 1.418 rad

$t_{cr} = \sqrt{\frac{4\times5.98}{314}(1.418 - 0.5017)}$
t_{cr} = 0.264 seconds

Equal Area Criterion Calculation for two generators feeding into an infinite bus:

The current feeding in to the infinite bus was calculated

$$I = \frac{Pe}{V * (pf)} \angle - cos^{-1}(pf)$$

$$I = \frac{1}{1 * 0.9} \angle - cos^{-1}(0.9)$$

$$I = 1.111 \angle - 25.8419°$$

The machine internal angle
E' /$\underline{\delta}$ = V_{bus} +jX_{eq} I

= 1/$\underline{0}$° + (j0.3735)(1.111/-25.8419°)
=1.238 /$\underline{17.537°}$ per unit

$P_e = \frac{|1.238|\times|1|}{0.3735} \sin\delta$

= 3.3146 sin δ ,
where $\delta = 17.537°$, hence δ_0 17.537°

Maximum angle δ_3 = 180°-17.537°
= 162.46° or 2.835 rad

Using the equal area criterion calculation and equating the accelerating and decelerating areas:

$$A_1 = \int_{\delta_0}^{\delta_{cr}} P_m \, d\delta = A_2 = \int_{\delta_{cr}}^{\delta_3} (P_{max} \sin\delta - P_m) d\delta$$

$$A_1 = \int_{0.3061}^{\delta_{cr}} 1 \, d\delta = A_2 = \int_{\delta_{cr}}^{2.8355} (3.3146 \sin\delta - 1) d\delta$$

$(\delta_{cr}$ -0.3061) = 3.3146 {cosδ_{cr} -cos(2.8355)}-{2.8355-δ_{cr}}
δ_{cr} – 0.3061 = 3.3146 cosδ_{cr} + 3.16 -2.8355+ δ_{cr}
-3.3146cosδ_{cr}= 0.6311
δ_{cr}= 1.762 rad

$t_{cr} = \sqrt{\frac{4\times2.99}{314}(1.762 - 0.3061)}$
t_{cr} = 0.235 seconds

Appendix C: Modified Euler Excel calculations

Single Generator Calculation

System data	
Generator transient reactance (X'd) in p.u	0.41
Transformer and line reactance (XT + XL) in p.u	0.337
Bus 1 voltage (24 kV) in p.u.	1
Bus 2 voltage (400 kV) in p.u.	1
Summary of power flow calculation results	
Pre-fault equivalent reactance (Xeq) in p.u	0.747
Power angle (delta) in radians	0.501721
Power angle (delta) in degrees	28.7465
Electric power (pe1) prior to fault	2.0793
Electric power (pe2) during fault	0
Electric power (pe3) after fault is cleared	2.0793

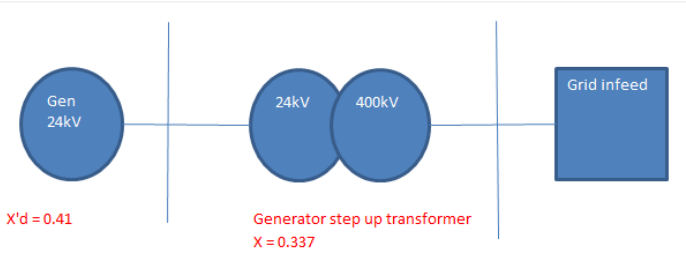

Transient Stability Example			
Mechanical power (p_m) =	1	p.u.	% From power flow calculations
Pre-fault maximum power (p_1max) =	2.0793	p.u.	% From power flow calculations
During fault maximum power (p_2max) =	0.0000	p.u.	% From power flow calculations
Post-fault maximum power (p_3max) =	2.0793	p.u.	% From power flow calculations
Initial (pre-fault) power angle (delta_0) =	0.5017	rad	% From power flow calculations
Frequency (f) =	50	Hz	% Frequency may be changed
Synchronous speed (omega_s) =	314.1593	rad/s	% omega_s = 2*pi*f
Machine inertia constant (H) =	5.98	p.u.-s	% Inertia constant may be changed
Clearance time (t_cl) =	0.27	s	% Fault clearance time may be changed
Step size (Delta t) =	0.01	s	% Time step for numerical method may be changed

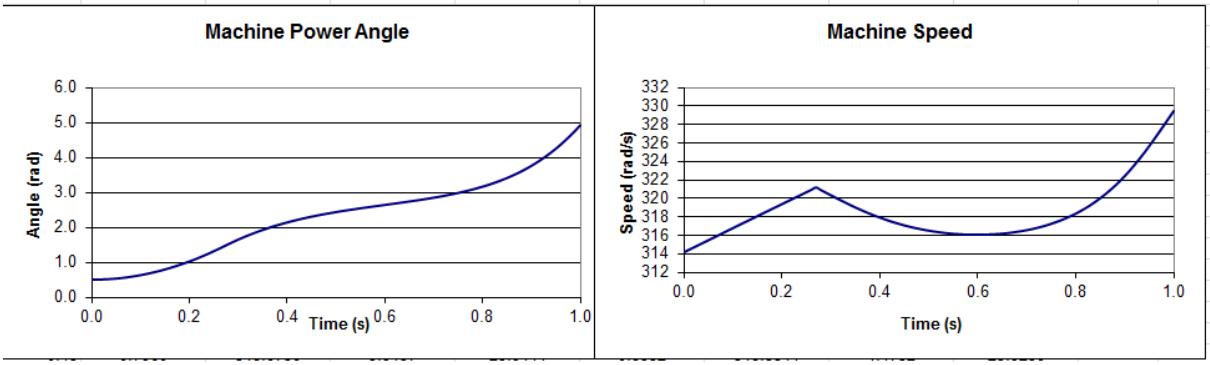

?

Two generators coupled to the HV busbar

System data	
Generator transient reactance (X'd)	0.205
Transformer and line reactance (XT + XL)	0.1685
Bus 1 voltage (24 kV) in p.u.	1
Bus 2 voltage (400 kV) in p.u.	1
Summary of power flow calculation results	
Pre-fault equivalent reactance (Xeq)	0.3735
Power angle (delta) in radians	0.306078391
Power angle (delta) in degrees	17.537
Electric power (pe1) prior to fault	3.3146
Electric power (pe2) during fault	0
Electric power (pe3) after fault is cleared	3.3146

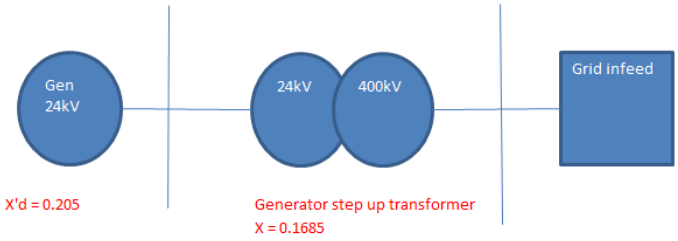

Transient Stability Example			
Mechanical power (p_m) =	1	p.u.	% From power flow calculations
Pre-fault maximum power (p_1max) =	3.3146	p.u.	% From power flow calculations
During fault maximum power (p_2max) =	0.0000	p.u.	% From power flow calculations
Post-fault maximum power (p_3max) =	3.3146	p.u.	% From power flow calculations
Initial (pre-fault) power angle (delta_0) =	0.3061	rad	% From power flow calculations
Frequency (f) =	50	Hz	% Frequency may be changed
Synchronous speed (omega_s) =	314.1593	rad/s	% omega_s = 2*pi*f
Machine inertia constant (H) =	2.99	p.u.-s	% Inertia constant may be changed
Clearance time (t_cl) =	0.24	s	% Fault clearance time may be changed
Step size (Delta t) =	0.01	s	% Time step for numerical method may be changed

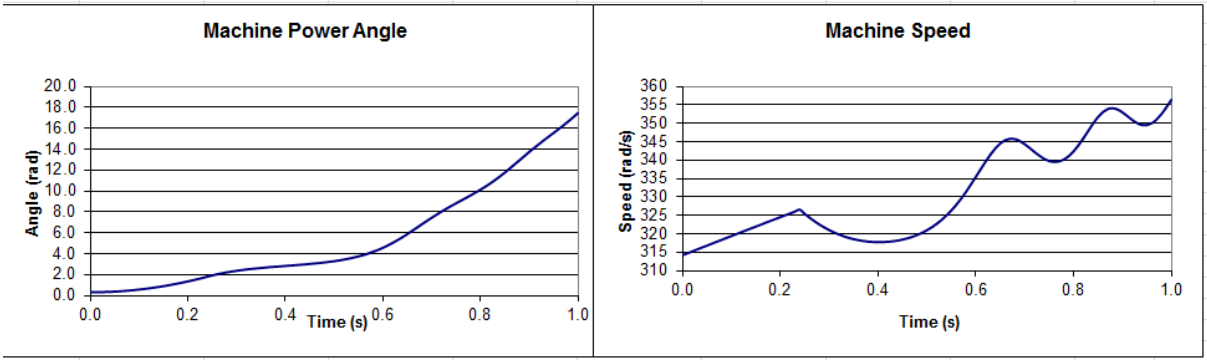

Appendix D: Input data

Grid information

Nominal voltage..... 400kV
Minimum voltage..... 380kV
Maximum voltage 420kV
Nominal frequency..... 50 Hz
Minimum frequency..... 49,5 Hz
Maximum frequency..... 50,5 Hz
Three phased fault maximum short-circuit power..... 22531 MVA (400kV)
Three phased fault minimum short circuit power..... 19271 MVA (400kV)
Single phased fault maximum short circuit power..... 8905 MVA (230kV)
Single phased fault maximum short circuit power ..... 7818 MVA (230kV)
Aperiodic time constant .....284 ms
R/X ratio 0,03

Generators Information

Rated apparent power..... 1080 MVA
Rated active power..... 972 MW
Rated power factor..... 0,9
Rated voltage..... 24kV
Stator voltage variation under normal conditions..... +/- 5%
Rated frequency..... 50 Hz
Direct axis synchronous reactance..... 2,596 p.u
Direct axis synchronous reactance (saturated)..... 2,424 p.u
Direct axis transient reactance..... 0,447 p.u
Direct axis transient reactance (saturated)..... 0,382 p.u
Direct axis sub-transient reactance..... 0,314 p.u
Direct axis sub-transient reactance (saturated)..... 0,232 p.u
Tolerance on reactance values..... +/-15%
Direct axis transient short circuit time constant..... 1,37 s
Direct axis sub-transient short circuit time constant..... 0,04 s
Aperiodic time constant..... 0,23 s
Inertia constant.....5,98

Generator step up transformer (GSUT) parameters

Rated apparent power..... 1245 MVA (3 X 415 MVA)
Rated voltage ratio..... 420 /24 kV
LV winding rated voltage.....24 kV
HV winding rated voltage.....400 kV /$\sqrt{3}$ kV
On load tap changer..... +/- 6 X 1,25%
Short circuit impedance on nominal tap..... 17,2% (+/- 7,5%)
Load loss..... 3016kW

Unit auxiliary transformer (UAT)

Rated apparent of HV winding..... 60 MVA
Rated apparent of MV1 winding..... 30 MVA
Rated apparent of MV2 winding..... 30 MVA
HV winding rated voltage..... 24 kV
MV1 winding rated voltage..... 6,9kV

MV2 winding rated voltage..... 6,9kV
Vector group symbol..... YNy0y0
LV1 and LV2 rated voltage..... 6,9kV
HV winding rated voltage..... 24kV
Short circuit impedance (HV/LV1 & HV/LV2)..... 9% (30MVA base)
Short circuit impedance (LV1/LV2)..... 23,1% (30MVA base)
Load losses..... 220kW

Line/Cable data:

Cable ID	Size (mm^2)	Length (m)	No. of cables per phase	R	X
UAT -LGA	500	125	4	0,06	0,099
UAT -LGD	500	106	4	0,06	0,099
LGA-LGB	500	28	1	0,0468	0,099
LGD-LGC	400	39	3	0,07955	0,101
LGB-LHA	400	23	1	0,07955	0,101
LGC-LHB	400	23	1	0,07955	0,101

Note : Ohms or Siemens/1000 m per conductor (cable) or per phase(line) at 20°C

Lumped load data can be found in Appendix A.

Appendix E: AVR block diagram

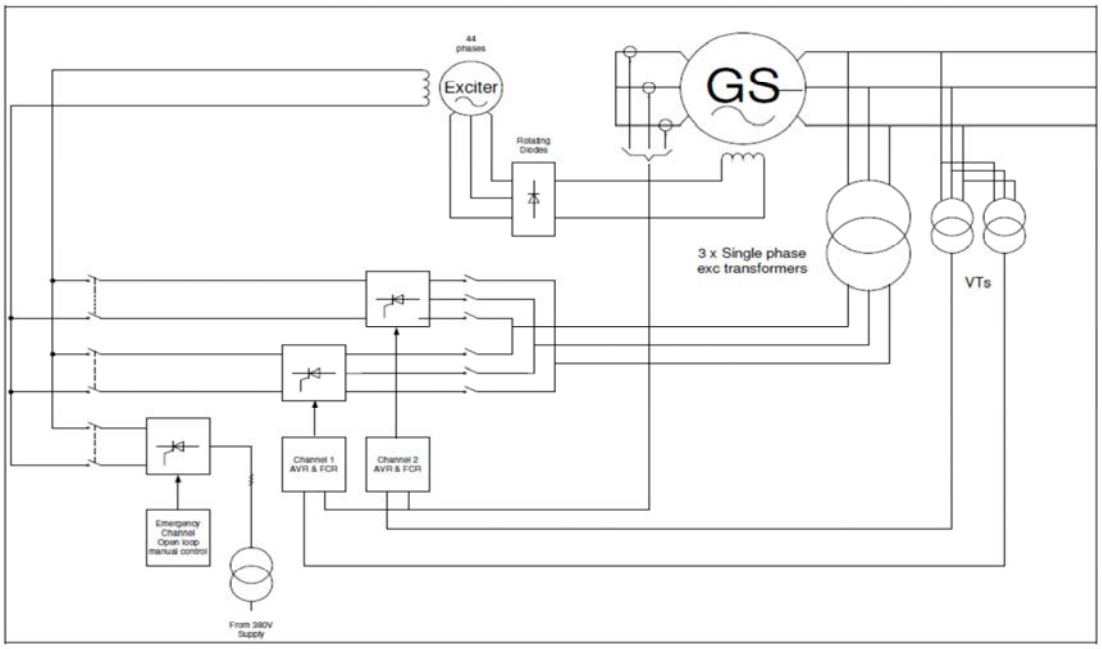

Appendix F: ST5B model in DIgSILENT

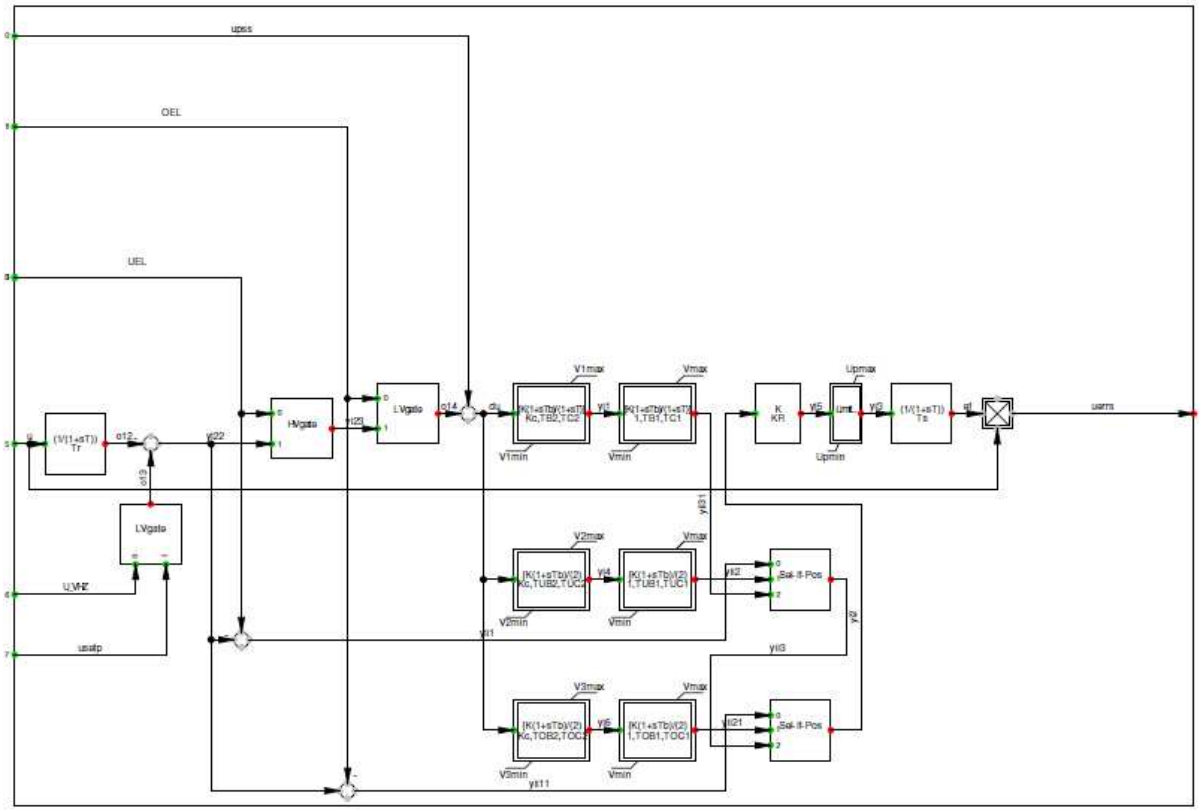

Appendix G: HV yard faults

Grid events

1986/08/29	Title: FAILURE OF THE KOEBERG ACACIA MANUAL START 12H00: THE KOEBERG ACACIA MANUAL START BUTTON WAS DEPRESSED AS PART OF A PERIODIC TEST - UNSUCCESSFUL. 2. THE CONTROL CIRCUIT LINKS IN THE HV YARD FOR THE MANUAL AND RESET ORDERS WERE FOUND OPEN. 3. 12H20: THE MANUAL START BUTTON WAS AGAIN DEPRESSED AND ACACIA STARTED UP SUCCESSFULLY BUT THE 132 KV BUS STRIP FAILED (TIMER FAILED).
1991/06/18	Title: TRIP OF RIETVLEI 132KV FEEDER (FS) DUE TO EARTH FAULT: 20H02: GRID DISTURBANCE TO BOTH 400 AND 132KV SYSTEMS TWICE DUE TO ARC AND TRIP. REGION CONTACTED FOR INFORMATION AND REPLIED THAT THEY WOULD TRY AND RECLOSED. THE BREAKER CLOSED AND IMMEDIATELY TRIPPED, CAUSING A FURTHER DISTURBANCE TO BOTH UNITS. SECURITY INFORMED CONTROL ROOM OF A CABLE LYING ON THE GROUND NEAR THE HV YARD. SHIFT MANAGER INVESTIGATED AND FOUND NEUTRAL CABLES DOWN BETWEEN 1ST AND 2ND PYLONS. BOTH UNIT 2 DIESELS STARTED AND ERF TRIPPED. TABLE VIEW BLACKED OUT. RESUPPLIED VIA 11KV NETWORK. WESTERN CAPE PERSONNEL INVESTIGATING
1993/06/15	Title: SIMULTANEOUS OUTAGE OF TWO UNITS AT ACACIA. ACACIA UNIT-1 WAS UNAVAILABLE FOR KOEBERG FROM 12:57 TO 15:06 ON 1993-06-15 TO LOCATE A DC EARTH FAULT. AS UNIT-3 WAS ALSO ON FORCED OUTAGE FOR STATOR REPAIRS, ACACIA WAS INOPERABLE IN TERMS OF THE KOEBERG TECH SPECS FOR THIS PERIOD (129 MINUTES), PLACING KOEBERG IN A FALL-BACK SITUATION. THE KOEBERG CONTROL OFFICER WAS KEPT FULLY INFORMED OF THE POSITION. NOTE: A DC EARTH FAULT SHOULD NOT CAUSE A START FAILURE BUT REQUIRES AN OUTAGE TO TRACE AND CLEAR. IN THE EVENT OF A START HAVING BEEN NECESSARY DURING THE OUTAGE, THE UNIT COULD HAVE BEEN RESTORED IN 10 TO 15 MINUTES. THE DC EARTH FAULT WAS TRACED TO BATTERY BOARD 1, TO WHICH UNIT-1 WAS SELECTED. THE UNIT WAS THEN CHANGED OVER TO BATTERY BOARD 2. SINCE CONTROL CIRCUITS HAD BEEN WORKED ON TO LOCATE THE FAULT, IT WAS DECIDED TO REQUALIFY THE UNIT BY STARTING IT ON MINIMUM LOAD. DURING THIS TEST THE AIR START DUCT RELIEF VALVE ON ENGINE 1A LIFTED MOMENTARILY. THE UNIT WAS THEREFORE HANDED BACK FOR SERVICE ON ENGINE 1B ONLY AND ARMED FOR KOEBERG AUTO START AY 15:06. AFTER ADJUSTING THE SIGNAL AIR PRESSURE REGULATOR, ENGINE 1A WAS TESTED BY RUNNING UP TO 1 4000 R/MIN AND FOUND SATISFACTORY. THE UNIT WAS HANDED BACK FOR SERVICE ON BOTH ENGINES AT 16:46. NOTE 1: THE BLOWING OF AIR START RELIEF VALVE DID NOT CAUSE A START FAILURE AND THE UNIT WAS IN FACT BROUGHT ON LOAD ON BOTH ENGINES. NOTE 2. THERE HAD BEEN A FORCED OUTAGE OF ENGINE 1A FROM 23:12 ON 93-06-05 TO 00:51 ON 93-06-06 (99 MINUTES) TO CHANGE THE AIR START CONTROL VALVE PRESSURE REGULATOR SEAT. A TEST START TO 6 000 R/MIN N2 SPEED PROVED SATISFACTORY. THE DC EARTH FAULT WAS TRACED TO THE ACACIA POWER STATION 132KV BREAKER WHICH WAS ALSO SELECTED TO BATTERY BOARD 1 (AND ULTIMATELY TO A JUNCTION BOX IN THE HV YARD). THIS BREAKER HAS BEEN ISOLATED ON THE 132KV SIDE FOR PURPOSE OF DEDICATING ACACIA TO KOEBERG AND THE EARTH FAULT WOULD NOT HAVE AFFECTED A START UP OF THE UNITS. A SECOND EARTH FAULT WAS TRACED TO AN INDICATING LAMP ON THE BATTERY CHARGER PANEL AND WAS CLEARED. BATTERY 1 WAS ALSO FOUND TO HAVE A HIGH RESISTANCE LEAKAGE TO EARTH WHICH IS TO BE

	CLEARED BY CLEANING CASING, TRESTLES AND FLOORS.THE RELEVANT LOG ENTRIES ARE ATTACHED. ACACIA UNIT1 AND 2 OPERABLE (STANDBY) AND DEDICATED TO KOEBERG. UNITS-1 AND 2 SELECTED TO BATTERY 1. ACACIA UNIT-3 ON FORCED OUTAGE FOR STATOR REWIND.
1994/05/09	Title: 400KV BUSZONE PROTECTION BLOCKED: 1. ON 6/05/94 AT 14:07 A BUSZONE ALARM WAS RECEIVED AT REGIONAL CONTROL FROM KOEBERG 400KV YARD. 2. FAULT WAS INVESTIGATED BY TEST (WEST) DEPARTMENT. 3. INVESTIGATION WAS ONGOING UNTIL MONDAY 09/05/94 WITHOUT ANY SUCCESS. PROBLEMS EXPERIENCED WERE: (A) LACK OF DETAIL DRAWINGS (B) NO SPARES AVAILABLE. 4. ON MONDAY 09/05/94 KOEBERG CONTROL ROOM WAS INFORMED OF THE PROBLEM BY NATIONAL CONTROL.5. KOEBERG PERSONNEL ASSISTED THE TEST (WEST) TECHNICIANS AND THE FAULT WAS ISOLATED ON MONDAY AT +- 19:00. 6. THE FAULT WAS TRACED TO A FAULTY SELF TEST FACILITY. THE TEST CURRENT OUTPUT OF THIS CARD WAS ISOLATED AND THE FAULT WAS CLEARED. 7. THE BUSZONE WAS RETURNED TO SERVICE WITH THE WEEKLY SELF TEST CYCLE INHIBITED. 8. DETAIL DRAWINGS AND THE REQUIRED SPARES WERE ORDERED BY THE TEST (WEST) TRANSMISSION GROUP. ATTACHED PLEASE FIND: (A) FAULT INVESTIGATION REPORT (B) ESKOM STANDARD IDENTIFYING TRANSMISSION GROUP'S ASSETS. (C) MEMO FROM GENERATION FINANCE MANAGER REGARDING OF KNPS HV YARD TO TRANSMISSION GROUP. (D) KCO LOG. NOTE: DECISIONS REGARDING THE GRID AND KOEBERG U2 LOADING AND PROTECTION SETTING CHANGES WERE TAKEN BY SYSTEM OPERATIONS (CHARLES GELDARD - NATIONAL CONTROL MANAGER)
1997/07/25	TITLE: Failure of PT-LGR-161 and sub optimum recovery: During a 6 monthly test of the Koeberg Autostart function, the breaker on the Koeberg side of the dedicated line failed to close, which rendered the 132kV supply at Koeberg inoperable. The consequence of this was that Unit-1 was put in a 36 hour fall-back (as the 132kV line was inoperable), and Unit-2 (which was supposed to have its 400kV Breaker open as the transformer was defective) had to keep its 400 kV breaker closed until the test was successfully completed. Although the response time of Test West to the call out was excellent some concerns were noted: (a) A lack of drawings at the HV Yard. (b) A lack of appropriate spares. From this, the additional concern was raised as to whether the maintenance on the dedicated line breakers is sufficient to avoid a similar fault in the future.
1998/08/12	TITLE: MVAR swing experienced on Unit-2 from - 100 to - 400 MVAR apparently coinciding with the opening of bus coupler A in the HV yard. DESCRIPTION/SEQUENCE OF EVENTS: Unit-2 informed by national Control that the 400 kV bus coupler A was to be o/s for 3 days. 11:35 - Bus coupler opened. 11:35 - Excitation voltage dropped to +- 22,5 kV MVAR's swing - 100 to - 400.
1999/03/19	TITLE: Loss of Acacia 132 kV dedicated line -: Grid disturbance noted in Unit Control Rooms followed by Acacia feeder 1 trip. Further investigation revealed the 132 kV Acacia line had snapped at the HV yard. LCO: LGx-2 (Loss of 132kV) entered. Both units in 36 hr fall-back to State 3B
2001/02/10	TITLE: Trip signal sent to 2GEV002TP and 400kV breaker during fire system PT (JPD181), causing water ingress in HV lung control box. INITIAL STATE: 2GEV002TP not energised, links in HV yard still open, 400kV breaker open.
2001/04/15	Title : Unit-2: 400kV and 24kV trip on earth fault resulting in Rx trip. Initial State: Rx 100% Pn. No work in progress, description: 03h15: Rx and turbine trip due to 24kV earth fault. Investigation in progress. It appears to be an earth fault between the 24kV and 400kV breakers. With the assistance of the Regional staff it would appear that the fault is on the white phase between the generator transformer and HV yard in one of the 7 SF6 sections. Region requires services of contractor to determine which section and thus make plans for repair. With it being obvious that the repair would take some time (+- 7 days) the unit commenced shutdown to state 3b. Final State: Unit-2 stable at

	hot shutdown. (Note: Subsequent identification of water hammer damage to supports on the feedwater line was linked to this event and is investigated under EPR No. 0056a/01) Recommendation 1: A review of the non-availability of the InSQL trend programme to record data during the critical period after the transient is required.
2002/07/13	PROBLEM TITLE: Voltage Transformer failure on Aurora no 1 feeder. INITIAL STATE: Unit 1-100% -Aurora no 1/ Koeberg breaker closed. Unit 2- Outage. PROBLEM SEQUENCE: 02:35 : OHZR- Aurora No.1: fault sustained. 05:13 : OLZR- Aurora No.1: informed by regional control of the possibility of taking the Aurora No.1 feeder out of service. . 05:21 : OLZR- Aurora No.1: feeder taken out of service. 16/07/2002 Confirmed with HV yard operator- that the Aurora No. 1 feeder is isolated for the replacement of the voltage transformer- red phase
2003/11/15	Title : HV Yard red phase earth fault and transformer 2GEV001TS Bucholtz 2nd stage trip & pressure relief valve operation Initial state: Plant state 2A, drain-down in progress, 400kV in service. Description: 22h58 51 sec - Red phase fault on 400kV busbar 1A initiated. 22h58 53 sec - 1GEV001TS Bucholtz 2nd stage fault and pressure relief valve operation resulted in 400kV breaker trip. Swop-over to 132kV initiated and I 2.1 used as guidance to mitigate incident. On investigation, there was clear indication that the pressure relief operated and gas noticed in Bucholtz at the unit transformer. In the HV yard, on the red phase section 1A chamber, debris and white powder noticed. Region control called out. NB: No switching occurred in the HV yard at the time of event. LCO LGX-1 entered and drain down aborted.
2003/11/15	Title: 400kV busbar 1A red phase earth fault, Initial State: Unit-2 at refuelling shutdown, 400kV breaker closed. Description: At about 19:00 there was a change-over supply from 132kV to 400kV following the closure of 2GEV001JA. at +- 22:57 there was an earth fault on 400kV busbar 1A red phase, 30 milli seconds later buszone protection operated (opening the bus section and bus coupler breakers), 45 milli seconds later 2GEV001JA tripped on Buchholtz/ pressure relief protection. Implement Corrective Actions: 2GEV001TS was replaced with 9GEV001TS. Earthing between HV yard and station was verified. Surge arresters were fitted on HV terminals of 2GEV001TS.
2007/02/18	Problem title: Blaauwberg 1 132kV feeder carrier line came adrift Reported by Protective Services that one of the carrier lines on BLAAUWBERG 1 132 KV feeder came adrift and is lying over the carpark. The line broke on the first pylon out of the HV Yard. Protective Services barricaded off the area. Region informed.
2007/06/10	Problem title: Koeberg/Acacia 400KV insulator broken off.Problem sequence: Region informed Koeberg that an insulator had broken off in the HV yard on the Koeberg/Acacia 400KV line. Line isolated and insulator replaced. Line returned to service.
2008/11/21	Affected component(s):0BSR 000GE Problem title: 0BSR 000GE - Two network failures on the 400kV grid have resulted in the Acacia Generators becoming unavailable to Koeberg in 2008. Both events have demonstrated the existence of a common mode failure mechanism between the preferred and 2nd grid supplies for Koeberg. Initial State: Acacia No 1 in SCO mode and armed for KAS. Acacia No 2 in SCO mode and armed for KAS Acacia No 3 on PTW. Koeberg Unit 1 at full Power (both events).Unit 2 in Outage 216 (first event). Unit 2 at full power (second event. Problem sequence: Failure No 1.On the 1st February 2008 at 20h41 Acacia Units No 1 and No 2 tripped as a result of a power interruption at the Acacia Substation. The power failure was as a result of the 400kV Acacia - Muldersvlei Line tripping as a result of an earth wire failure. The alternate 400kV line into the Acacia Substation was on permit at the time, this as a result of a failed SF6 to Air Bushing in the Koeberg HV Yard. Failure No 2. On the 13 October 2008 at 05h42 Acacia Units No 1 and No 2 tripped as a result of a power interruption at the Acacia Substation. The power failure was as a result of an earth wire becoming entangled with a truck on the N7 highway and subsequently coming into contact with the Koeberg -Acacia Line and Acacia - Muldersvlei Line investigation. On the 5th November 2008 a meeting was held at Peaking Generation to discuss the above two events and to determine if there was a common made failure mechanism between the preferred grid (400kV network) and the

	2nd supply (132kV supply) derived from Acacia Power Station. At the meeting it was determined that we do in fact have a common made failure mechanism. Commonality being the inadvertent activation of the Loss Of Field Protection Relays on the Acacia Generators. These relays affected by a loss of supply on the 132kV busbars; this being the case for both instances while connected to the preferred grid in SCO mode
2009/02/07	Problem title: Grid disturbance. Initial State: Unit 2 @ 99.1%Pn Problem sequence: At 19:20 2009/02/07, a grid disturbance, possibly caused by lightning, caused an auto reclose on the Koeberg/Acacia 400KV line. 2GPA017AA (UNDERVOLTAGE OR FREQ FUSE FAULT, was later reset by 2GPA100TO), 2GPB001AA (SYSTEM UPDATE UNHEALTHY), and 2GEV006AA (OLTC BLOCKED) sustained. Unit 1 was supplied by the 132KV network at the time, and had an automatic no-load start-up of 1LHP and 1LHQ diesels. Security reported indications of arcing in the HV yard. Region Control informed to investigate. .
2010/03/11	Problem title: Loss Of N2 Pressure On 1GEV001JA and 400KV Bus Coupler-B. Initial State: 6B Problem sequence: At 02H09 on 2010-03-11 a loss of N2 pressure alarm on 1GEV001JA sustained. With this alarm sustained 1GEV001JA is interlocked closed and will not open on fault conditions. 45 minutes later at 02H54, a loss of N2 pressure on 400kv bus coupler B alarm also sustained. With this alarm sustained the bus coupler is interlocked closed. Region control informed and alarms acknowledged and cleared locally on HV yard
2010/09/04	Problem title: Start-up Of Emergency Diesel Generators. Initial State: Plant state 1 with both 1LHA and 1LHB boards supplied by 132Kv offsite power. Problem sequence: While National and Region Control were trying re-energize the faulty 400Kv busbar 2A, the 400/132Kv coupling transformer 1 tripped and this power disturbance caused a automatic start-up of both emergency diesel generators. Fuel unloading suspended. Power supply to both 1LHA and 1LHB confirmed to be from offsite power 132Kv, both diesel generators stopped and placed on standby. Fuel unloading recommenced. Suggested Corrective Actions : National and Region Control Centres to ensure that proper communication protocol is maintained at all times, the KCO to be informed of all switching in the Koeberg HV yard
2010/10/06	Problem title: 400 kV breaker tripped on the first two attempts to close it during GEV transformer back energisation Initial State: 400 kV breaker open Problem sequence: On the 6 October 2010, during back energisation of the GEV transformers, the 400 kV breaker tripped instantaneously on closure. Investigation found that the trip was initiated by the YTG “Switch onto Standstill” relay situated in the Koeberg HV yard, which operated due to the high in rush magnetising current. The high in rush current was experienced due to the installation of the new Smit transformer, 1 GEV 003 TP. The output of the YTG relay was inhibited, and a second attempt to close the 400 kV breaker was made on the 7 October. The breaker again tripped, due to the combination of poor Koeberg relay logic design and operation of the BFR (Breaker Fail Relay) in the HV yard. The BFR relay had operated as it was given a permissive to operate due to the Smit transformer in rush current
2010/12/05	Problem title: Glowing Hot connection in HV Yard Initial State: Unit 1 97%Pn and Unit 2 99%Pn Problem sequence: A Hot connection was reported in the HV Yard, and the SRO on shift commenced investigation to locate the problem. The location of the glowing (hot connection) was found to be on top of the fourth upright gantry where the 3 earthing wires join from the first pylons of Stikland and Muldersvlei. HV Yard Technician called out to investigate further and to effect repairs.
2011/04/26	Problem title: Unit 1 loss of load owing to flashover in HV Yard Initial State:Unit 1 at 99.6% Pn, 977MWe Problem sequence: 05h05 26/4/2011 Acacia 400kV feeder tripped [owing to suspected fault at HV yard] Unit 1 shed load to 90MWe ,at which point it was limited by LVA operation. Unit stabilised and LVA limitation reset.Acacia 400 kV line reclosed by National Control with KCO concurrence and Unit load increased to approx 285 MWe thereafter until 05h57. 05h57 26/4/2011 Acacia 132kV [dedicated 132kV supply] feeder tripped on a reported flashover in the HV yard .OTS 3.LGx 2 declared. Unit 1 power limited to 35%Pn, 290 MWe while LCO 3.LGX 2 is in force. Additional information from Shift manager log: 400kV At 05h18, the

Muldersvlei / Acacia line tripped due to a red phase CT flashover in the Acacia HV yard. The Acacia/Koeberg line tripped in sympathy due a suspected incorrect setting on an impedance relay in the Koeberg HV Yard. This relay's zone 1 protection should look at the area from the Koeberg 400 kV breaker to the Acacia 400 kV breaker, but was looking past the Acacia 400kV breaker into the Acacia / Muldersvlei line where the fault occurred (overreaching). As a result of the temporary loss of load, Unit 1 shed load to 90MWe as a result of LVA operation. The unit was then stabilised, and the LVA limitation reset. The Acacia 400 kV line was re-closed by National Control with KCO concurrence and Unit 1 load increased to approx 285 MWe thereafter. Due to the over-reaching of the zone 1 protection, it has been switched off until the System Operator provides a new setting. The line protection is now provided by zone 2 protection, in addition to the installed Differential protection on the Koeberg/Acacia line. 132kV .There was also a totally isolated incident on the 132kV Acacia Koeberg line. At 05h57, the dedicated 132kV supply to Koeberg tripped. The line trip is being attributed to pollution on the 132 kV white phase line trap insulator. OTS 3.LGx 2 was declared. Unit 1 load increase and Unit 2 fuel reload was suspended. The insulator was Insul-coated after the incident in 2006, however, a flashover still occurred due to pollution despite the application of this coating. Transmission cleaned the insulators and applied a silicon grease coating over the Insul-coating. The line was re-energised and KAS armed at 11h30. Unit 1 load increase started (at reduced rate due to fuel defects) and Unit 2 fuel reload resumed.

Appendix H: DIgSILENT plots for Emergency Diesel Generator

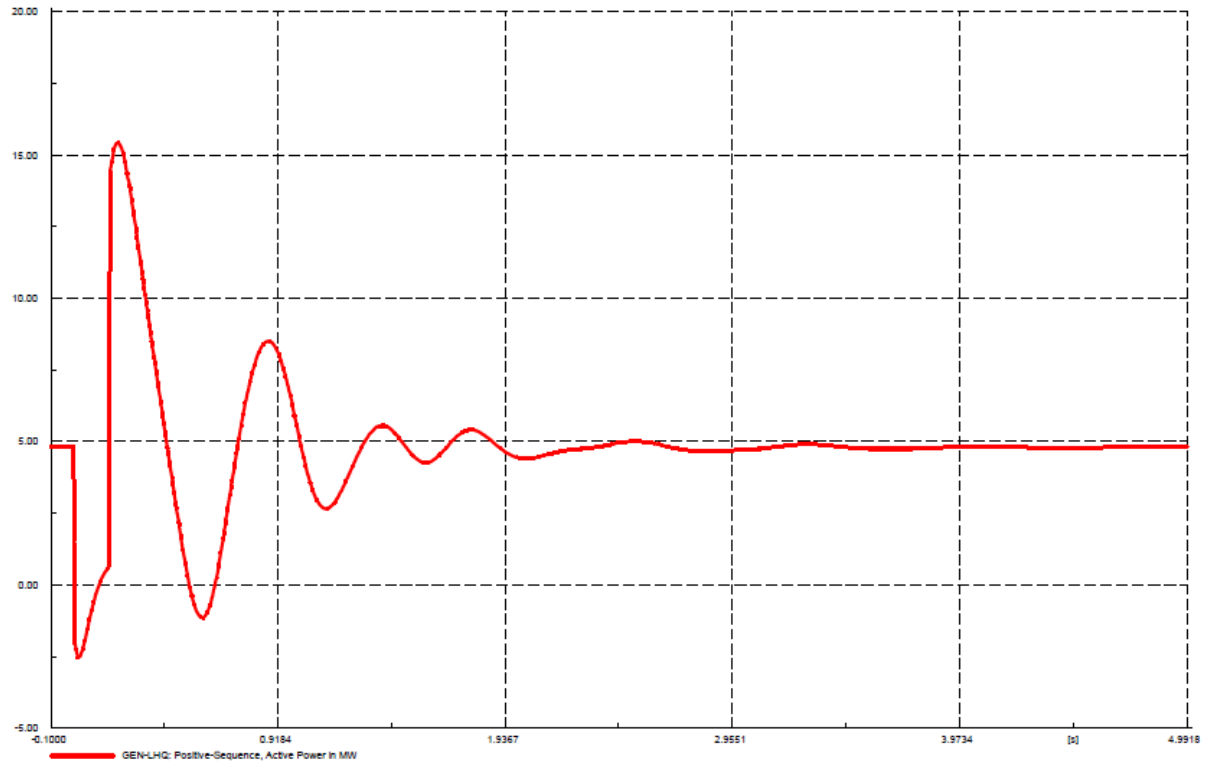

Figure H 1

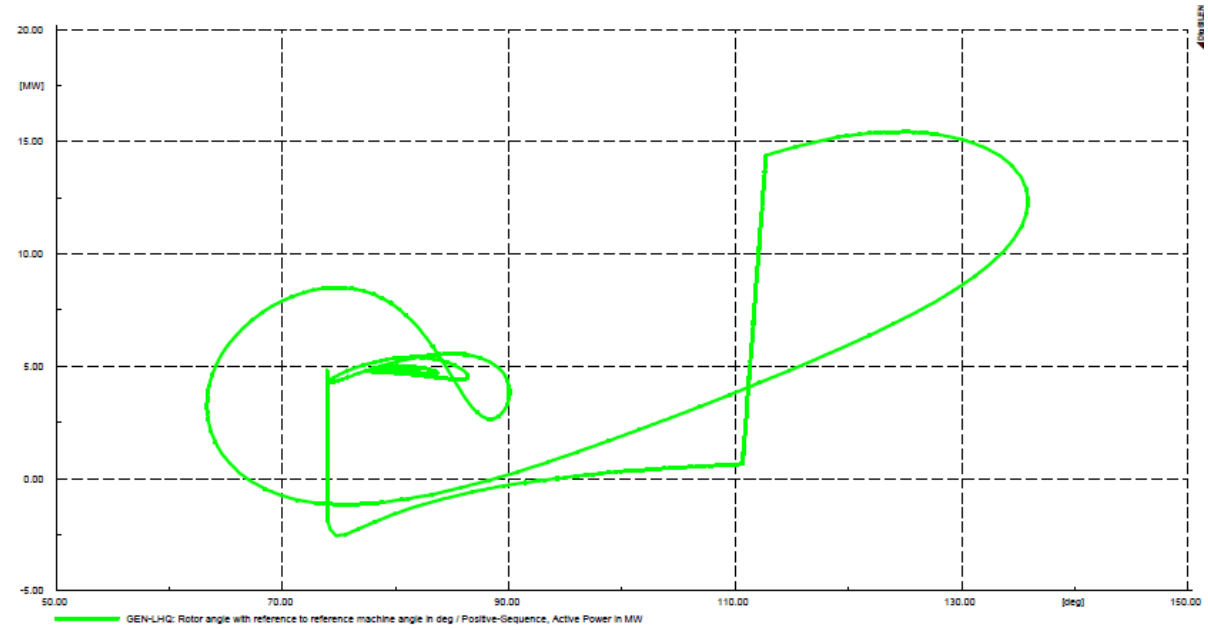

Figure H-2: P-δ curve

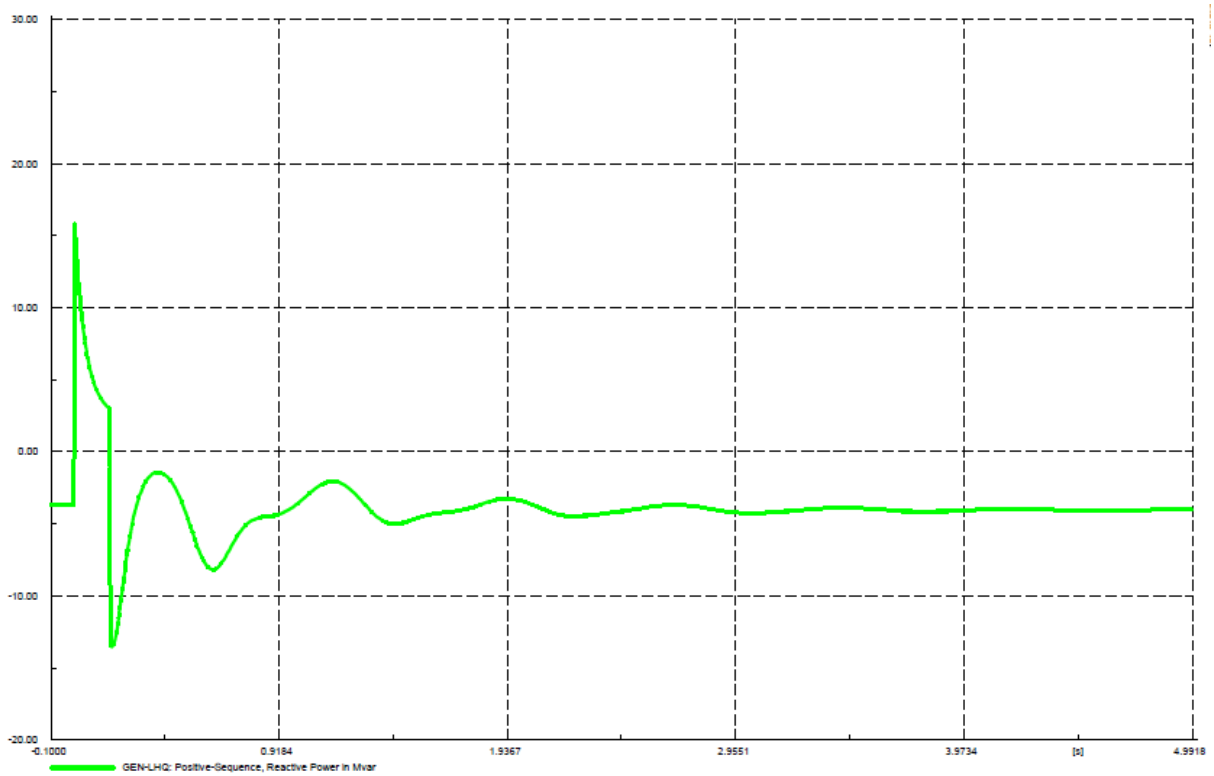

Figure H-3 : Reactive power plot

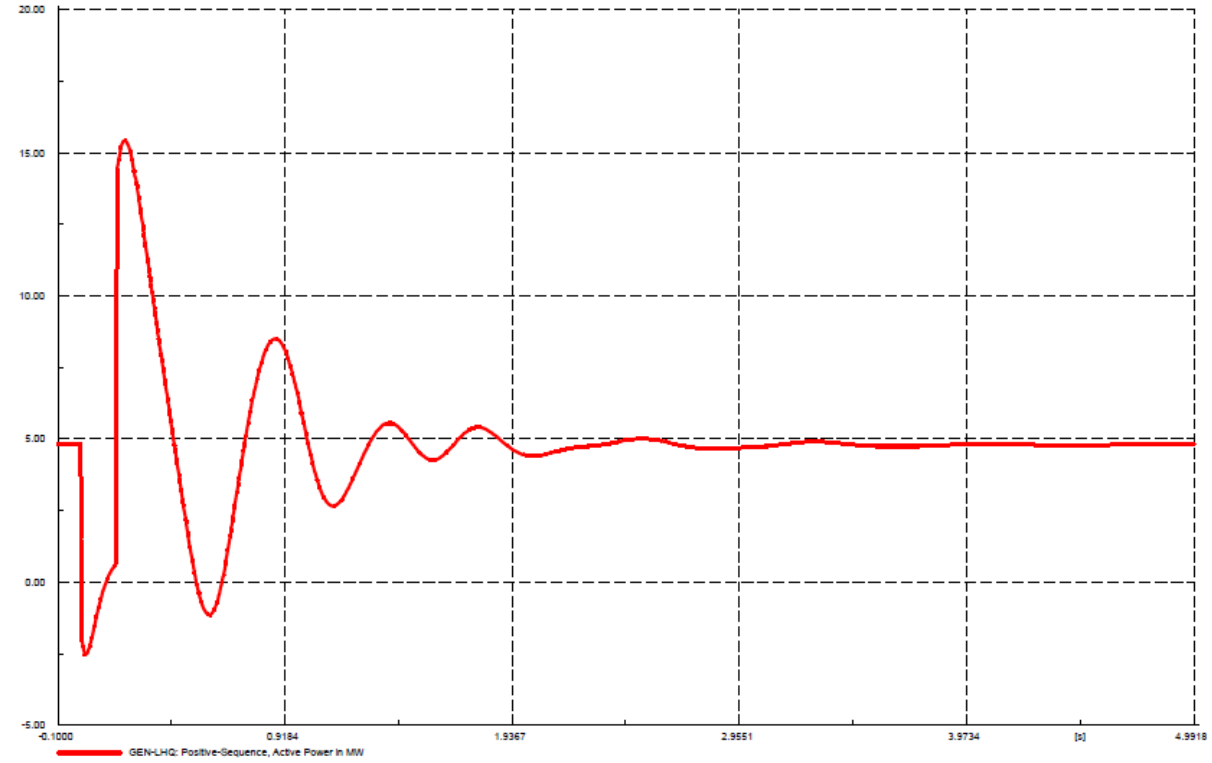

Figure H-4: Active power plot

Appendix I: 400kV network including generation capacity